Nasa CR 65268

Final Report

HIGH ENTHALPY GAS HEATER

Prepared for
NASA Manned Spacecraft Center
Structures and Mechanics Division
Entry Environment Simulation Branch
2101 Webster-Seabrook Road
Houston, Texas 77058

Contract No. NAS9-3564

EOS Report 6320-Final

30 December 1965

E
O
S
ELECTRO-OPTICAL SYSTEMS, INC.
A Subsidiary of Xerox Corporation
300 N. Halstead Street, Pasadena, California

N66-20997
(ACCESSION NUMBER) (THRU)
169 1
(PAGES) (CODE)
CR 65268 33
(NASA CR OR TMX OR AD NUMBER) (CATEGORY)
FACILITY FORM 602

LIBRARY COPY

JAN 06 1965

MANNED SPACECRAFT CENTER
HOUSTON, TEXAS

GPO PRICE $ _____

CFSTI PRICE(S) $ _____

Hard copy (HC) ___

Microfiche (MF) ___

ff 653 July 65

Final Report

HIGH ENTHALPY GAS HEATER

Prepared for
NASA Manned Spacecraft Center
Structures and Mechanics Division
Entry Environment Simulation Branch
2101 Webster-Seabrook Road
Houston, Texas 77058

Contract No. NAS9-3564

EOS Report 6320-Final

30 December 1965

Prepared by

Robert Richter, Project Engineer
Rolf D. Buhler

Approved by

Rolf D. Buhler, Manager
PLASMA TECHNOLOGY LABORATORY

Approved by

E. L. Katz, Manager
SPACE TECHNOLOGY GROUP

ELECTRO-OPTICAL SYSTEMS, INC. — PASADENA, CALIFORNIA
A Subsidiary of Xerox Corporation

Abstract

A 1-MW High-Enthalpy Constricted Arc Heater was developed and delivered, which is suitable for materials and structural testing. The heater has a single upstream cathode, a segmented 2-cm diameter constrictor, and 30 anode pins located in the supersonic nozzle. The heater has the following demonstrated design point performance:

Mass averaged enthalpy (with air or nitrogen)	9.3×10^7 j/kg (40,000 Btu/lb)
Stagnation pressure	~ 1.2 atm
Current	1540 amp
Efficiency	59 percent

The heater has been operated over a broad range of stagnation pressures (up to 2 atm), enthalpies (to 57,000 Btu/lb), and power levels (to 1 MW) with exceptional jet stability. A five-hour life test resulted in no appreciable component deterioration or measurable performance change. Complete experimental performance maps are presented.

Semi-empirical design charts and scaling rules for larger constricted arc heaters are also included. They indicate the general feasibility of a 10-MW heater with enthalpy-pressure performance capabilities similar to those of the 1-MW model.

An axisymmetric (Hall-arc jet) accelerator with an arc power of approximately 0.5 MW was designed and fabricated. The accelerator was tested with nitrogen at tank pressures to 7 mm Hg, and its capability for continuous operation was demonstrated. Pitot pressure profiles were obtained.

ACKNOWLEDGEMENTS

This program was carried out under Contract NAS 9-3564 under the technical direction of Mr. D. Greenshields and Mr. John Grimaud, Structures and Mechanics Division, NASA Manned Spacecraft Center. Their guidance through technical discussions is gratefully acknowledged. The writers are also indebted to numerous associates, both in and outside this company for valuable suggestions and discussions.

The staff of the Magneto Plasmadynamics Branch of the NASA/Ames Research Center under Mr. Howard Stine supplied considerable assistance and information for this project, at the request of the Technical Monitor. This includes the computer runs listed and much other pertinent experimental and theoretical information supplied by Messrs. C. Shepard and V. Watson from their own arc heater studies. The writers wish to express their thanks for this important assistance, and hope that this most fruitful exchange of information will continue in the future.

Within Electro-Optical Systems the following staff members made major contributions to the success of this project: Dr. Gary Marlotte (input for, and evaluation of, the computer calculations), Messrs. Charles Deichler, Nolan Archer, Joe Crepeau and Oscar Muller (heater fabrication, installation and testing), Mr. Robert Swope (detail design), and Messrs. Cecil Shepard and Ty Jacobs (test facilities, instrumentation).

Mr. Lloyd Popish was responsible for the editing and production of the reports and the Heater Manual.

The authors wish to thank these and several other staff members for their enthusiastic, effective, and patient participation in this work.

CONTENTS

1.	INTRODUCTION	1-1
2.	HEATER DESIGN AND DEVELOPMENT APPROACH	2-1
	2.1 Preliminary Considerations - Some Basic Choices and Alternatives in Arc Heater Design	2-1
	2.2 Theoretical Calculations and Design Optimization Procedures	2-4
3.	TEST EQUIPMENT, MEASUREMENTS, AND PROCEDURES	3-1
	3.1 Facilities and Equipment	3-1
	3.1.1 Test Facility	3-1
	3.1.2 Heater Installation	3-1
	3.1.3 Coolant Water Supply	3-4
	3.1.4 Electric Power Supply	3-4
	3.2 Measurements	3-4
	3.2.1 Coolant Flow Measurement	3-4
	3.2.2 Power Measurement	3-4
	3.2.3 Gas Flow Measurement	3-5
	3.2.4 Temperature Measurement	3-5
	3.2.5 Enthalpy Determination	3-5
4.	TESTING AND EVALUATION OF LABORATORY MODEL HEATER	4-1
	4.1 Testing of Laboratory Model Heater	4-1
	4.2 Test Results Obtained with the Laboratory Test Heater: Their Correlation and Evaluation	4-9
	4.2.1 Correlation Between Total Enthalpy, Constrictor Exit Pressure, and Mass Flow Rate for Choked Flow Conditions	4-9
	4.2.2 Electric Parameters	4-15
	4.2.3 Energy Transfer to the Constrictor Wall	4-27
	4.2.4 Heater Efficiency	4-30
	4.2.5 Testing with Simulated Air	4-33

CONTENTS (contd)

5. ONE MEGAWATT MATERIALS TEST HEATER (Materials Test Heater, Model HE-1MW) 5-1

5.1 Materials Test Heater, Model HE-1MW, Design 5-1

5.2 Materials Test Heater, Model HE-1MW, Operation 5-2

5.3 Life and Endurance Test of Materials Test Heater, Model HE-1MW 5-9

6. EXTRAPOLATION TO LARGE-SIZE CONSTRICTED-ARC HEATERS 6-1

6.1 A Combined Analytical and Experimental Approach to the Design of Large-Diameter Constricted-Arc Heaters 6-3

6.2 Design and Performance Calculations for a 10-Megawatt Constricted-Arc Heater 6-6

7. AXISYMMETRIC MHD ACCELERATOR 7-1

7.1 Purpose 7-1

7.2 Design of the Axisymmetric MHD Accelerator 7-1

7.3 Testing of the Axisymmetric MHD Accelerator 7-2

7.4 Measurements 7-6

7.5 Results 7-6

8. SUMMARY AND CONCLUSIONS 8-1

8.1 Objectives 8-1

8.2 Discussion of Results 8-1

APPENDIX A — ARC COLUMN MEASUREMENTS WITH THE 0.5-CM I.D. CASCADE APPARATUS

APPENDIX B — COMPUTER CALCULATIONS

REFERENCES

ILLUSTRATIONS

3-1	Laboratory Model Heater Installed on Vacuum Chamber	3-2
3-2	Materials Test Heater Model HE-1MW Mounted on Vacuum Chamber Flange	3-3
4-1	Constrictor Segments	4-3
4-2	Assembled Nozzle Section of Laboratory Model Heater	4-4
4-3	Nozzle Section with Anode Pins (front view)	4-5
4-4	Cathode Housing with Cathode Insulator and Cathode	4-6
4-5	Vacuum Tank Lid for Laboratory Model Heater with Anode Pins Manifolds and Coolant Distribution Fixtures	4-7
4-6	Laboratory Model Heater (5 Segment Configuration) Installed	4-8
4-7	Analytical Correlation Between Critical Flow Parameter and the Total Enthalpy	4-11
4-8	Correlation Between the Pressure at the Entrance and the Pressure at the Exit of the 2-cm-Diameter Constricted Arc Heater for Five Mass Flow Rates and Critical Exit Conditions	4-13
4-9	Correlation of the Choked Flow Parameter with the Mean Total Enthalpy (Nitrogen)	4-14
4-10	Operating Map for a 2-cm-Diameter Constricted Arc with Critical Exit Conditions	4-16
4-11	Comparison Between the Enthalpy Determined by Energy Balance and the Enthalpy Determined by Throat Pressure Measurement for the 2-cm-Diameter Constricted Arc Heater with Critical Exit Conditions	4-17
4-12	Correlation Between Total Voltage and Arc Current for the 2-cm-Diameter Constricted Arc Heater	4-19
4-13	Correlation Between Arc Voltage and Arc Current for the 2-cm-Diameter Constricted Arc Heater	4-20
4-14	Correlation Between Total Power and Arc Current for the 2-cm-Diameter Constricted Arc Heater	4-21
4-15	Correlation Between Throat Pressure and Arc Current for the 2-cm-Diameter Constricted Arc Heater	4-22

ILLUSTRATIONS (contd)

4-16	Correlation Between Total Enthalpy and Arc Current for the 2-cm-Diameter Constricted Arc Heater	4-23
4-17	Cross-Correlation of Test Data Measured with the 2-cm-Diameter Constricted Arc Heater	4-25
4-18	Accumulated Arc Voltage Along the 2-cm-Diameter Constricted Arc Heater	4-26
4-19	Correlation of Energy Transfer to Constrictor Wall for the 2-cm-Diameter Constricted Arc Heater	4-29
4-20	Energy Transfer to Constrictor Wall of the 2-cm-Diameter Constricted Arc Heater	4-31
4-21	Total Power Loss to the Constrictor Wall of the 2-cm-Diameter Constricted Arc Heater	4-32
4-22	Efficiency of the 2-cm-Diameter Constricted Arc Heater as a Function of Arc Current and Mass Flow Rate	4-34
4-23	Efficiency of the 2-cm-Diameter Constricted Arc Heater as a Function of Total Enthalpy and Mass Flow Rate	4-35
4-24	Efficiency of the 2-cm-Diameter Constricted Arc Heater as a Function of Arc Current and Throat Pressure	4-36
4-25	Correlation Between Entrance Pressure and Exit Pressure of the 2-cm-Diameter Constricted Arc Heater Operating with Simulated Air at Choked Exit Conditions	4-37
4-26	Total Voltage-Arc Current Relation for Simulated Air	4-38
5-1	High Enthalpy Gas Heater Assembly - Model HEGH-2	5-3
5-2	Materials Test Heater, Model HE-1MW (nozzle view)	5-4
5-3	Materials Test Heater, Model HE-1MW (rear view)	5-5
5-4	Exploded View of Materials Test Heater, Model HE-1MW	5-6
5-5	Schematic of Materials Test Heater, Electrical System, Coolant, and Gas Flow	5-7
5-6	Performance Chart for Materials Test Heater, Model HE-1MW (Enthalpy vs Total Power)	5-13
5-7	Efficiency of Materials Test Heater, Model HE-1MW at Life Test Operating Points	5-14
5-8	Performance Chart for Materials Test Heater, Model HE-1MW (Throat Pressure versus Total Power)	5-15
5-9	Total Voltage - Arc Current Characteristics of Materials Test Heater, Model HE-1MW	5-16
5-10	Comparison of Vital Heater Components (Anode Pins, Cathode, and Cathode Insulator) Before and After Life Test	5-17

ILLUSTRATIONS (contd)

6-1	Correlation Between Arc Current, Total Voltage, and Constrictor Length for a 10 Megawatt Constricted Arc Heater	6-8
6-2	Design Chart for a 10 Megawatt Constricted Arc Heater	6-10
6-3	Design Chart for a 10 Megawatt Constricted Arc Heater	6-11
6-4	Design Chart for a 10 Megawatt Constricted Arc Heater	6-12
7-1	Hall Current Accelerator Assembly	7-3
7-2	Hall Current Accelerator Installation on Vacuum Tank Lid	7-4
7-3	Hall Current Accelerator with Magnetic Field Coil	7-5
7-4	Pitot Pressure Distribution of Hall Current Accelerator Operating with 6 g/sec Nitrogen	7-7
7-5	Pitot Pressure Distribution of Hall Current Accelerator Operating with 4 g/sec Nitrogen	7-8

SYMBOLS AND UNITS

In general, the MKS system of units is used for all equations. In the discussion and on some of the charts, other units were occasionally used, generally for convenience or in quoting numbers familiar to many readers. Thus, gas flow rates are frequently given in grams/second, wall heat loads in kilowatt/square centimeter, input power in kilowatt or in megawatt, etc.

In writing the empirical heater design relations, it was not practical to nondimensionalize the empirical constants. As a result, the numerical values of the constants should only be used in conjunction with the MKS system. The reader should refer, in each case, to the defining equation (given in the table below) whenever numerical values of the empirical constants are to be used.

A	Cross sectional area of flow passage, m^2
C_c	Empirical mass flow factor (Eq. 4-6)
C_E	Defined by Eq. 4-6
C_Q	Empirical wall heat load factor (Eq. 6-10)
D	Diameter, m
E	Electric field, volt/m
I	Arc current, amp
K_A	Defined by Eq. 6-7
K_L	Defined by Eq. 4-13
K_V	Defined by Eq. 4-6
L	Constrictor length, m
$\dot{M}$	Gas mass flow rate, kg/sec
P_T	Total input power, W
R	Constrictor radius, m
T	Temperature, ^{o}K
V_A	Arc potential drop, volt
V_a	Anode potential drop, volt
V_B	Potential across ballast resistors, volt
V_c	Cathode potential drop, volt
V_T	Total potential drop, volt
$\dot{W}_{H_2O}$	Water flow rate, kg/sec

c	Specific heat of water, joules/kg-^{o}K
h_t	Total enthalpy, joules/kg
k_E	Local electric field factor, defined in Eq. 4-7, volt/m
n	Exponent of current (Eq. 4-13)
p	Pressure, newtons/m^2
p^*	Pressure at sonic throat, newtons/m^2
p_a	Atmospheric pressure, newtons/m^2
$\dot{q}_A$	Energy transfer per unit area, W/m^2
$\dot{q}_L$	Energy transfer per unit constrictor length, W/m
s	Pressure exponent (Eq. 6-1)
t	Pressure exponent (Eq. 6-2)
v	Velocity, m/sec
v^*	Sonic velocity, m/sec
z	Axial distance, m
z'	Nondimensional axial distance z/L
γ	Specific heat ratio
η	Efficiency
ξ	Defined by Eq. 6-2
ϕ	Heat conduction potential, $\int_o^T k(T)\, dT$

1. INTRODUCTION

This report documents the objectives, methodology, and progress of a program undertaken to design, develop, and fabricate a 1-MW, high-enthalpy, constricted-arc type materials test heater. This project was motivated by two factors. The first was the need for materials test jets of appreciably higher enthalpies than those available. The second was the knowledge of recent advances in arc heater and gas accelerator research which made the required 1 MW high-enthalpy materials test heater a realistic development goal.

High enthalpy test jets are required (a) for the simulation of atmospheric entry conditions at very high flight speeds (on the order of 15 km/sec and higher) and (b) more generally, for imposing very high heat loads on material test samples and vehicle components under relatively low pressure conditions.

The project had as its objectives the following heater performance goals:

1. The development and delivery of a constricted arc gas heater suitable for routine materials testing with nitrogen, air, and other gas mixtures simulating planetary atmospheres, and having the following performance capabilities:

Mass averaged enthalpy	9.3×10^7 joules/kg (40,000 Btu/lb)
Input power level (nominal)	1 MW
Minimum heating efficiency (at maximum enthalpy)	50%
Stagnation pressure range	~ 0.5 - 2.0 atm
Minimum life (without maintenance)	5 hours

2. The feasibility demonstration of an axisymmetric (Hall-current type) MHD gas accelerator ultimately capable of simulating still higher entry flight speeds (higher enthalpies) than those given above.

The materials test heater was to be designed to be compatible with the existing dc power supply, cooling water supply, and test tank at the NASA-MSC Entry Environments Simulation Laboratory. Also, the heater would be life tested under conditions closely approximating a materials testing operation, including frequent starting and shutdown sequences, long and short duration runs, and repeated cycling through a sequence of typical operating points (to demonstrate repeatability).

A corollary goal was the development and accumulation of arc heater design information and calculations to permit the realistic planning and eventual development of large ($\sim$ 10-MW class) materials test heaters for the same performance level as the present 1 MW heater.

The original premise that a 1 MW-class heater with the given performance would be feasible was based partly on theoretical calculations (Refs. 1 and 2) and partly on small-scale experiments with the Maecker cascade-type arc research apparatus (Ref. 3). Shortly before this project was started, results from a NASA-Ames high enthalpy constricted arc heater (1/2-inch diameter) became available (Ref. 4) which confirmed the previous theoretical predictions.

When this project was started, the initial effort was put into cross-correlating all this existing information and attempting to scale it up to the 1 MW level, using the existing scaling rules for constricted arc columns. In particular, the existing choked mass flow versus pressure and enthalpy points of Shepard were immediately useful for the choice of the proper constrictor size (see Section 4). Some additional small-scale (1/2-cm diameter) cascade tests were also run during this period, to explore the effects of segment and insulator thicknesses on the potential gradients and the enthalpies reached and to test the reliability of purely theoretical predictions. Some details are given in Appendix A.

Also during the first part of the project, additional numerical constricted arc-gas flow calculations were carried out by the staff of the Magnetoplasmadynamics Branch of the Ames Research Center, in support of this development program. Computer integrations were run for the 50 to 100 kW (1/2-cm constrictor), for the 1 MW (2-cm constrictor), and for the 10 MW heater size regimes, to serve as a basis for design and performance predictions, and for subsequent comparisons with the experimental results. These theoretical results and some limited comparisons with experimental data are discussed in Appendix B.

The development of the 1 MW materials test heater was carried out in two major steps. First, a flexible "laboratory model" heater was built in stages. This was used for the electrode development, for the determination of a proper constrictor length, and for the generation of accurate experimental performance maps. This work is described in Section 4. Second, after the required performance was attained and the internal heater design configuration was firm, the final materials test heater assembly was designed, suitable for ease of handling, installation, and maintenance at the NASA-MSC Entry Environments Simulation facility. This heater was then successfully life tested for five hours prior to delivery. The materials test heater and its life test are described in Section 5.

In Section 6, the experimental and theoretical information obtained is presented in the form of semiempirical design charts and rules for MW-class constricted-arc heaters. A tentative design point region for a 10-MW high enthalpy heater is shown, which indicates the general feasibility and promise of such a heater at least as far as constrictor heat loads are concerned.

The design, check-out, and preliminary performance tests of the axisymmetric (Hall-arc jet type) MHD accelerator were carried out concurrently with the arc heater development, as described in Section 7.

In Section 8, the most important results and conclusions of this project are summarized and discussed.

2. HEATER DESIGN AND DEVELOPMENT APPROACH

2.1 Preliminary Considerations - Some Basic Choices and Alternatives in Arc Heater Design

The direct heating of a gas by an arc may be accomplished by a variety of design approaches and heater configurations. For example, the gas flow may be coaxial to the arc or perpendicular to it; the arc can be rotated within a chamber of nearly stationary gas; the electrodes may be consumable (the original Gerdien idea) or nonconsumable; and so forth.

Experience and some basic thinking, however, will quickly rule out many of these alternatives, for the design of heaters under consideration for this program. In fact, it is widely agreed, although difficult to conclusively prove, that the most efficient way of raising a gas to highest practical enthalpies, at least with dc power, is by passing the gas coaxially through the arc, in a constrictor of suitable size and length.

Once it is decided to develop a dc-heater of the constrictor type (or coaxial flow-arc), the remaining design alternatives are primarily related to the locations and general design of the two or more electrodes which must be at opposite ends of the constrictor(s). The constrictor diameter can be readily determined for any particular set of operating conditions. The first choice is which electrode to put at the upstream end of the constrictor and which at the downstream end, to achieve a simple constrictor design. When pairs of constrictors are used ("Double-Gerdien" approach) then both or all electrodes can be "upstream." The numbers and sizes of constrictors to be used could also be optimized but the use of more than one entails the use of a mixing or plenum chamber, and the difficult problems associated with it.

It is difficult to evaluate precisely the relative advantages and disadvantages of the single constrictor as compared with the double constrictor (Double-Gerdien) configurations, but the performance potential of both should be nearly the same at high pressures. The advantage of electrode corrosion protection by operating with two "upstream" electrodes in the Gerdien type arc can also be achieved with a cavity electrode in a single constrictor. For low pressures and extremely high enthalpies the single constrictor design appears most favorable since there is no plenum chamber in which the gas energy is dissipated. The single constrictor design also permits the placing of one electrode set, e.g., the anodes, downstream of the throat in the low-pressure part of the supersonic nozzle. This greatly reduces the spot formation tendency on the anodes and has worked extremely well in practice.

The advantages offered by the single constrictor design are thus (1) that either low-pressure or high-pressure anodes may be used and; (2) the mechanical simplicity of axisymmetric construction. Because of these advantages the EOS group chose the single constrictor configuration over the double (or multiple) constrictor approaches. Once this decision is made, the following important choices remain regarding the electrodes:

1. Location of the anode upstream or downstream of the constrictor.
2. Location of the downstream electrode upstream or downstream of the nozzle throat (if supersonic testing is contemplated).
3. Primary method of electrode cooling (transpiration or internal water cooling).
4. Electrode materials.
5. Location of inlets for oxidizing gases.
6. Necessity of inert gas shielding for either electrode, and gas to be used.
7. Submerged or cavity electrodes versus electrodes in contact with main gas stream.

8. Single or multiple electrodes (with individual ballast resistors) for either anode or cathode.
9. Method of artificial arc movement to be used on either electrode, if any (vortex flow and/or magnetic fields), together with sizes and shapes of the electrodes.

A complete and unbiased investigation of all these choices would have led far beyond the scope of this program. Since the primary objective of the program was to develop, life test and deliver, a high-enthalpy materials test heater within one year, it was necessary to immediately choose that one approach and design configuration which, based on prior experience and calculations, offered the greatest probability of success.

On this basis the following initial choices were made:

1. Single constrictor design with constant diameter, which implies choking to occur at the constrictor exit.
2. Single tungsten cathode located at upstream end of constrictor.
3. Multiple pin anodes located in the supersonic nozzle, as the first choice.

Single tungsten cathodes for the 1000-2000 amperes regime at 1 to 2 atm pressure were known to be feasible, though in past experience some cathode erosion occured. The problem was to minimize erosion by proper cathode and gas flow design. Multiple cathodes were a possible alternate, but it was not clear whether this would really reduce the overall erosion rate. Inert gas shieldings of the cathode would be automatically provided by the upstream location of the cathode (choice 2 above).

Multiple anode pins in the low-pressure portion of the expansion nozzle were the first choice. This design configuration would completely eliminate the problem of test jet rotation associated with a single anode and rotating arc attachment point. At the time EOS was firming heater design plans, C. Shepard (NASA Ames Research Center) had

successfully demonstrated the operation of multiple anodes.* Other anode designs were considered as possible alternates should they be required. From the start it was expected that several different anodes might be required to accommodate the full range of operating conditions (outlet pressures) of which these heaters are capable. However, the use of a vacuum tank for testing, i.e., a low pressure supersonic test jet, was specified as the usual test mode for this heater. The anode design objective was for a diffused anode attachment achieved by low pressure and argon shielding. The current of each anode attachment was to be limited to 50 amps which appeared to be tolerable even with a contracted spot.

Some of the radically different design approaches such as transpiration-cooled electrodes were ruled out because of uncertainties and limited time. However, the laboratory model heater provides flexibility to permit extensive study of several of the other design variables. For example, the oxidizing gas inlets can be located at any distance along the constrictor length. The recess of the anode pins can be optimized, as can the quantity and type of anode bleed (shielding) gas. Such studies would be possible without modification to the heater.

2.2 Theoretical Calculations and Design Optimization Procedures

When the project was initiated it was expected that general dimensionless heater design charts could be developed in a manner similar to that used in developing dimensionless charts for long (asymptotic) flow-arc columns. The hope was that all existing information on similar heaters (from small-scale experiments, a few full-scale experiments, and purely theoretical studies) could be correlated and evaluated to yield data for the 1-MW heater design and design estimates for future 10-MW heaters.

---

*The writers had the opportunity to witness one of the earliest runs of the 1-inch diameter Ames high-enthalpy heater.

This approach proved to be more difficult and less fruitful than expected. The reasons are manifold and will only be briefly discussed here. First, most scaling rules are very different for the small conduction-governed and the large radiation-governed arcs. Therefore any very general scaling procedure which includes conduction-governed, radiation-governed, as well as mixed cases, such as the scaling rules of Marlotte and Cann (Ref. 3) for simple arc columns, are complicated and difficult to use for design charts. A second difficulty is that the usual heater scaling theories, Stine-Watson (Ref. 4), Patt etc, use the "corresponding infinite or asymptotic" arc column solution as the point of departure. This corresponding asymptotic solution, however, is not known for either the experienced or the theoretical data points which were to be correlated. In fact, for the heaters under study, a corresponding asymptotic flow-arc solution cannot exist in the strict sense, because here the choking point is always at the heater exit, i.e., before the gas reaches the full asymptotic mean enthalpy. A new general scaling approach is therefore needed which departs from the choking (or heater outlet) point rather than the "corresponding asymptotic" flow-arc; but this has not yet been worked out.

One other finding influenced the heater design approach which was eventually used. There are still considerable difficulties and uncertainties involved in the use of the theoretical calculation of the flow-arc solution (by numerical integration). The uncertainties are in the gas transport properties (density of emitted radiation, thermal and electric conductivities), and in the omission of self-absorption of radiation energy and of possible turbulence. Both self-absorption and turbulence tend to become more important with increasing constrictor sizes and increasing pressures. In addition to these uncertainties there may also be other difficulties which have not yet been isolated.

In any case, the computer integrations did not agree well with the experimental results. (This is discussed in more detail in Appendix B). It was evident that less confidence could be placed in the computer results, in terms of actual heater design, than had been anticipated. As a result, a more strongly empirical approach was chosen for both the design of the 1-MW heater developed in this program phase, and the performance predictions for the 10-MW heater.

One very general and useful design chart was obtained initially, pertaining to the choked flow condition at the heater "throat", i.e., at the constrictor outlet where the choking must occur. The chart correlates the mass flow per unit of cross sectional area. With the critical pressure and the mass-averaged enthalpy at the constrictor exit. This correlation (discussed in Section 4) immediately fixes the constrictor size, for a given desired throat pressure, mass flow rate and total enthalpy.

The following approach was thus taken for the design of the 1-MW heater:

1. A "design point" was chosen, based on the specified heater enthalpy, minimum overall heater efficiency and a throat pressure half of the desired stagnation pressure.
2. Corresponding to this "design point" a constrictor diameter was calculated from the mass flow-enthalpy-pressure correlation.
3. The remaining major variables to be determined were then the constrictor length or the current (the choice of either one of these fixes the other), the nozzle angle and length and the number of anode pins. These quantities were determined or chosen largely on an empirical basis, as will be discussed in the following paragraphs.

   The initially estimated "design point" was taken as follows:

mass-flow averaged total enthalpy	$\bar{h}_t$	= 9.3×10^7 joules/kg ($\sim$ 40,000 Btu/lb)
power in gas (minimum) (50% of total heater power)	W_g	= 500 kW
mass flow rate	$\dot{M}$	= 5.37 g/sec
throat (constrictor exit) pressure	p^*	= 0.50 atm

The throat pressure of one half atmosphere corresponds to about 1 atm upstream stagnation pressure, which is in the middle of the expected heater operating range ($p_o \sim 0.5 - 2.0$ atm). The "design" enthalpy and estimated efficiency were chosen on the basis of the original contractual agreement. The resulting calculated constrictor radius was then adjusted to accommodate the nearest standard reamer size .

constrictor diameter, 2R = 1.985 cm

= 0.7813 in.

The nozzle length and angle were selected somewhat arbitrarily, based on a nozzle exit diameter of 4.962 inch (12.6 cm) for an assumed desirable range of test pressures and Mach numbers. A straight conical nozzle was chosen for simplicity, with a relatively large half angle (26 degrees) to make the nozzle as short as practical. It was felt that later, for very specific test Mach numbers and flow uniformity requirements, more elaborate nozzle shapes could be evolved. For the initial tests 30 pin anodes were used. These were fitted into a simple anode ring near the nozzle exit. With this arrangement additional anode pins could be placed in the nozzle if necessary. The number of anode pins corresponded to an estimated safe current limit of 50 amp per pin.

The remaining design value of the constrictor length was based on the desired maximum arc current of 1500 amps at full power of one megawatt. This current-power relation was chosen as a good match for the existing NASA-MSC rectifier power supply. The constrictor length had to be determined experimentally in the manner described in Section 4.

The initial choice of the constrictor diameter proved to be very good as was established by the test results of the laboratory heater (see Section 4).

The final mass flow rate at the "design" enthalpy and the corresponding constrictor pressure were slightly higher than the initial estimates, since the heater efficiency was higher than 50 percent on which the first design values were based.

3. TEST EQUIPMENT, MEASUREMENTS, AND PROCEDURES

3.1 Facilities and Equipment

3.1.1 Test Facility

The testing of the 1-MW laboratory model heater, the ultrahigh enthalpy accelerator, and the materials test heater, was conducted in the Plasma Laboratory of EOS. All heaters were tested in a 6 x 3 foot water-cooled vacuum tank which is equipped with a copper coil heat exchanger. A vacuum of 5 mm Hg can be maintained with a gas flow rate of 6 g/sec in the tank.

3.1.2 Heater Installation

The heaters were installed on vacuum flanges which were mounted on dollies for ease of handling. The laboratory test heater and the materials test heater were mounted on their flanges and are shown in Figs. 3-1 and 3-2. In the laboratory test heater, the cooling water was delivered to the segments by individual water lines which permitted the measurement of the flow rate through each individual flow circuit of the heater, and the temperature rise of the cooling water in each segment. In the materials test heater, the component cooling water is supplied from two manifolds which are part of the support structure of the heater.

For the monitoring of the current carried by each individual anode pin of the laboratory model heater, 30 voltmeters were connected across the anode pin ballast resistors. Since the test results of the laboratory model heater indicated that the ballast resistance of 1.4 ohms for each anode pin was sufficient to assure the desired current distribution over all 30 anode pins, voltage measurements across the ballast resistors in the materials test heater were unnecessary.

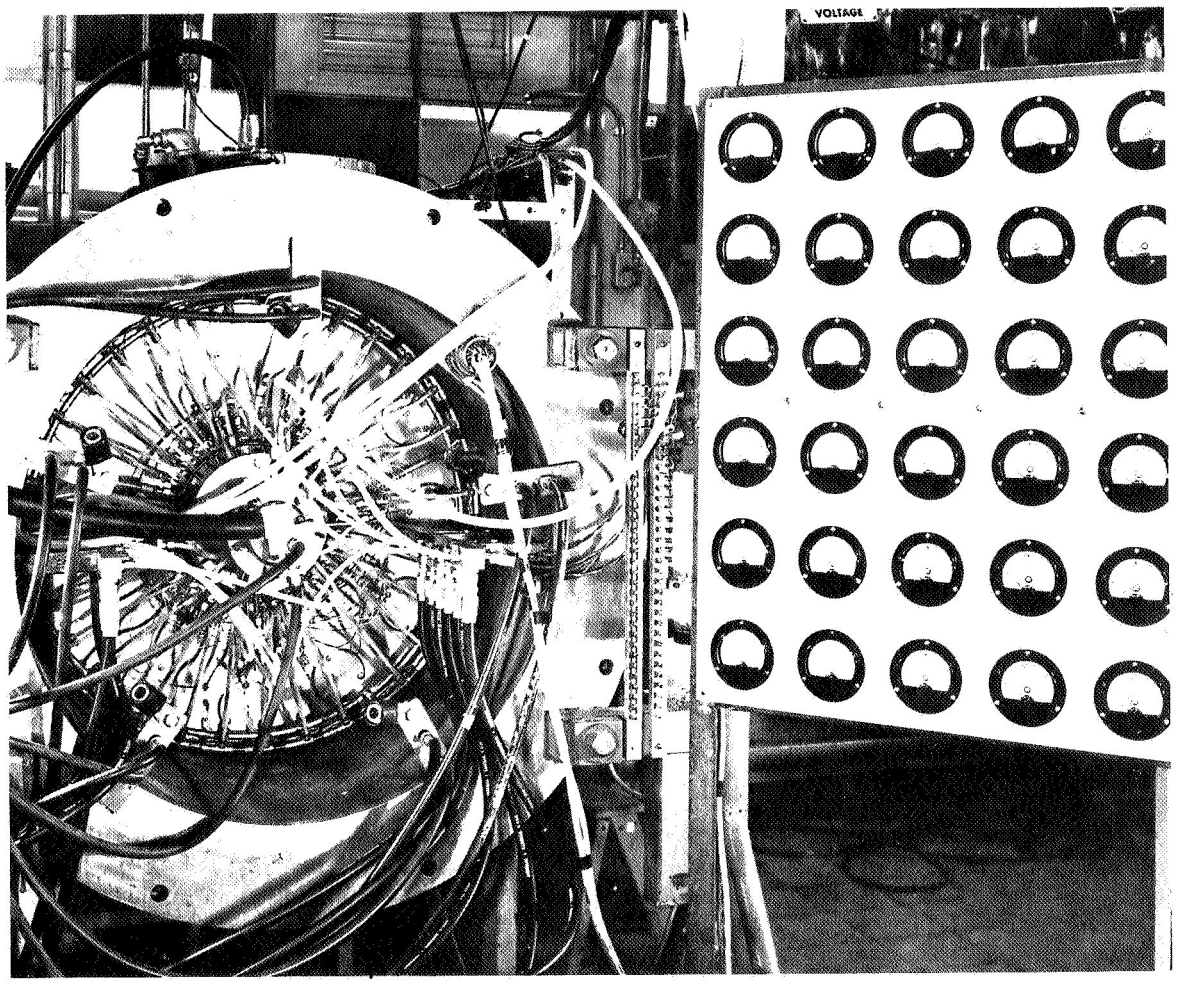

FIG. 3-1 LABORATORY MODEL HEATER INSTALLED ON VACUUM CHAMBER

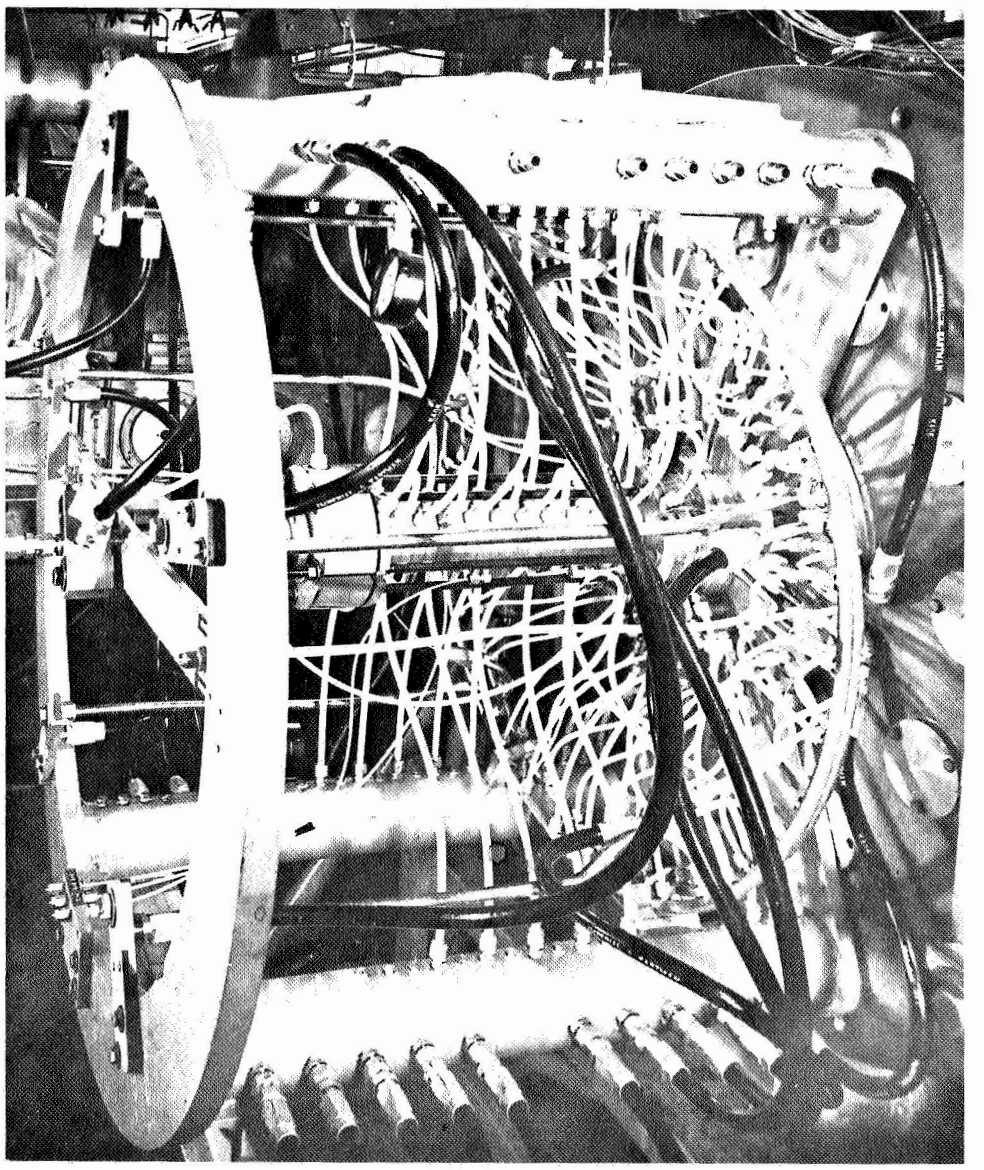

FIG. 3-2 MATERIALS TEST HEATER MODEL HE-1MW MOUNTED ON VACUUM CHAMBER FLANGE

3.1.3 Coolant Water Supply

Cooling water for the heaters and the heat exchanger was provided from two sources: a 1000 psig water supply, capable of delivering 200 gpm of recirculated chemically treated water, and a 200 psig supply, capable of delivering 100 gpm from the water main.

3.1.4 Electric Power Supply

The electrical power for the heater was delivered by a 600 kW rated A. O. Smith rectifier power supply which can be operated at almost double its rated capacity for 10 minutes. In addition, six rectifiers, each with a rated capacity of 50 kW, were available.

3.2 Measurements

3.2.1 Coolant Flow Measurement

The water flow rates were measured with two water flow panels each having twelve separate water circuits. The 200 psig water flow panel measures, with individual mercury columns, the pressure drops across commercial precision flow orifices. The 1000 psig water flow rates are determined from the pressure drops across commercial precision orifices measured with a single differential pressure gage (Mid-West Instrument). Each water flow panel was calibrated by weighing the total water flow, during a given time interval, at several pressure differentials.

3.2.2 Power Measurement

The electrical power input to the heater was determined from the product of the arc current and total voltage. Both electrical values were measured with a Rowan D.C. Volt-Amp Panel Model DR 630/631 Serial No. 001. The instruments of the panel are guaranteed to measure voltage and current with ±1 percent full-scale accuracy. The calibration of the two instruments indicated that they performed within the specified accuracy (Calibration Test No. 00518, 24 June 1965).

3.2.3 Gas Flow Measurement

All gas flow rates were measured with sonic orifices. Each orifice was calibrated with a wet test meter (AL 17) or against a calibrated orifice, depending on the orifice size. The orifices were mounted on a flow panel on which the upstream pressures as well as the downstream pressures were measured with 1/4 percent Gasco pressure gages.

3.2.4 Temperature Measurement

The temperature rise in the cooling water circuit was measured with commercial shielded copper-constantan thermocouples whose differential output was displayed on a digital voltmeter. Before each power run, the temperature rise of the water due to friction (pumping power conversion) was established (zero reading) and subtracted from the total temperature rise measured during arc operation.

3.2.5 Enthalpy Determination

The total mass-averaged enthalpy delivered by the heater was determined by two methods, one of which was based on the following relation:

$$h_t = \frac{P_T - \dot{W}_{H_2O}\, c\, \Delta T}{\dot{M}} + h_B$$

where

h_t = total mass-averaged enthalpy

P_T = total electrical power input

$\dot{W}_{H_2O}$ = coolant water flow rate

h_B = base enthalpy of gas

c = specific heat of water

$\dot{M}$ = gas mass flow rate

The other method employed the theoretical relation between throat pressure, enthalpy, mass flow rate, and throat area

$$\frac{\dot{M}}{C_c p^* A^*} = f(h_t)$$

This relation incorporates a correction factor C_c, which takes into account the nonuniformity of the enthalpy distribution and the viscous effects at the constrictor exit. The correction factor was determined by a comparison of enthalpies measured by the first method.

The possible error in the total mass averaged enthalpy evaluated by the first method can be estimated from

$$\frac{\Delta h_t}{h_t} = \frac{\frac{\Delta V}{V} + \frac{\Delta I}{I} + \frac{c\Delta T\ \dot{W}_{H_2O}}{V_T I_A}\left(\frac{\Delta \dot{W}_{H_2O}}{\dot{W}_{H_2O}} + \frac{\Delta (T)}{\Delta T}\right) + \left(1 - \frac{c\dot{W}_{H_2O}\ \Delta T}{V_T\ I_A}\right)\frac{\Delta \dot{M}}{\dot{M}}}{1 - \frac{c\Delta T\ \dot{W}_{H_2O}}{V_T I_A}}$$

When using realistic values for all possible errors of the operating parameters measured, one finds a possible error in the enthalpy determined by the above equation to be:

$$\frac{\Delta h_t}{h_t} \approx \pm 13\%$$

For the error analysis of the second method, the approximate relation

$$h_t = \left(\frac{p^* A^* C_c}{\dot{M}}\right)^{\frac{1}{2}} = C_1^{\frac{1}{2}} \frac{p^{*\frac{1}{2}}}{\dot{M}^{\frac{1}{2}}}$$

can be written, so that

$$\left| \frac{\Delta h_t}{h_t} \right| = \frac{1}{2} \left(\left| \frac{\Delta p^*}{p^*} \right| + \left| \frac{\Delta \dot{M}}{\dot{M}} \right| \right) + \frac{1}{2} \frac{\Delta C_1}{C_1}$$

With realistic values for possible errors in pressure and mass flow rate,

$$\frac{\Delta h_t}{h_t} \approx \pm 1.5\% + \frac{1}{2} \frac{\Delta C_1}{C_1}$$

where

$$\frac{\Delta C_1}{C_1} = \frac{\Delta A^*}{A^*} + \frac{\Delta C_c}{C_c}$$

When the tests for the determination of the constant C_c were performed, all measurements were made with great care over a wide range of operating conditions. The accuracy of the correction factor should, therefore, be considerably better than the accuracy of an individually determined, mass-averaged enthalpy determined by the first method. One can estimate

$$\frac{\Delta C_1}{C_1} \approx \pm 5\%$$

so that the second method will determine the total enthalpy with a possible maximum error of

$$\frac{\Delta h_t}{h_t} \approx \pm 6.5\%$$

which is only half the possible maximum error for individual enthalpies determined by the heat balance method.

4. TESTING AND EVALUATION OF LABORATORY MODEL HEATER

Testing of the laboratory heater was performed with two general objectives in mind. The first objective was the testing and verification of the basic constricted-arc heater design with all critical components. The second objective was to establish design procedures for constricted-arc heaters in the 1 MW power size and for heaters of larger power capacity, i.e. up to 10 MW, by means of consistent test data and their correlations. The test data obtained in the course of the testing program, and their correlations and evaluations, are presented in the form that led to the satisfactory completion of the second objective. This is indicated by the design charts established for a 10-megawatt constricted-arc heater presented in Section 6.

4.1 Testing of Laboratory Model Heater

The testing of the laboratory model heater had three basic objectives:

1. Evaluation of the constrictor segments, the cathode and the anode design.
2. Experimental determination of the constrictor length for full power input of 1 megawatt at 1500 amps.
3. Determination of flow rate and efficiency at the design point of 40,000 Btu/lb (9.3×10^7 joules/kg) at 1 megawatt total power input.

Evaluation of Constrictor Segments, Cathode and the Anode Design

The constrictor segments, the cathode and the anode design were evaluated with a heater configuration consisting of five (5) constrictor segments, the complete nozzle and anode section with 30 anode pins, and a 3/4-inch-diameter cathode with a 0.60-inch-diameter tungsten tip. The constrictor segments, the nozzle section, the cathode assembly, the test

tank lid with the anode pin manifolds, and the assembled first test configuration of the heater are shown in Figs. 4-1 to 4-6. This configuration was tested up to the full design current of 1500 amps with a nitrogen flow rate of 5.37 g/sec. In this configuration, the anode pins as well as the cathode performed without any indication of problem. The constrictor segments remained in their original condition.

The second configuration of the heater consisted of 15 constrictor segments, i.e. a constrictor of 9.1 inch in length. This configuration was tested up to 1500 amps successfully.

Determination of Constrictor Length and Heat Transfer to Constrictor

During the testing of the 9.1-inch constrictor, the heat transfer to the constrictor wall was measured and extensive correlations between arc current and total voltage were made. These tests gave the first indication that the energy transfer to the constrictor wall was predominantly a function of the arc current. Extrapolation from the two constrictor lengths tested indicated that the total power of 1 megawatt could be dissipated in the heater at 1500 amps with a 12.75 inch (32.4 cm) long constrictor at a gas flow rate of approximately 6 g/sec.

Six more constrictor segments were added to the constrictor to bring its total length to 32.4 cm. When this configuration was tested at 1500 amps, problems were encountered with the cathode. Even with a new cathode of the original design, the ablation of the tungsten tip persisted when reaching an arc current of approximately 1450 amps. The cathode was redesigned. Its diameter was increased to 1 inch and the tungsten tip diameter was made 0.700 inch. Small modifications on the cathode housing and the associated components had to be made to accommodate the new cathode. With these changes the heater was operated up to the full current of 1500 amps and full power of 1 megawatt. The heater was tested with nitrogen and with simulated air.

The main gas flow was injected into the constrictor near the cathode tip.

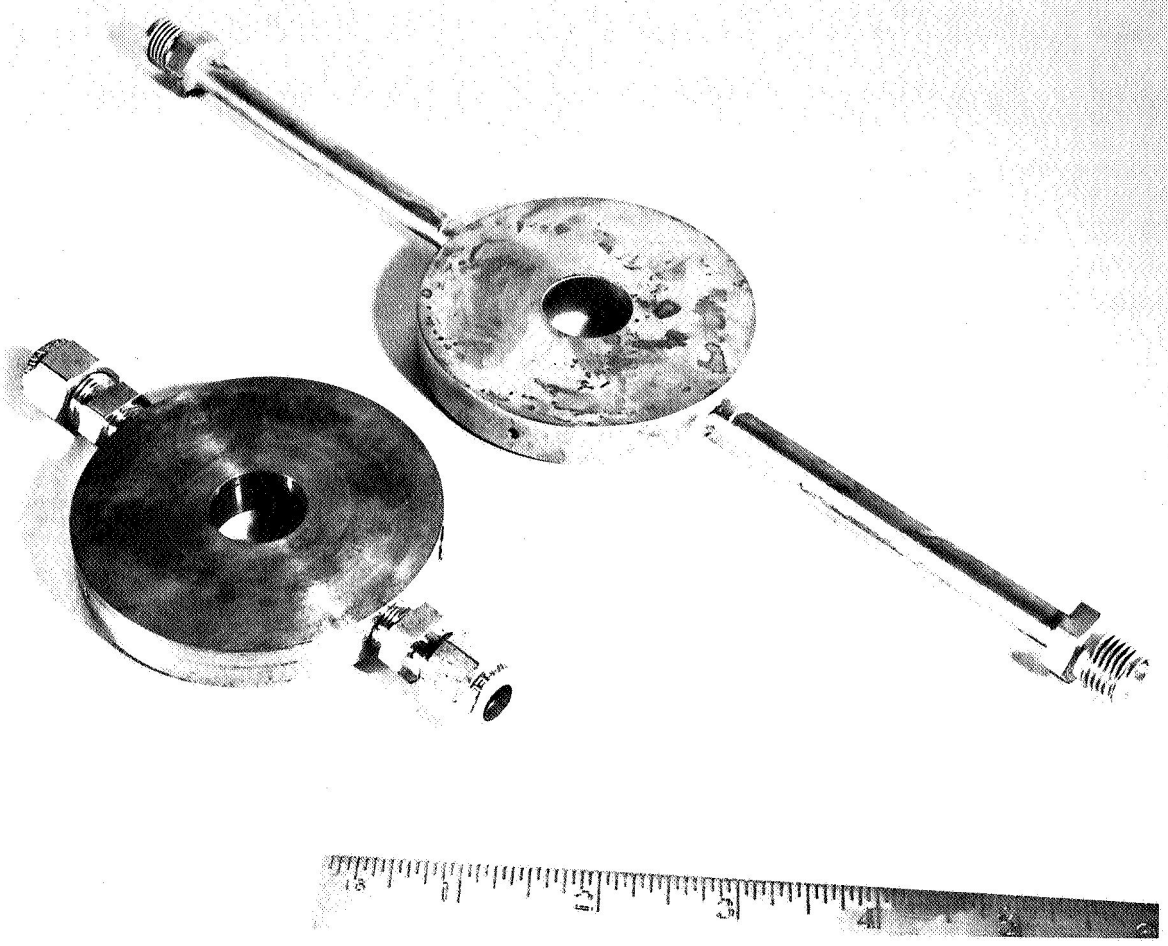

FIG. 4-1 CONSTRICTOR SEGMENTS

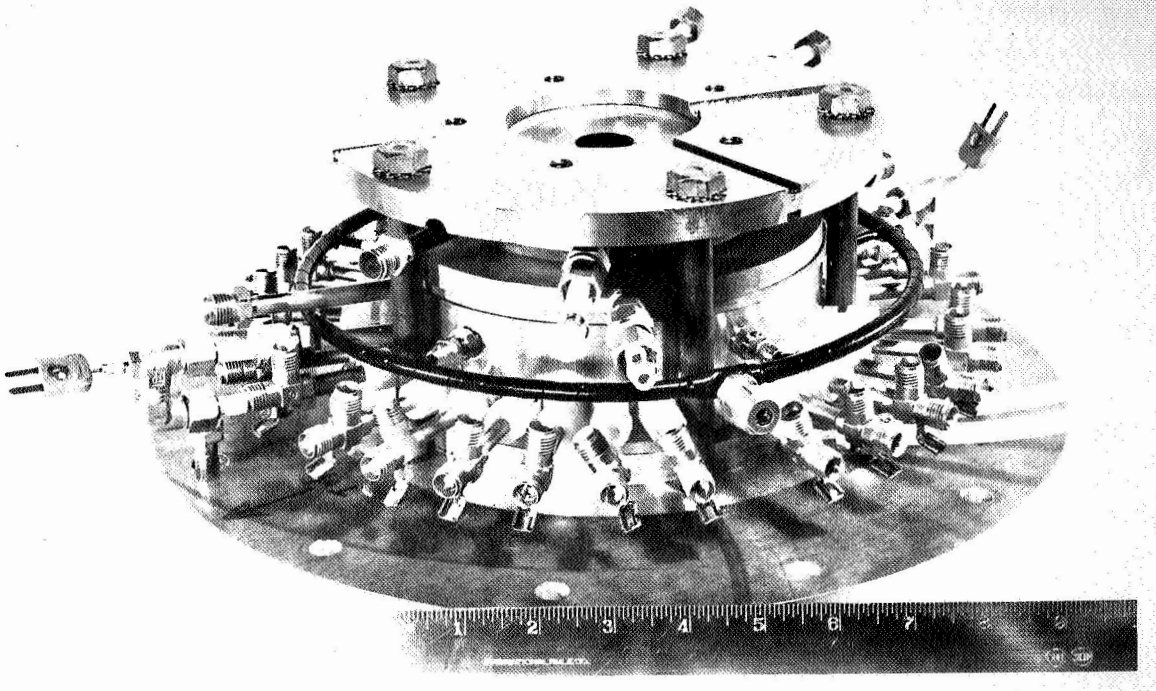

FIG. 4-2 ASSEMBLED NOZZLE SECTION OF LABORATORY MODEL HEATER

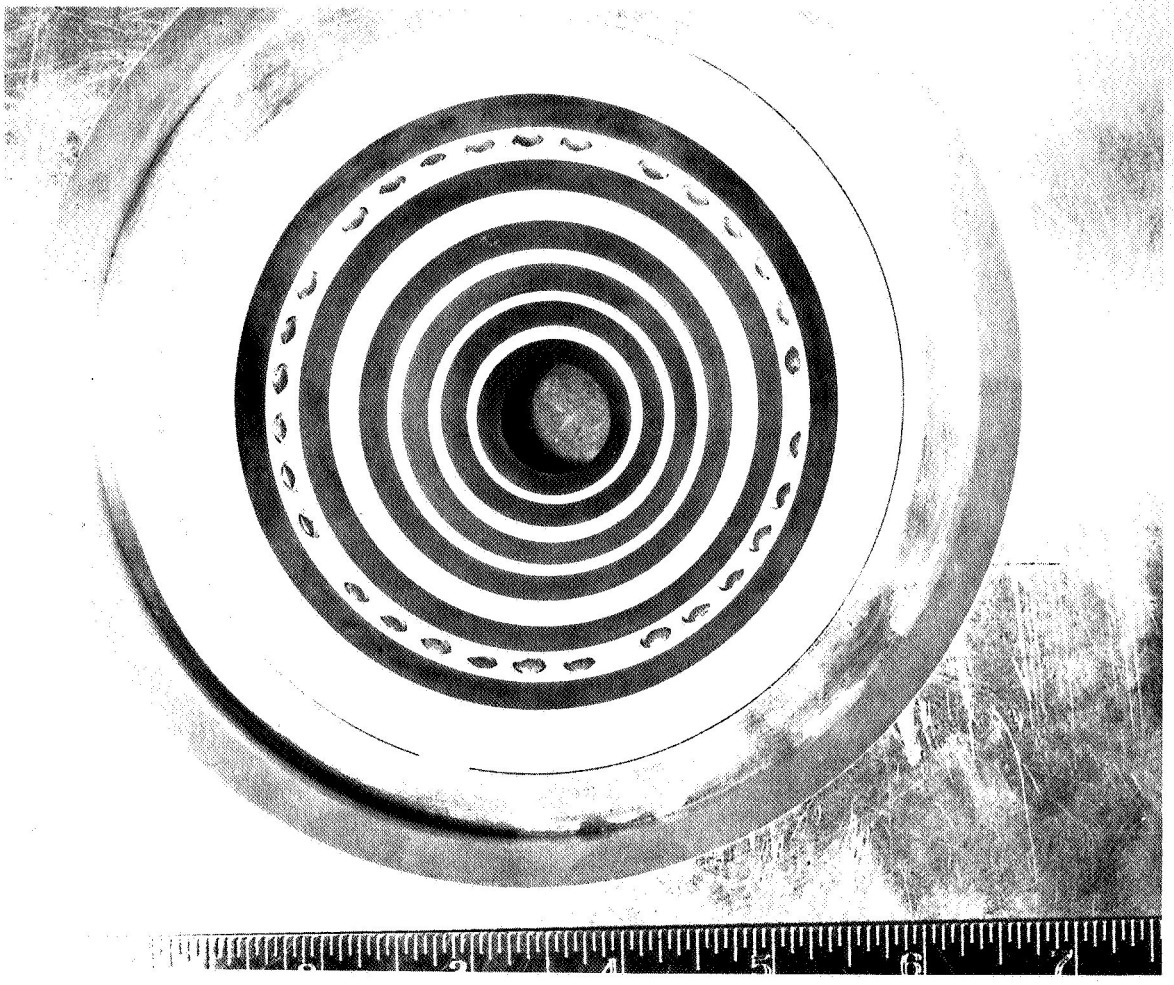

FIG. 4-3 NOZZLE SECTION WITH ANODE PINS (FRONT VIEW)

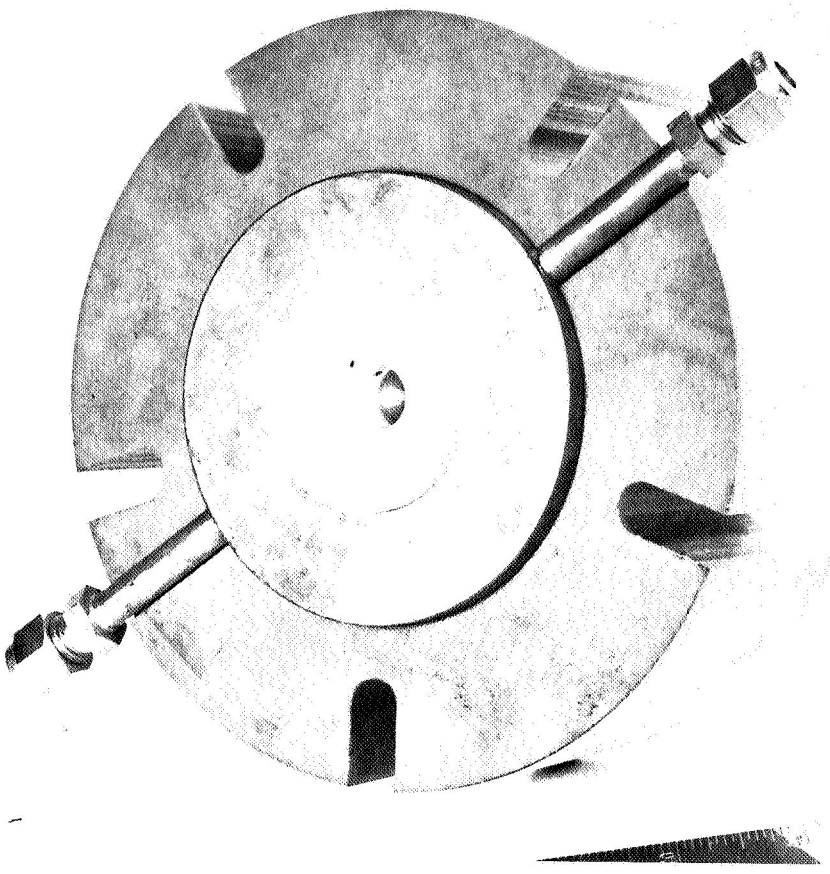

FIG. 4-4 CATHODE HOUSING WITH CATHODE INSULATOR AND CATHODE

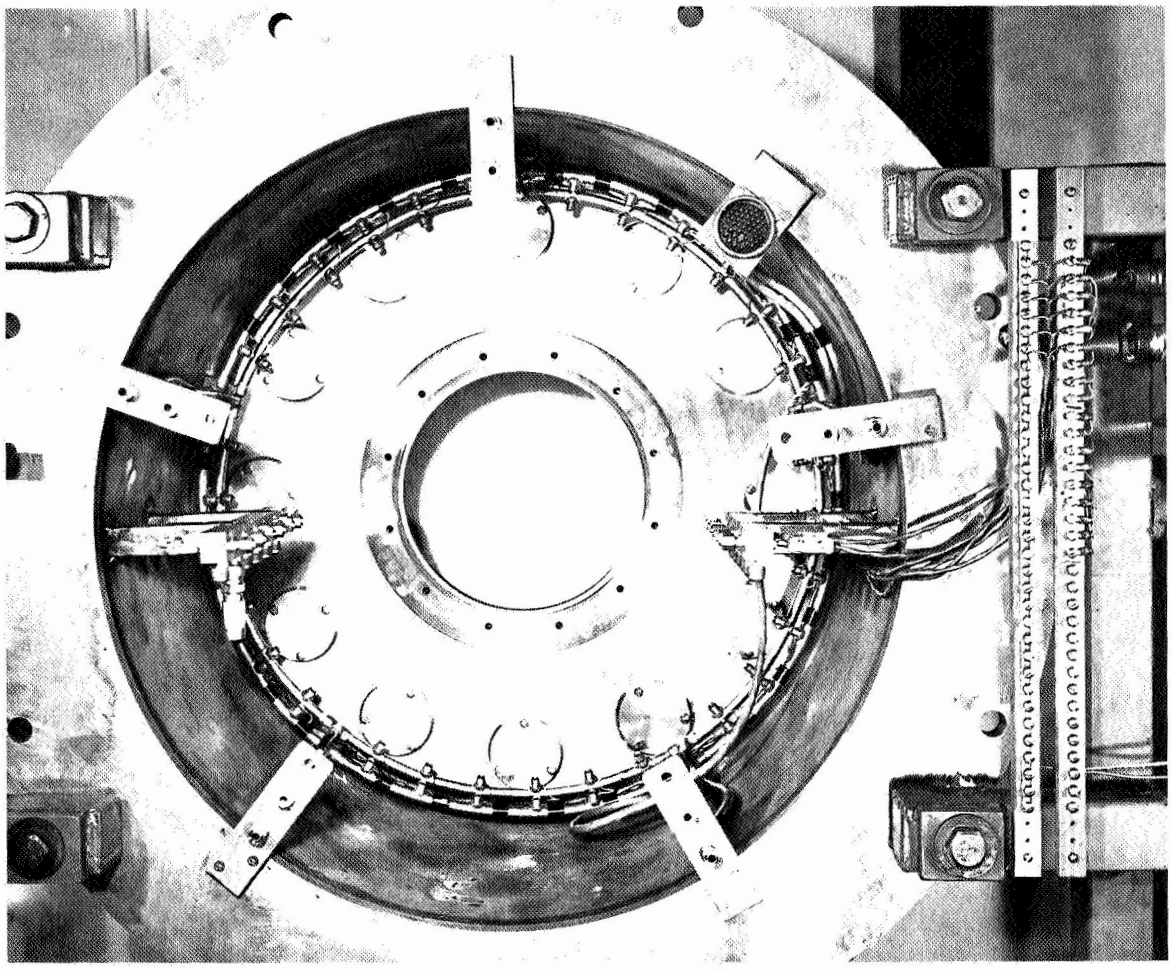

FIG. 4-5 VACUUM TANK LID FOR LABORATORY MODEL HEATER WITH ANODE PINS MANIFOLDS AND COOLANT DISTRIBUTION FIXTURES

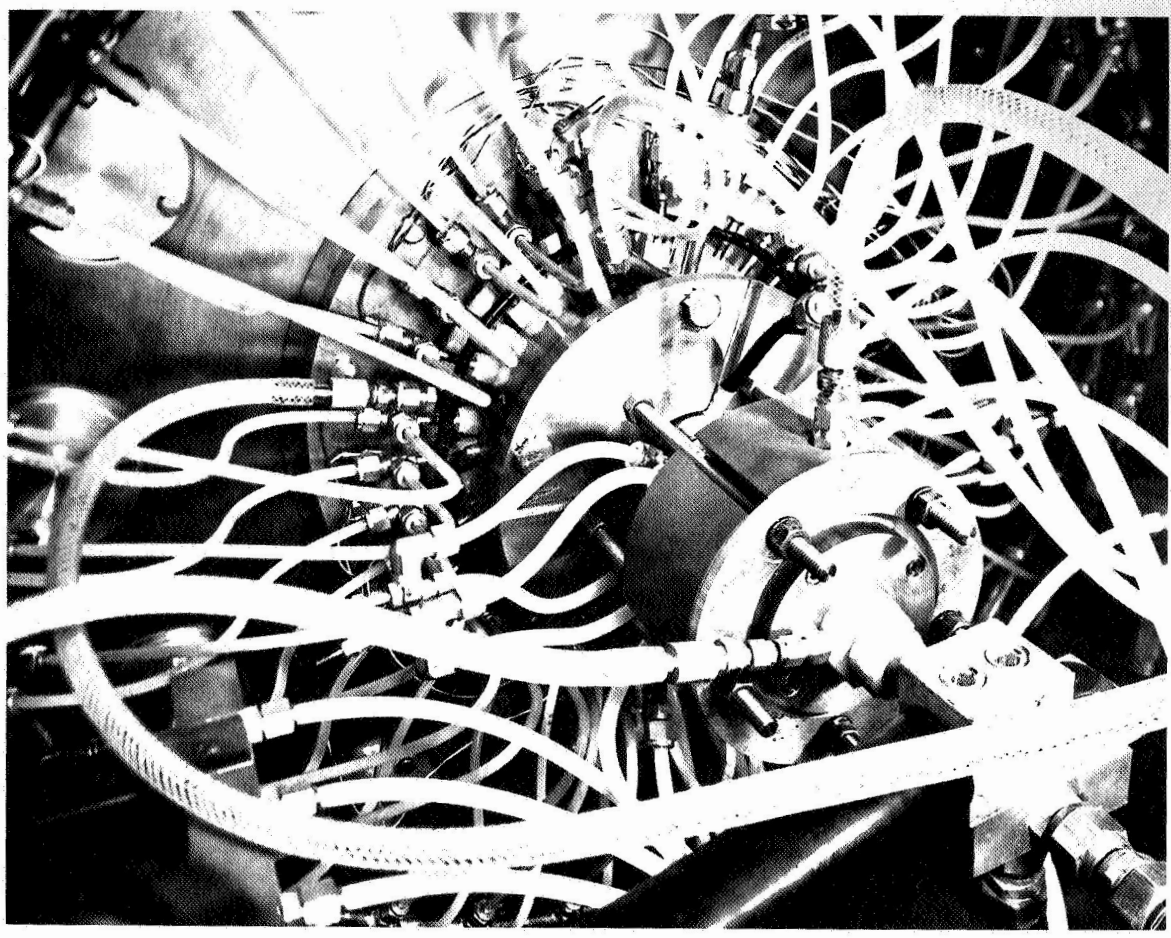

FIG. 4-6 LABORATORY MODEL HEATER (5 SEGMENT CONFIGURATION) INSTALLED

When operating the heater with simulated air, the oxygen was injected into the heater between the fifteenth and sixteenth segment downstream of the cathode. This was found necessary to prevent the oxygen from affecting the tungsten of the cathode.

The test results obtained with the 12.75 inch (32.4 cm) long constrictor configuration of the laboratory model heater are discussed in the following paragraphs.

4.2 Test Results Obtained with the Laboratory Test Heater: Their Correlation and Evaluation

4.2.1 Correlation Between Total Enthalpy, Constrictor Exit Pressure, and Mass Flow Rate for Choked Flow Conditions

The following relations all apply to the constricted-arc heater which exhausts directly into a vacuum tank, without an intervening mixing chamber or "second" nozzle throat. For this case, an analytic correlation between the total enthalpy, the static pressure at the exit of the constrictor, and the total mass-flow rate can be found.

$$\frac{v^* \rho^*}{p^*} = f(h_t) \tag{4-1}$$

If the following assumptions for the condition at the constrictor exit are made:

1. One-dimensional flow, i.e., uniform velocity and enthalpy distribution, no frictional effects
2. "Chemical" (species distribution) and thermodynamic equilibrium
3. Sonic flow conditions

then it is also true that

$$\frac{\dot{M}}{A^* p^*} = \frac{v^* \rho^*}{p^*} \tag{4-2}$$

where $v^* = f(h, p^*)$ = throat (sonic) velocity

$\rho^* = f(h, p^*)$ = throat (sonic) density

and the total enthalpy is

$$h_t = h + \frac{v^{*2}}{2} \tag{4-3}$$

The relation (Eq. 4-1) was verified for both nitrogen and air up to very high temperatures ($\sim 15{,}000^{\circ}K$), by using the equilibrium thermodynamic properties of these gases given respectively in Ref. 5 and Ref. 6. The plots of $\rho^* v^*/p^*$ vs h_t for different pressures (0.1 to 10 atmospheres) fall all on the same curve, with engineering accuracy. The curve for nitrogen is shown in Fig. 4-7. For a very wide range of enthalpies, the mean slope of the mass-flow parameter is -0.52. For a perfect gas it would be constant and -0.50. For such a gas

$$\frac{\rho^* v^*}{p^*} (h_t)^{.5} = \text{constant (for perfect gas)} = \gamma \left\{\frac{\gamma + 1}{\gamma - 1}\right\}^{1/2} \qquad (4\text{-}4a)$$

From the one-dimensional flow calculations using the latest real gas tables for nitrogen (Ref.) it turned out that

$$\frac{\rho^* v^*}{p^*} (h_t)^{.5} = \text{a weak function of } h_t \text{ only (one-dimensional flow, equilibrium nitrogen)} \qquad (4\text{-}4b)$$

At the beginning of the program the curve which accurately represents the simple one-dimensional flow of equilibrium nitrogen (or air) was compared with the available experimental data from a 1/2-inch-diameter constricted arc heater at NASA/Ames Research Center.(*) The Ames experimental data, however, were given in terms of the upstream stagnation pressure, p_o. A measured throat pressure was not available for that heater. From analytical and theoretical consideration, a relation between throat pressure and upstream stagnation pressure was assumed

$$\frac{p^*}{p_o} \approx \text{Constant} \qquad (4\text{-}5)$$

(*) Furnished to this project by C. Shepard and H. Stine (Head), Magnetoplasmadynamics Branch

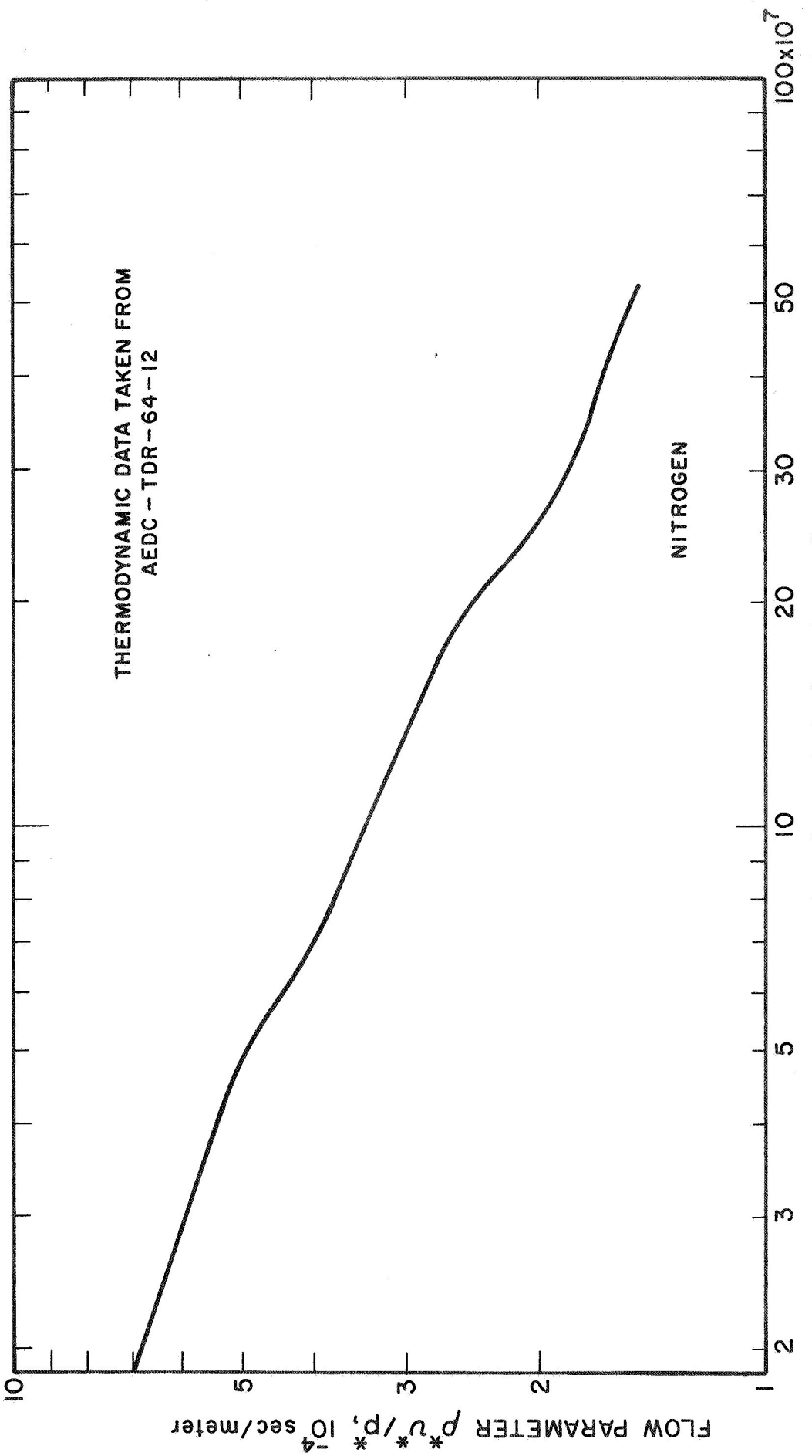

FIG. 4-7 ANALYTICAL CORRELATION BETWEEN CRITICAL FLOW PARAMETER AND THE TOTAL ENTHALPY

Assuming the constant factor to be 0.53, the experimental data were referred to as the calculated throat pressure and correlated with the theoretical curve. The precise value for the ratio between throat pressure and stagnation pressure chosen (within a few percent) was not critical because it was only important to establish that the experimental data follow the theoretical curve. The validity of using a constant for the pressure ratio p^*/p_o was later verified by measurements such as those shown in Fig. 4-8. This correlation shows that the ratio of the measured pressures at the first segment, p_1 (which is slightly lower than p_o), to that of the exit segment p_2, remained constant at a value of 0.49. The important fact is that neither enthalpy, flow rates nor absolute pressure level have any appreciable effect on the sonic throat to inlet pressure ratio of the constrictor, within the regime of interest.

The Shepard mass-flow data were thus converted to

$$h_t = f\left(\frac{1}{0.53}\,\frac{\dot{M}}{p_o A^*}\right),$$

and compared with the one-dimensional analytic values of Fig. 4-7. This comparison is shown in Fig. 4-9. It was found that the mean curve through the converted test data runs parallel. This indicated that the experimental data can be closely approximated by the one-dimensional analytic curve, though a small constant correction factor might have to be applied to bring the experimental data into full agreement with the theoretical curve. This correction factor lumps together all the effects neglected in the simple one-dimensional flow model, i.e., nonuniform enthalpy and velocity distribution, friction (boundary layer), etc. The factor was found for the 1 MW heater, i.e. for the 1.9895 cm diameter constrictor, to be $C_c = 0.9674$; this led to the quasi-theoretical relation

$$\frac{\dot{M}}{C_c A^* p^*} = \frac{\rho^* v^*}{p^*} = f(h_t) \qquad (4\text{-}6)$$

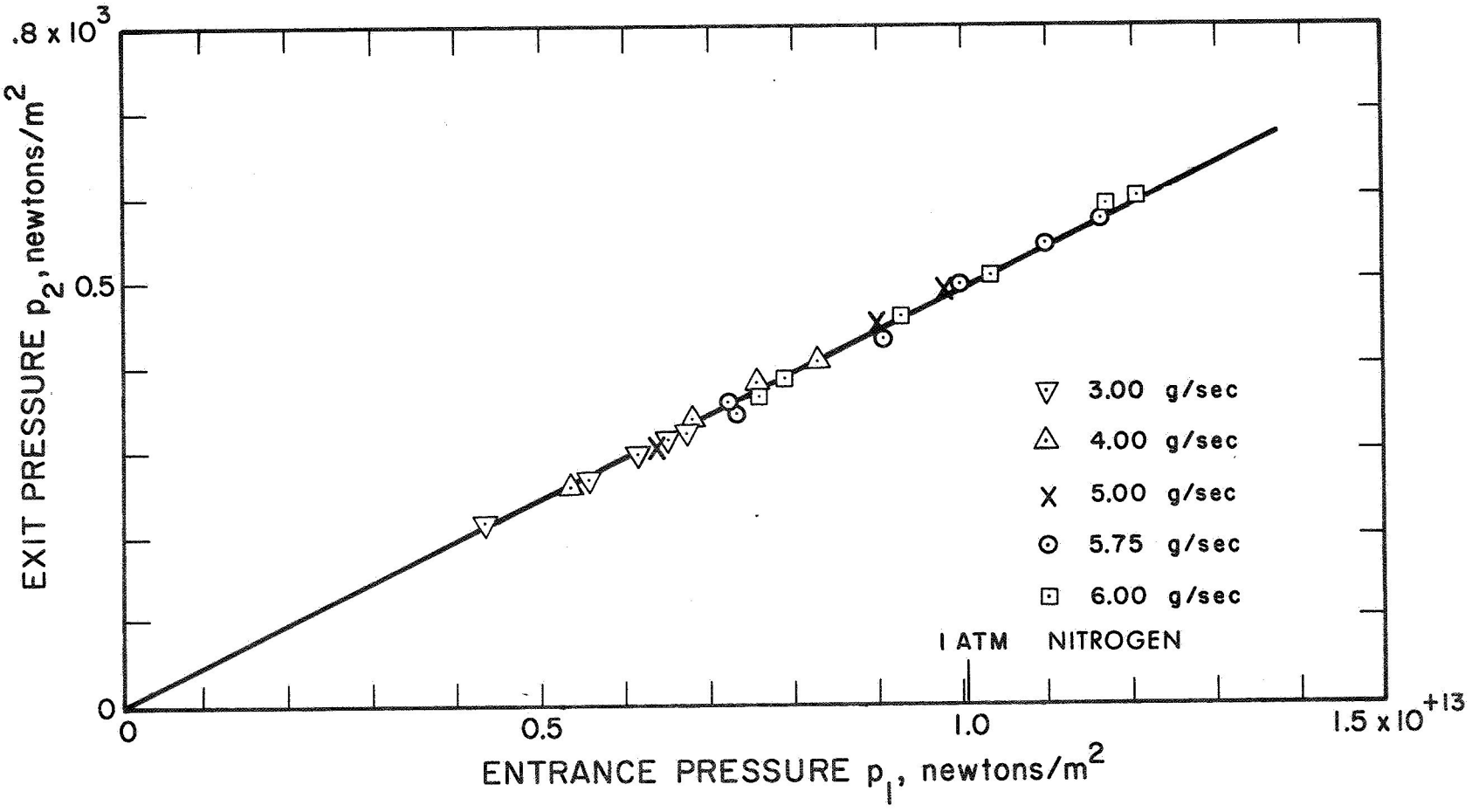

FIG. 4-8 CORRELATION BETWEEN THE PRESSURE AT THE ENTRANCE AND THE PRESSURE AT THE EXIT OF THE 2-cm-DIAMETER CONSTRICTED ARC HEATER FOR FIVE MASS FLOW RATES AND CRITICAL EXIT CONDITIONS

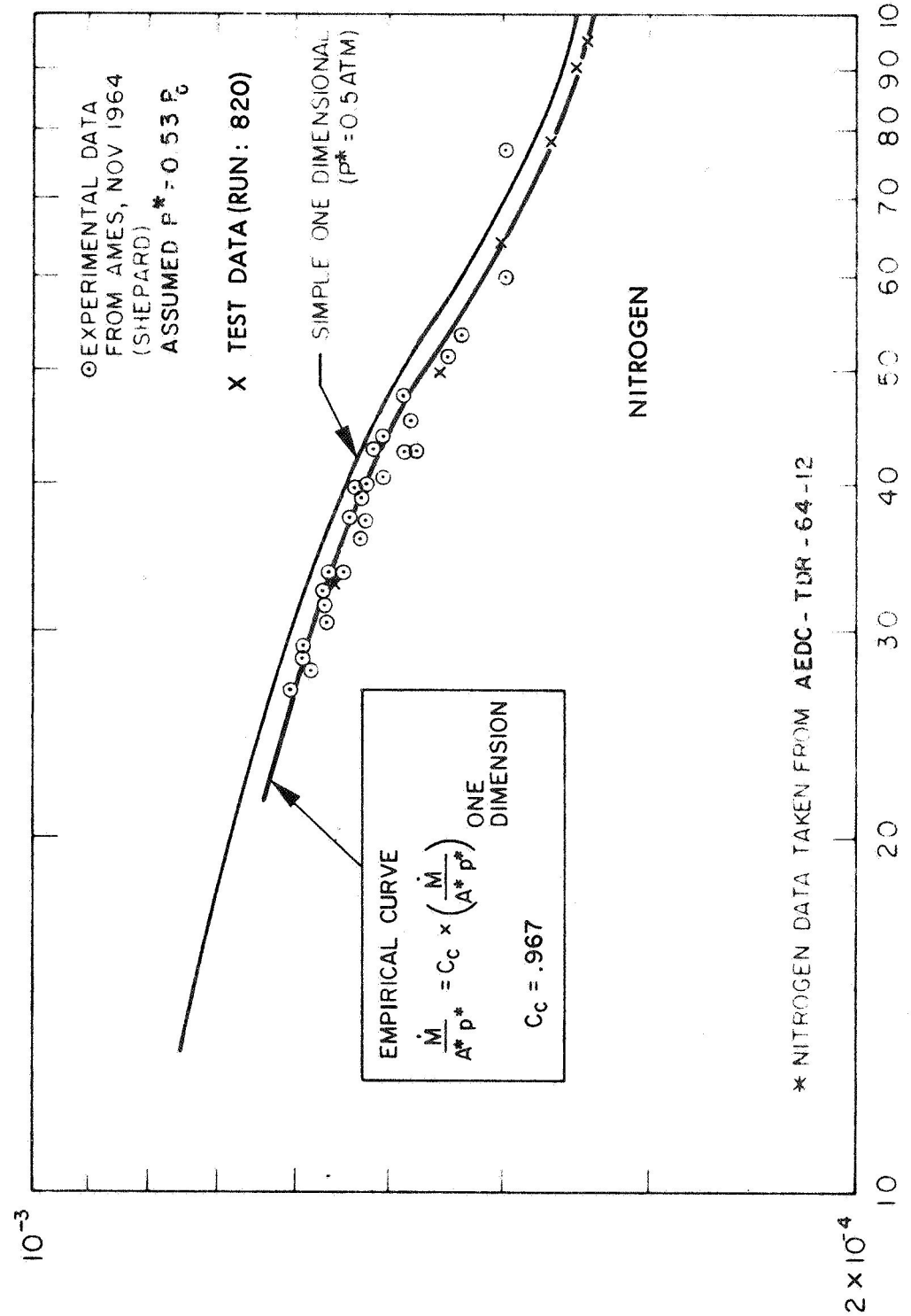

FIG. 4-9 CORRELATION OF THE CHOKED FLOW PARAMETER WITH THE MEAN TOTAL ENTHALPY (NITROGEN)

For larger heaters in which boundary layer effects are smaller and the enthalpy becomes more uniform (higher Reynolds numbers) the correction factor may approach unity.

The thus established mass flow relation (Eq. 4-3) is utilized to construct a heater operating map for a given constrictor size in terms of the same variables. Such a map, for a 2 cm diameter constrictor, is shown in Fig. 4-10.

This map can be used to determine the mass averaged total enthalpy at the throat from the measured throat pressure and mass flow. This is very useful because the enthalpy determined from an energy balance is not always readily available (e.g., for short runs or during a run). In addition, this method furnishes an independent simple check on the total enthalpy obtained by the energy balance. The good consistency between the "throat pressure" enthalpy or "choked flow" enthalpy and the enthalpy determined directly from the energy balance is shown in Fig. 4-11. The scatter is well within the experimental accuracy which was discussed in Section 3.

A map similar to that of Fig. 4-10, but with the power in the gas (instead of the mass flow rate) as a parameter, can easily be drawn. On these maps, the possible operating range for a given heater in terms of maximum pressure versus enthalpy for given gas power can be sketched out.

4.2.2 Electric Parameters

Following is the correlation of arc voltages and currents with the gas dynamic parameters and the constrictor dimensions.

The total voltage of the heater is given by the relation:

$$V_T = \int_0^L E \, dz + V_c + V_a + V_{BR} \qquad (4\text{-}7)$$

where

V_T = total heater potential, (volt)

L = length of arc, (m)

E = electric field, (volt/m)

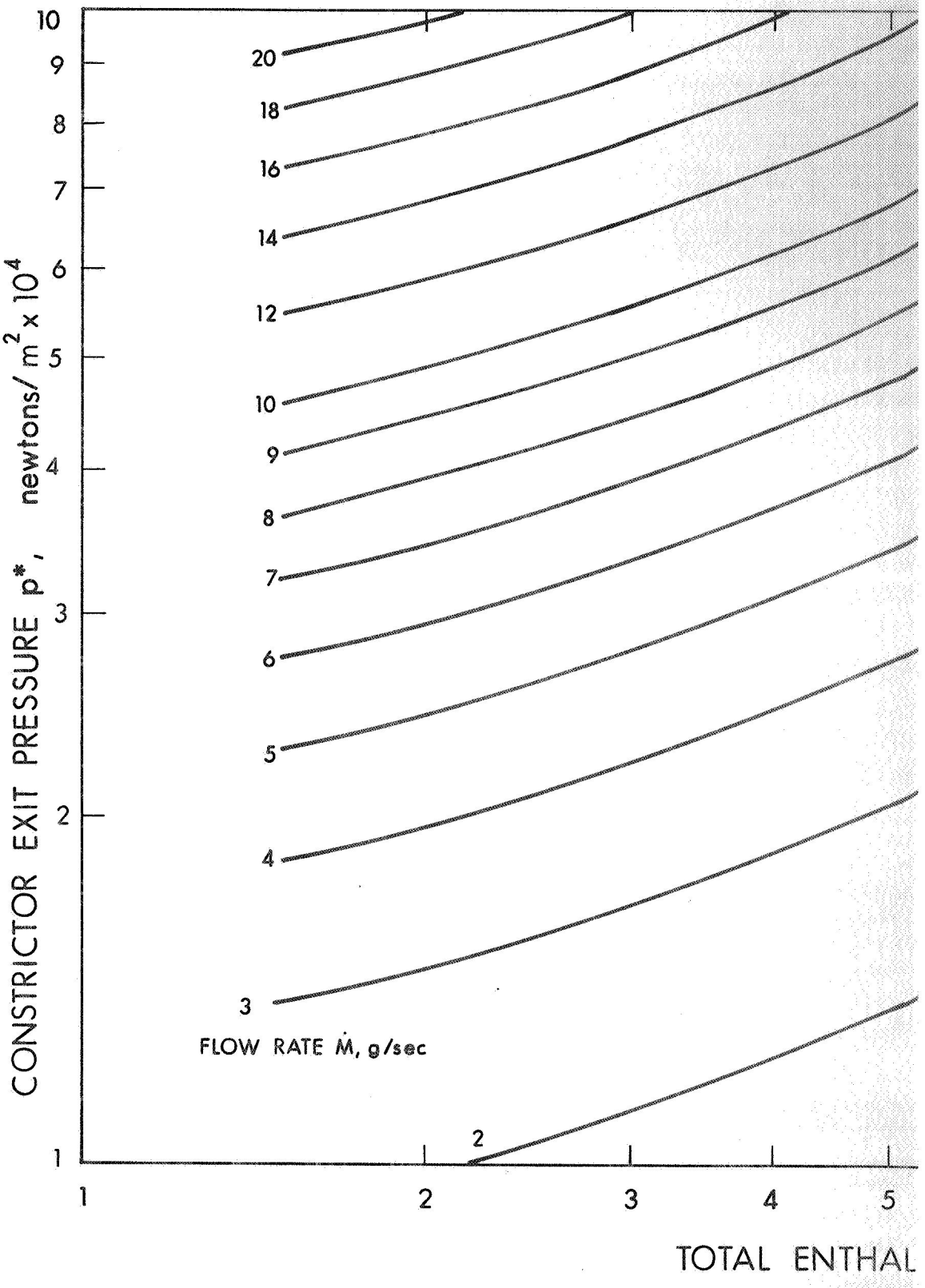

FIG. 4-10 OPERATING MAP FOR A 2-cm-DIAMETER CONSTRICTED ARC JET

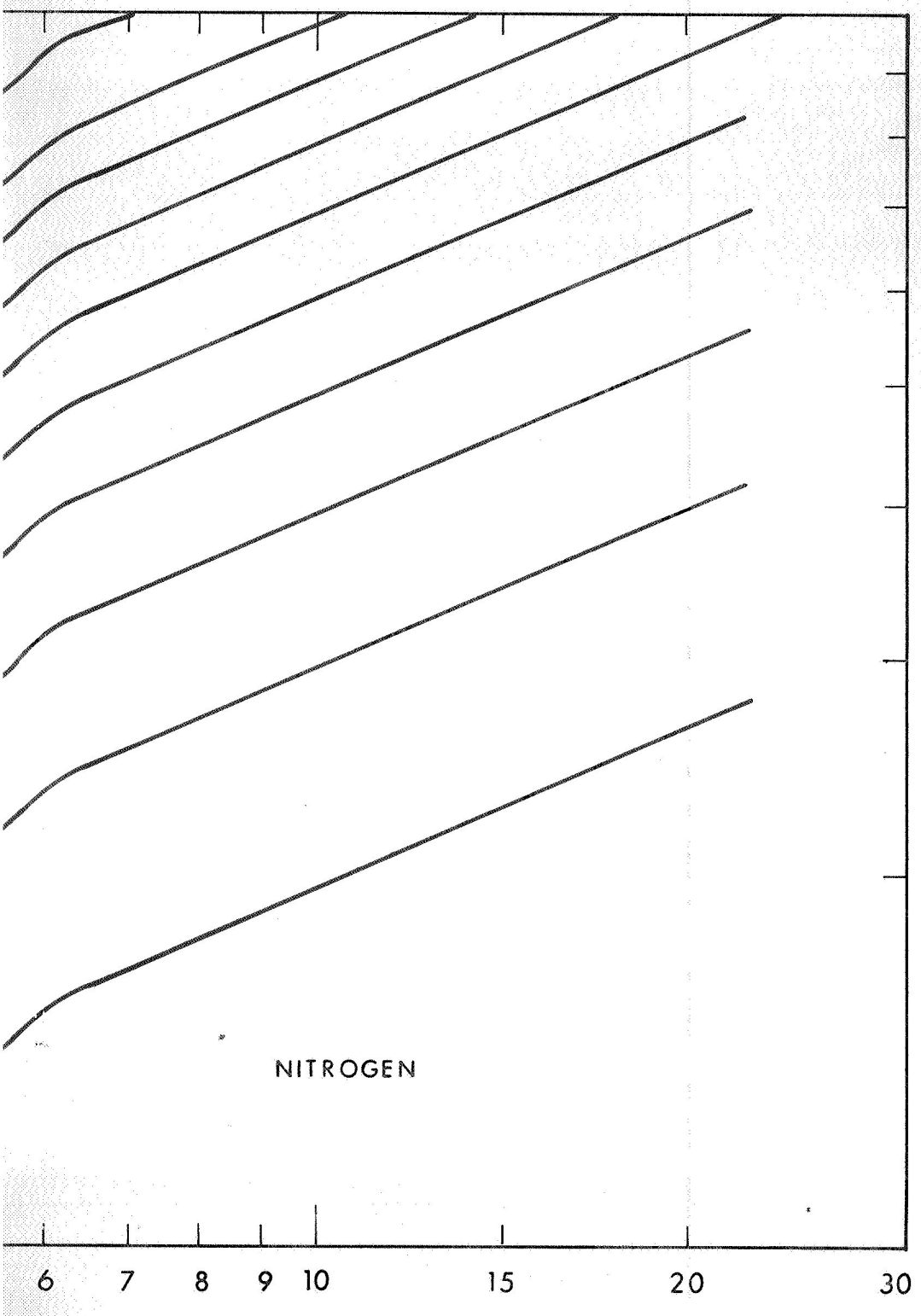

CRITICAL EXIT CONDITIONS

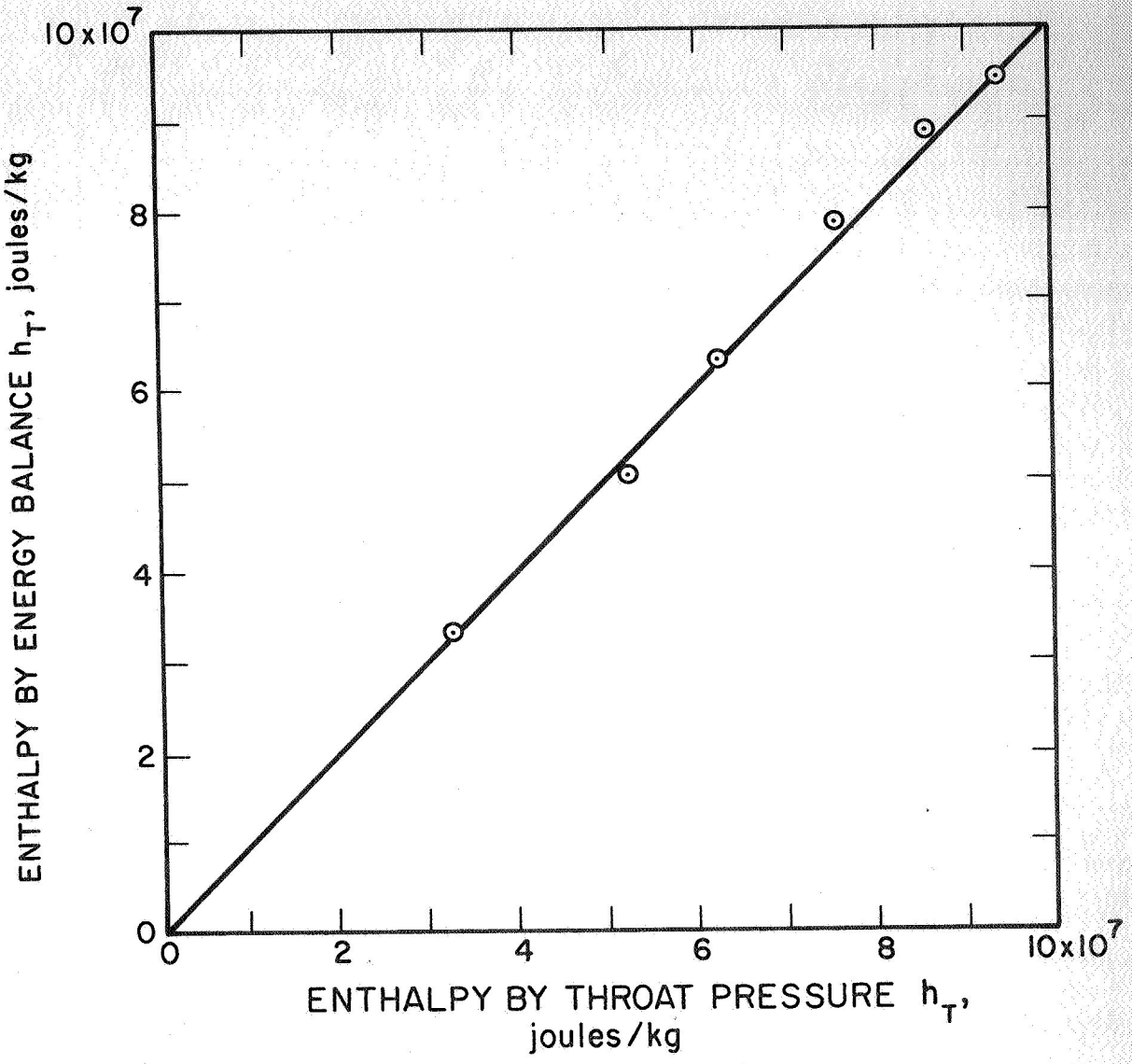

FIG. 4-11 COMPARISON BETWEEN THE ENTHALPY DETERMINED BY ENERGY BALANCE AND THE ENTHALPY DETERMINED BY THROAT PRESSURE MEASUREMENT FOR THE 2-cm-DIAMETER CONSTRICTED ARC HEATER WITH CRITICAL EXIT CONDITIONS

V_c = cathode drop voltage, (volt)

V_a = anode drop voltage, (volt)

V_{BR} = ballast resistor voltage (if applicable),(volt)

z = distance along the constrictor, (m)

and the arc voltage is being considered to be represented by the term

$$V_A = \int_0^L E\, dz = \int_{\text{constrictor}} Edz + \int_{\text{nozzle}} Edz \qquad (4\text{-}8)$$

The latter breakdown is desirable when the design and optimization of the constrictor is discussed.

In Fig. 4-12 the total heater voltage as measured during the tests, is plotted against the current, with mass flow as the parameter. In Fig. 4-13 the arc voltage alone (as defined above) is shown as a function of the arc current and the mass flow rate. The total heater voltage rises more steeply with current than the arc voltage because of the anode ballast resistors. The arc voltage rise with increasing current at constant mass flow is mostly a pressure effect, as will be shown. In Fig. 4-14 the total heater input power is given as a function of the arc current and flow rate. The throat pressure as a function of arc current and flow rate is presented in Fig. 4-15.

In Fig. 4-16 the enthalpy is correlated with the arc current, with constant mass flow values as the parameter. The enthalpy curves have a slope of 1.0 while the pressure curves in Fig. 4-15 have a slope of roughly 0.5.

Gross correlation of all the presented data yields a result of great practical importance and of theoretical significance. The arc voltages were plotted against the throat pressure, first with the enthalpy and then with the arc current as the constant parameter.

618842

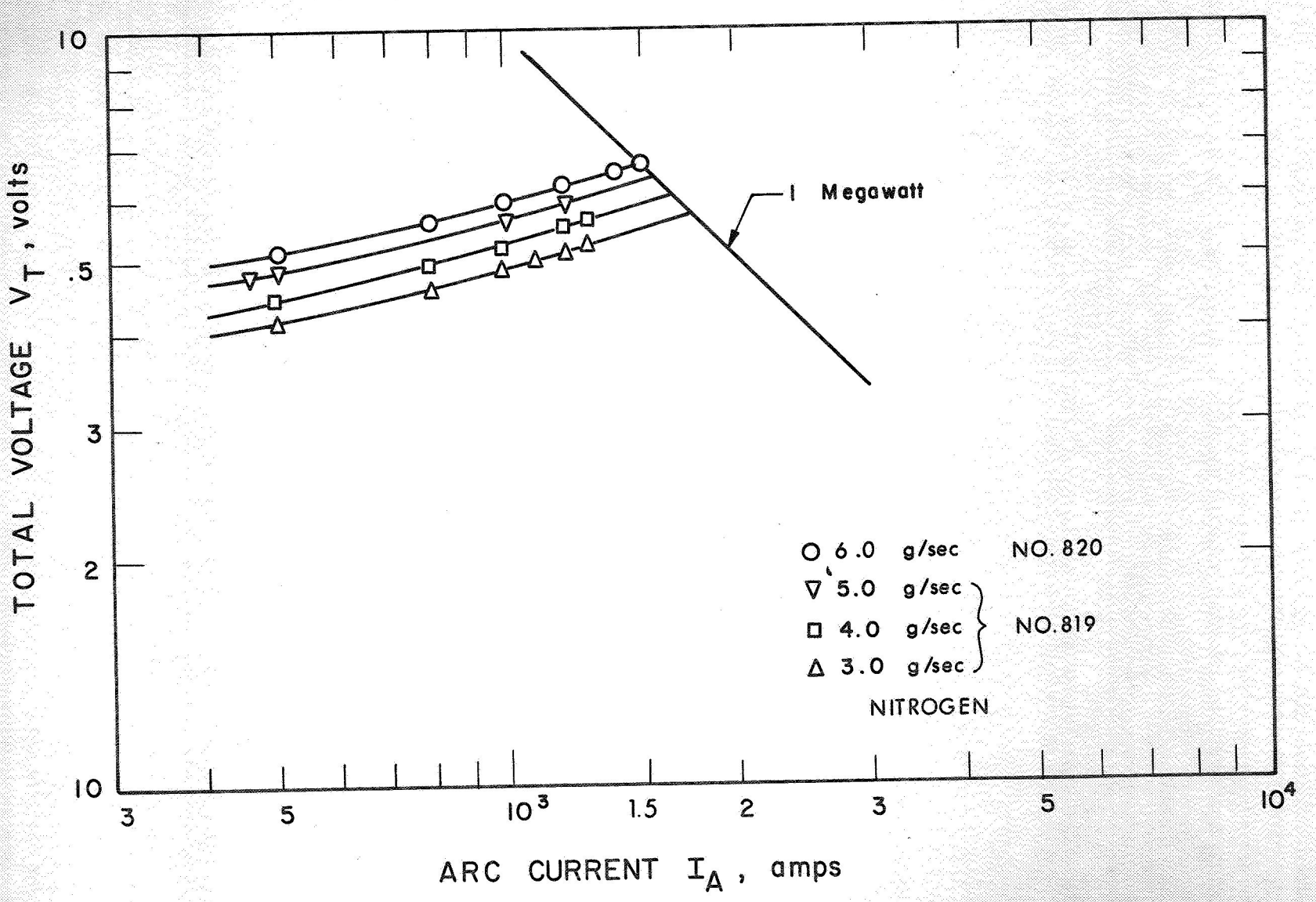

FIG. 4-12 CORRELATION BETWEEN TOTAL VOLTAGE AND ARC CURRENT FOR THE 2-cm-DIAMETER CONSTRICTED ARC HEATER

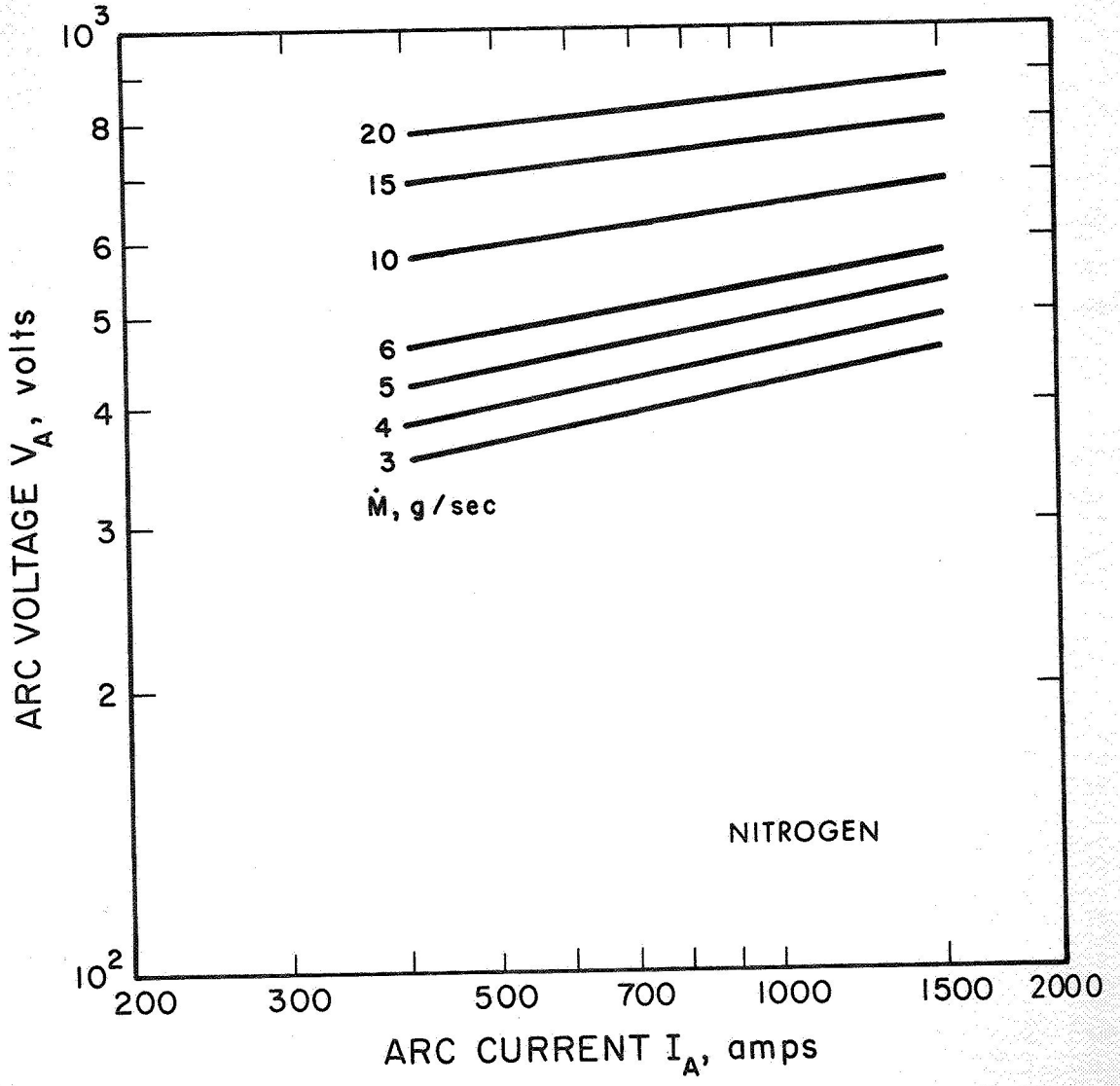

FIG. 4-13 CORRELATION BETWEEN ARC VOLTAGE AND ARC CURRENT FOR THE 2-cm-DIAMETER CONSTRICTED ARC HEATER

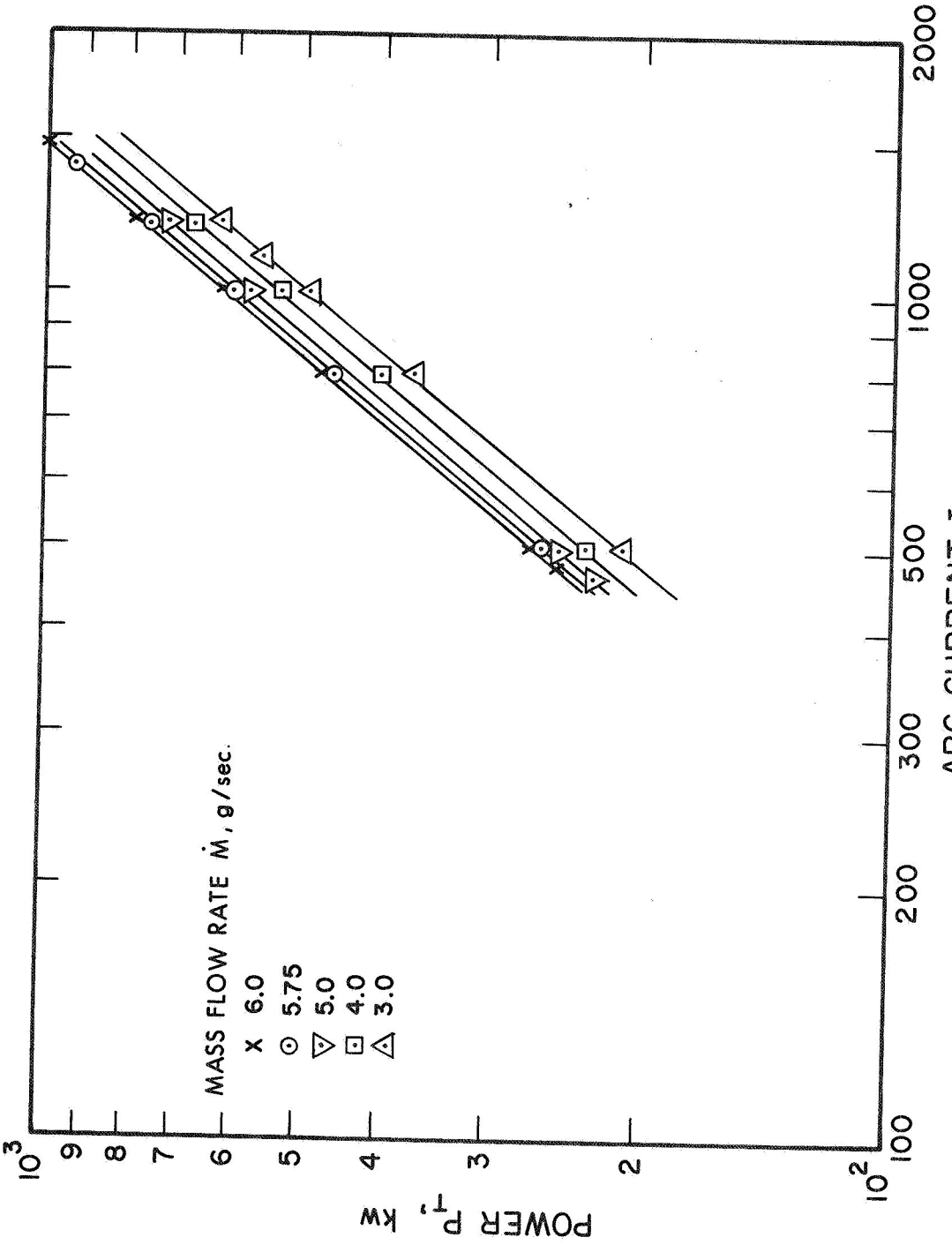

FIG. 4-14 CORRELATION BETWEEN TOTAL POWER AND ARC CURRENT FOR THE 2-cm-DIAMETER CONSTRICTED ARC HEATER

849

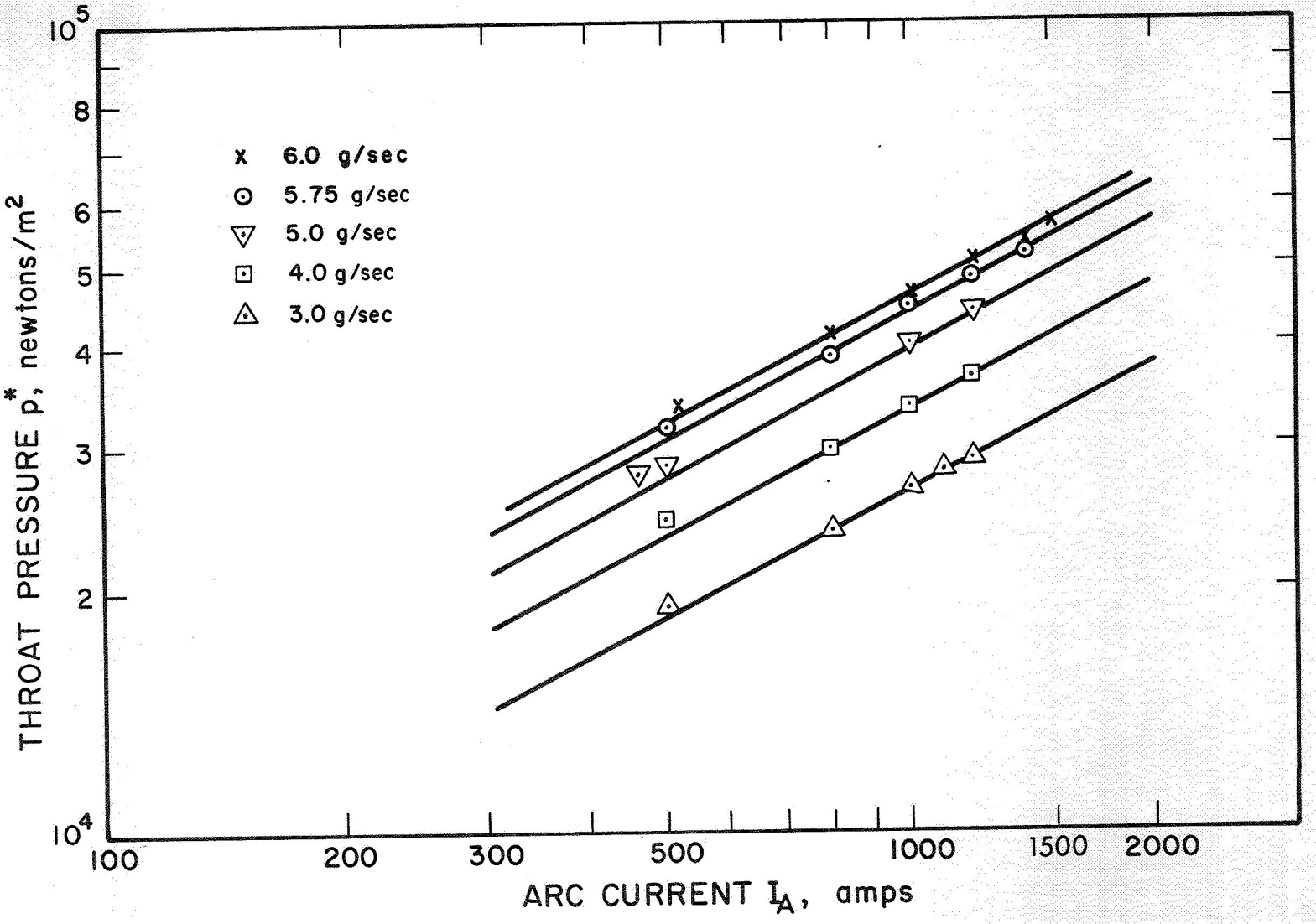

FIG. 4-15 CORRELATION BETWEEN THROAT PRESSURE AND ARC CURRENT FOR THE 2-cm-DIAMETER CONSTRICTED ARC HEATER

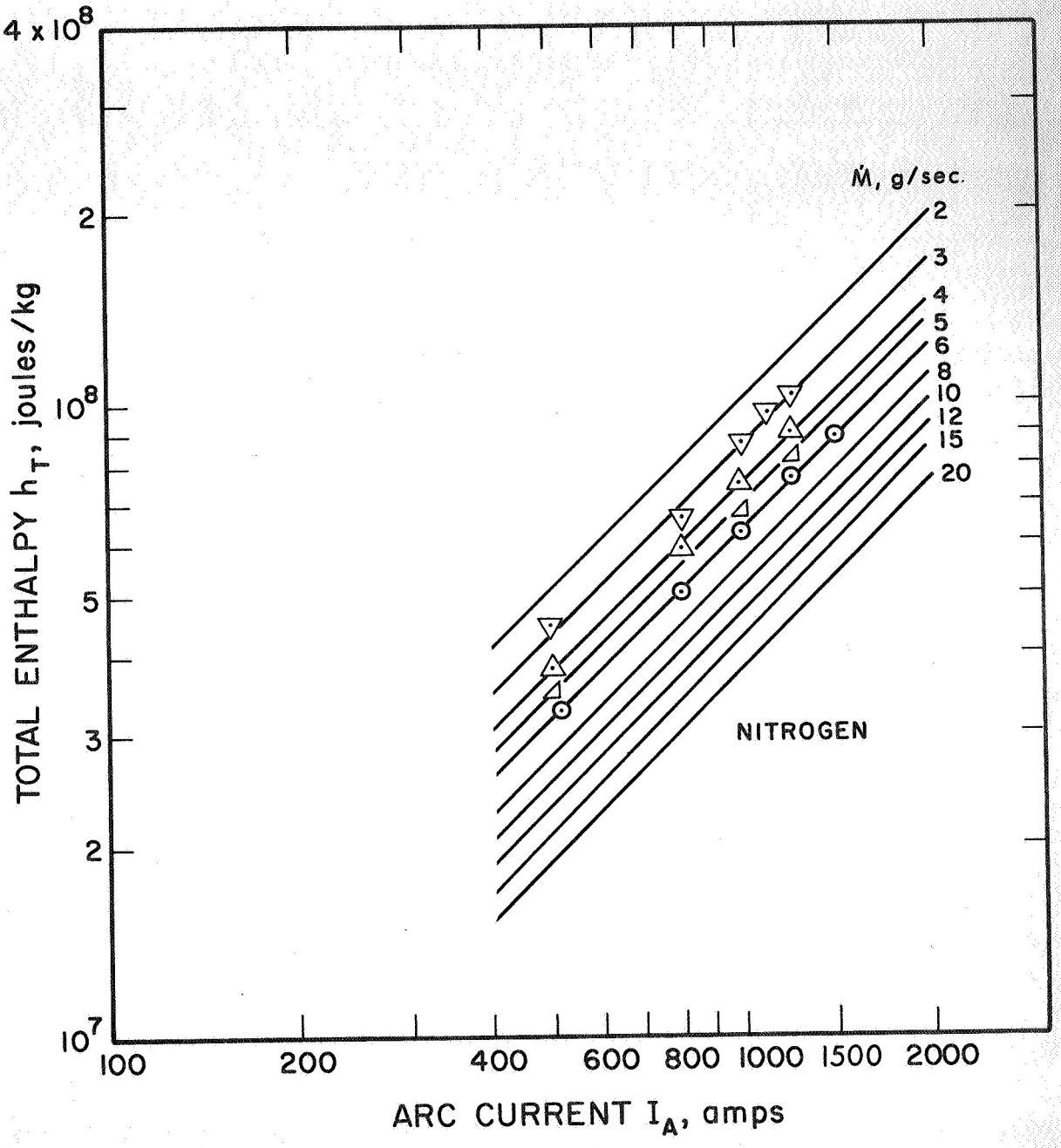

FIG. 4-16 CORRELATION BETWEEN TOTAL ENTHALPY AND ARC CURRENT FOR THE 2-cm-DIAMETER CONSTRICTED ARC HEATER

The very significant result found (Fig. 4-17) is that the voltage is substantially a function only of the pressure, and is nearly independent of all other parameters. This is true within the range of the parameters covered and within the accuracy required for design calculations. This result is expressed by

$$V_A \approx LK_v \left(\frac{p^*}{p_a}\right)^{1/2} \qquad (4\text{-}9)$$

where p_a is atmospheric reference pressure. It is evident that plotting the arc voltage against the inlet pressure would have yielded a similar correlation different only in the constant factor K_v. When different empirical trends are compared they are found to be quite consistent. They can be approximated by the very simple relations:

$$V_A \sim \propto (p^*)^{1/2} \qquad \text{Empirical, Fig. 4-17} \qquad (4\text{-}10a)$$

$$h_t \sim \propto I \dot{M}^{-.42} \qquad \text{Empirical, Fig. 4-16} \qquad (4\text{-}10b)$$

$$p^* \sim \propto I^{1/2} \dot{M}^{1/2} \qquad \text{Empirical, Fig. 4-15} \qquad (4\text{-}10c)$$

Since all pressures along the constrictor are proportional to the throat pressure, we can immediately conclude from the relation 4-9 that the potential gradient, E, along the constrictor must have the same functional dependence on the pressure, namely:

$$E(z) \approx k_E \left(\frac{p(z)}{p_a}\right)^{1/2} \qquad (4\text{-}11)$$

The same pressure dependence can be obtained from the detailed potential gradients along the constrictor of one single operating point. Fig. 4-18 shows the potential and voltage gradients along the constrictor at a current of 1008 A and a mass flow rate of 6 g/sec of nitrogen. The gradients range from ~ 18.8 V/cm near the inlet to ~ 13.6 V/cm near the outlet. The ratio is almost precisely $\sqrt{2}$, i.e., the square root of the pressure ratio. This would indicate that, even in the inlet region of the heater near the cathode, the voltage gradient appears to be largely dependent only on the pressure.

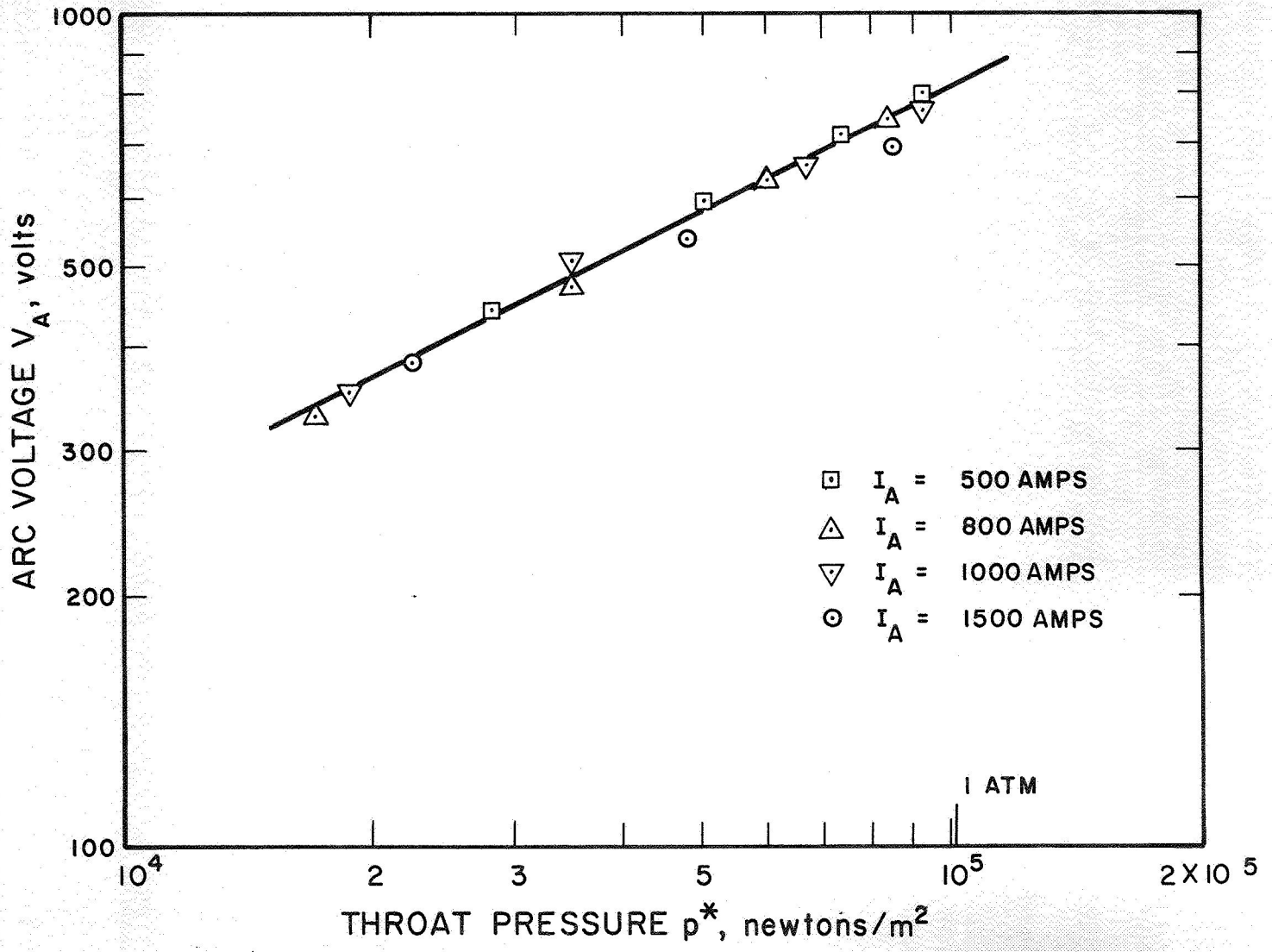

FIG. 4-17 CROSS-CORRELATION OF TEST DATA MEASURED WITH THE 2-cm-DIAMETER CONSTRICTED ARC HEATER

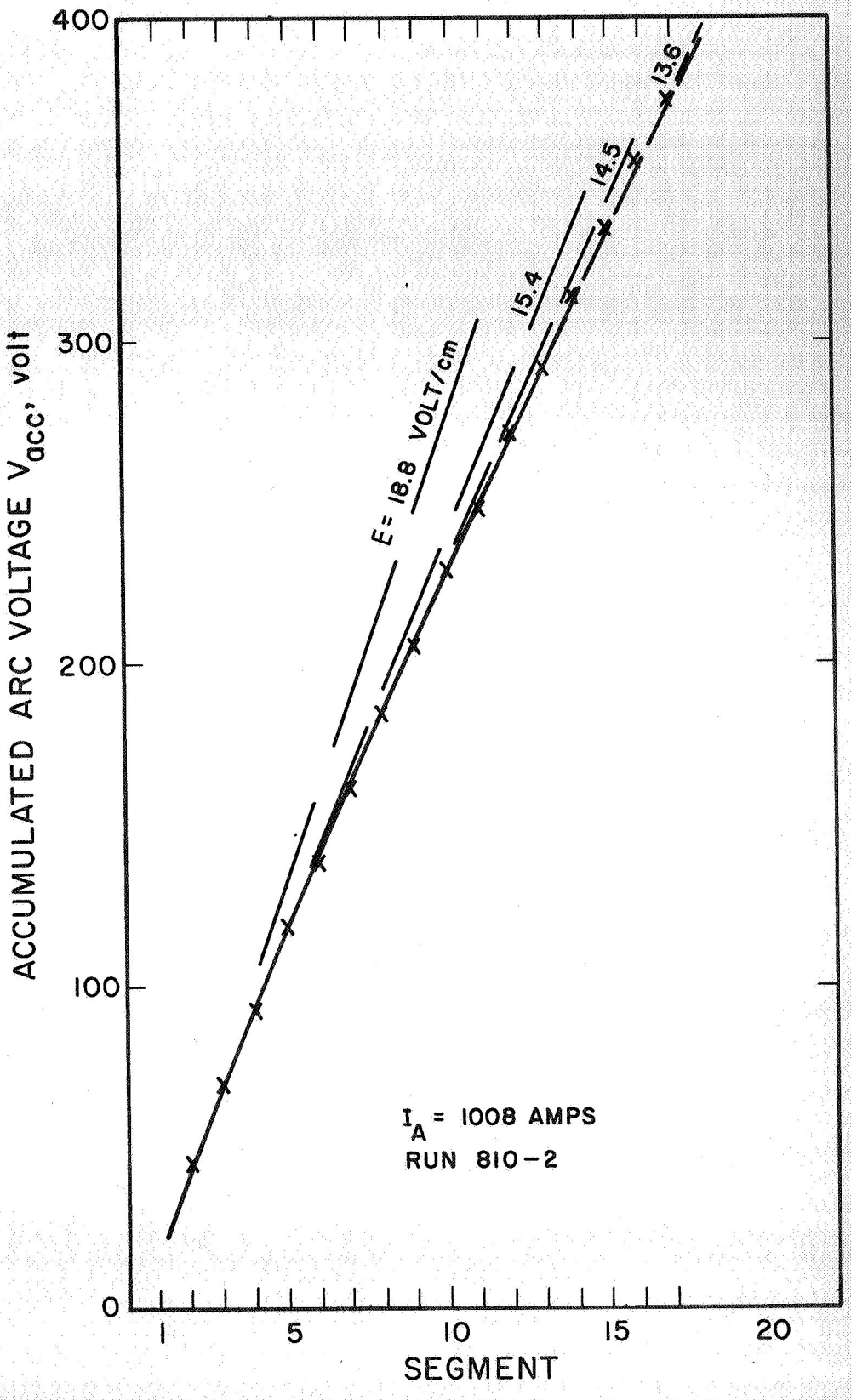

FIG. 4-18 ACCUMULATED ARC VOLTAGE ALONG THE 2-cm-DIAMETER CONSTRICTED ARC HEATER

Measurements along the constrictor, like those of Fig. 4-18, can furnish the constant $k_E = E(p)/(p/p_a)^{1/2}$ directly. This constant can also be obtained from the relation between arc voltage and pressure as shown in Fig. 4-17. Because of the almost linear pressure drop along the constrictor, one can write

$$\frac{p(z)}{p^*} = 2 - \frac{z}{L} \tag{4-12}$$

Then the relation between measured arc voltage and throat pressure is

$$V_A = \int_o^L E(z)\, dz = \int_o^L k_E \left(\frac{p}{p_a}\right)^{1/2}(z)\, dz \tag{4-13}$$

Inserting Eq. 4-12 into Eq. 4-13 and setting $z/L = z'$,

$$V_A = k_E \left(\frac{p^*}{p_a}\right)^{1/2} L \int_o^1 (2-z')^{1/2} dz' \tag{4-14}$$

one finds

$$k_E = 0.807 \frac{V_A}{L} \left(\frac{p_a}{p^*}\right)^{1/2} \quad [V/m] \tag{4-15}$$

From the correlation of the test results, the constants k_E and K_v (Eq. 4-6) were found to be

$$k_E = 1.804 \times 10^3 \quad [V/m]$$

$$K_v = k_E/0.807 = 2.235 \times 10^3 \quad [V/m]$$

4.2.3 Energy Transfer to the Constrictor Wall

In large arc heaters, a most difficult quantity to comprehend analytically and to predict with any accuracy is the heat transfer to the constrictor wall. Yet, this quantity is critical for the prediction of the two essential performance criteria, the heater efficiency, and enthalpy-pressure performance envelope which is feasible with an allowable wall heat load.

The complete energy transfer to the constrictor wall depends on a large number of parameters and conditions. Some of the more important ones are the gas temperature profile across the constrictor, the radiant emission and self absorption properties of all gas layers, the reflectivity, reactivity, roughness of the constrictor wall surface, the magnitude of turbulent energy and mass transport (reacting species), the heat conduction and molecular recombination near the wall, and the symmetry and stability of the discharge as well as the flow. None of these can be reliably predicted yet by analytical means alone.

For the 1.9845 cm diameter constrictor, radiation appears to dominate the energy transfer to the constrictor wall, but conduction and turbulent convection still contribute a relatively important part of the total heat transfer, especially near the constrictor outlet. The combined test results of the laboratory model heater and the small arc column (Appendix A) indicate the maximum convection heat transfer in the laboratory model heater to be approximately 10 percent. The numerical computer calculations by Watson, which assume purely laminar flow, still predicted about half of the heat transfer near the outlet to come from conduction (Appendix B). Unfortunately, the energy transfer rates produced by these computer calculations neither agree in magnitude nor in axial distribution with those measured in the 2 cm diameter constricted arc heater. We are therefore forced to rely to a large extent upon purely empirical correlations at this stage.

The important empirical result was that at the higher currents the heat losses to the constrictor wall depend substantially only on the current. This correlation is shown in Fig. 4-19, for the whole constrictor as well as for a group of 3 individual segments. These test results suggest an energy transfer dependency for the 2 cm diameter heater with current of the form

$$\dot{Q}_L \approx K_L I^n \qquad (4\text{-}16)$$

where $n \sim 1.62$.

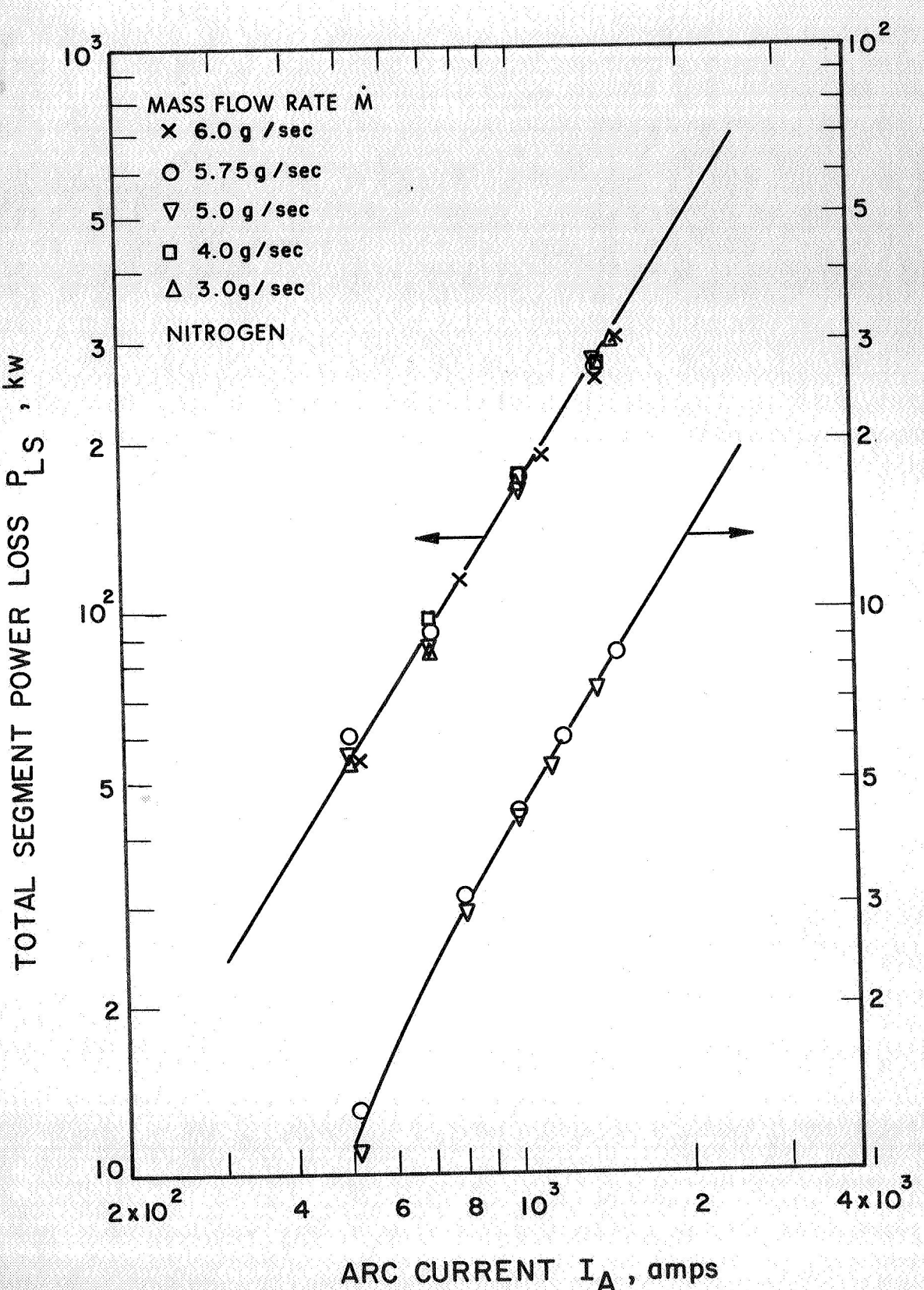

FIG. 4-19 CORRELATION OF ENERGY TRANSFER TO CONSTRICTOR WALL FOR THE 2-cm-DIAMETER CONSTRICTED ARC HEATER

73618853

Thus, whatever effect pressure, mass flow, and enthalpy have on the energy transfer to the wall, these effects seem to appear only in such a combination as to be proportional to a simple power of the current, at least for a given arc constrictor which operates with choked outlet flow.

Relation 4-16 was derived from test results that produced the heat load distribution along the constrictor for different currents. This is shown in Fig. 4-20. The heat load distributions for all current levels are rather flat. The correlation of the wall heat loss with the enthalpy alone, which was fairly good for the small 1/2 cm research cascade (see Appendix A), fails here, as is shown in Fig. 4-21. Such a correlation would be typical for a strongly conduction-governed or convection-governed energy transfer process.

The experimental wall heat loads on the 1.984 cm diameter constrictor are seen (Fig. 4-20) to be moderate. Typically, they are $\sim$ 1.3 to 1.4 kW/cm^2 for the 1500 amps arc current, and proportionately lower at lower currents. These heat loads are based on the entire constrictor wall including the boron nitride surface area.

4.2.4 Heater Efficiency

With the empirical correlations which were found for the electric field and the energy transfer to the constrictor wall, it is now possible to arrive at a correlation between the operating parameters of the heater and the efficiency.

The total electric power consumed in the constricted arc heater is

$$P_T = I \left\{ \int_0^L E \, dz + V_a + V_c + R_B \, I \right\} \qquad (4\text{-}17)$$

Inserting now the relation for the arc voltage from Eq. 4-15, solved for V_A,

$$V_A = \int_0^L E \, dz = 1.239 \times L \, k_E \left(\frac{p^*}{p_a}\right)^{1/2} \qquad (4\text{-}18)$$

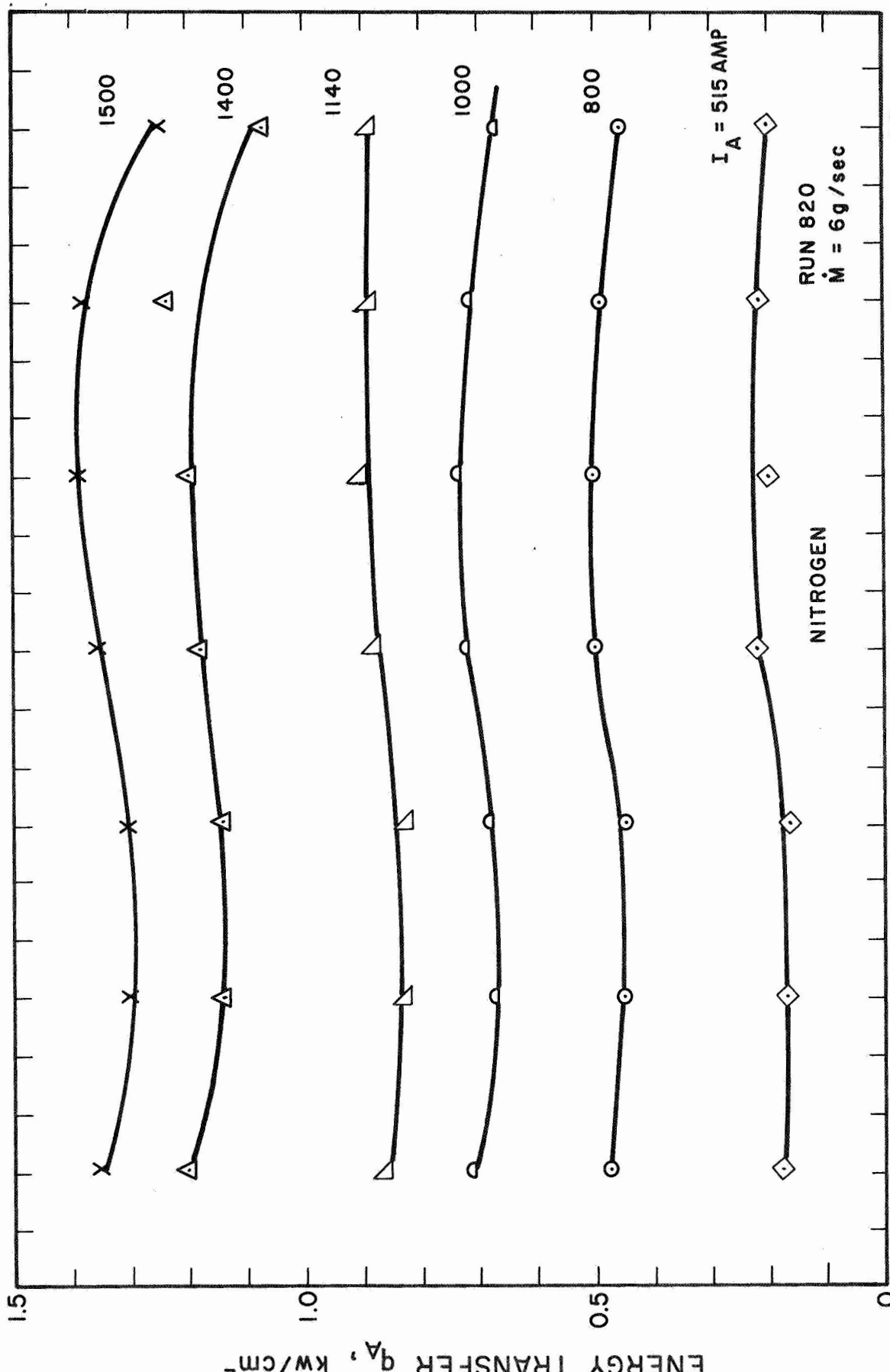

FIG. 4-20 ENERGY TRANSFER TO CONSTRICTOR WALL OF THE 2-cm-DIAMETER CONSTRICTED ARC HEATER

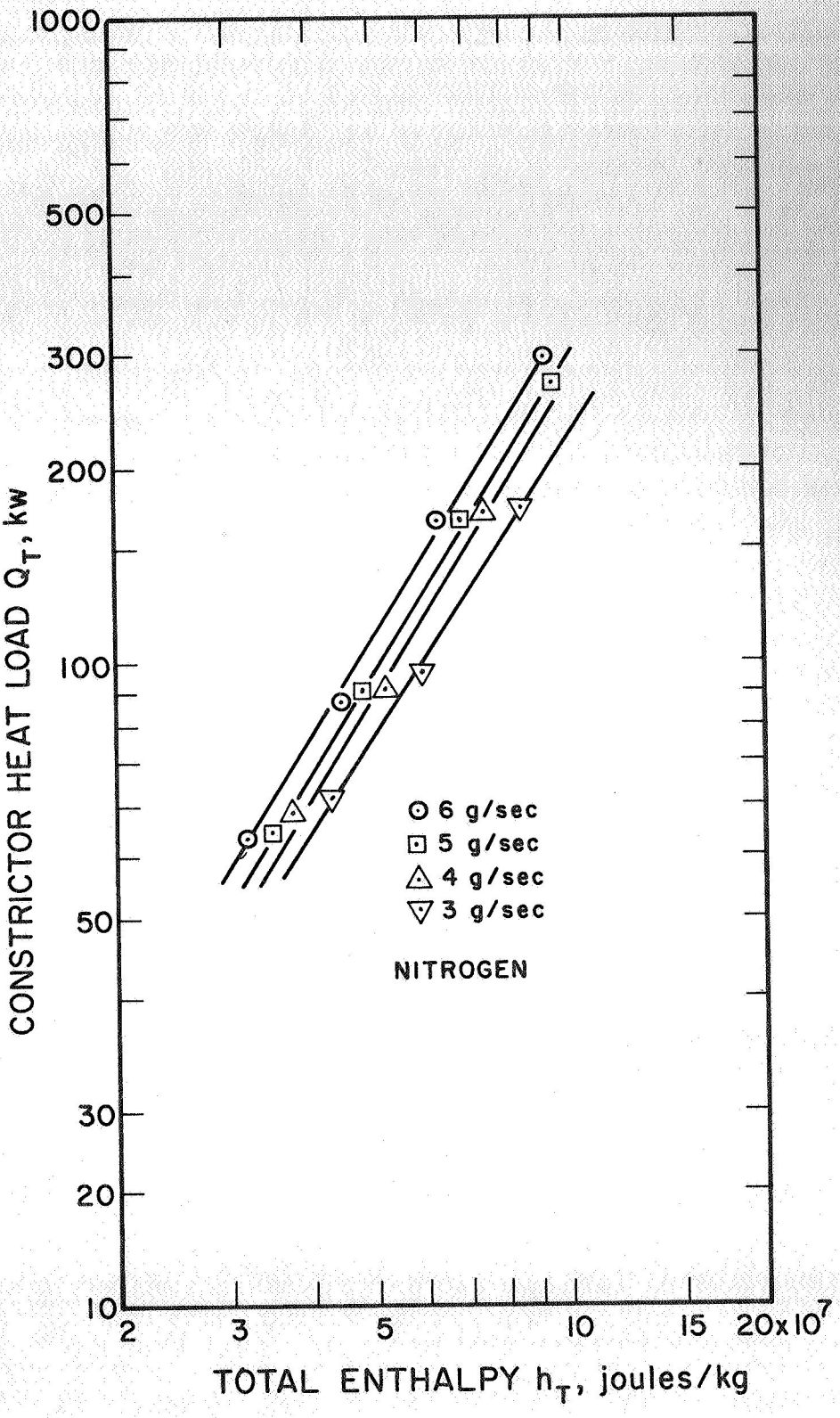

FIG. 4-21 TOTAL POWER LOSS TO THE CONSTRICTOR WALL OF THE 2-cm-DIAMETER CONSTRICTED ARC HEATER

The total power is then

$$P_T = I \left(1.239 \times L\, k_E \left(\frac{p^*}{p_a}\right)^{1/2} + V_A + V_C + R_B\, I\right) \qquad (4\text{-}19)$$

The power in the gas is the difference between the total electric power and the total loss. The total loss is comprised of the electrode losses due to the electrode voltage drop, $I\,(V_a + V_c)$; the power into the ballast resistance, $R_B I^2$; and the energy transfer to the constrictor wall, which was found to be $LK_L I^n$. The efficiency of the heater is, therefore,

$$\eta = \frac{P_T - P_L}{P_T}$$

$$= 1 - \frac{L\, K_L\, I^{n-1} + (V_a + V_c + R_B I)}{1.239 \times L\, k_E \left(\frac{p^*}{p_a}\right)^{1/2} + (V_a + V_c + R_B I)} \qquad (4\text{-}20)$$

From Eq. 4-20 one can recognize the dependency of the efficiency on the arc current. This agrees with the test results, which are shown in Fig. 4-22 and Fig. 4-23 as measured.

The semi-empirical equation (Eq. 4-20) and the test results show that the efficiency decreases with increasing current (at fixed p*), and increases with increasing throat pressure (or mass flow) at fixed current. This is shown in Fig. 4-24 which is a cross plot of data presented in previous figures.

4.2.5 Testing with Simulated Air

The laboratory model heater was also tested with simulated air. Some deviation from the correlations which were presented for nitrogen were found. The main reason for these variations lies in the change of the pressure distribution along the length of the constrictor. This change is due to the injection of 20 percent of the total gas flow approximately 2/3 of the constrictor length downstream of the cathode. This becomes apparent from the difference in the pressure relation between the upstream pressure p_1 and the downstream pressure p_2 as shown in Fig. 4-25. The total voltage-arc current relation for the tests with simulated air is shown in Fig. 4-26.

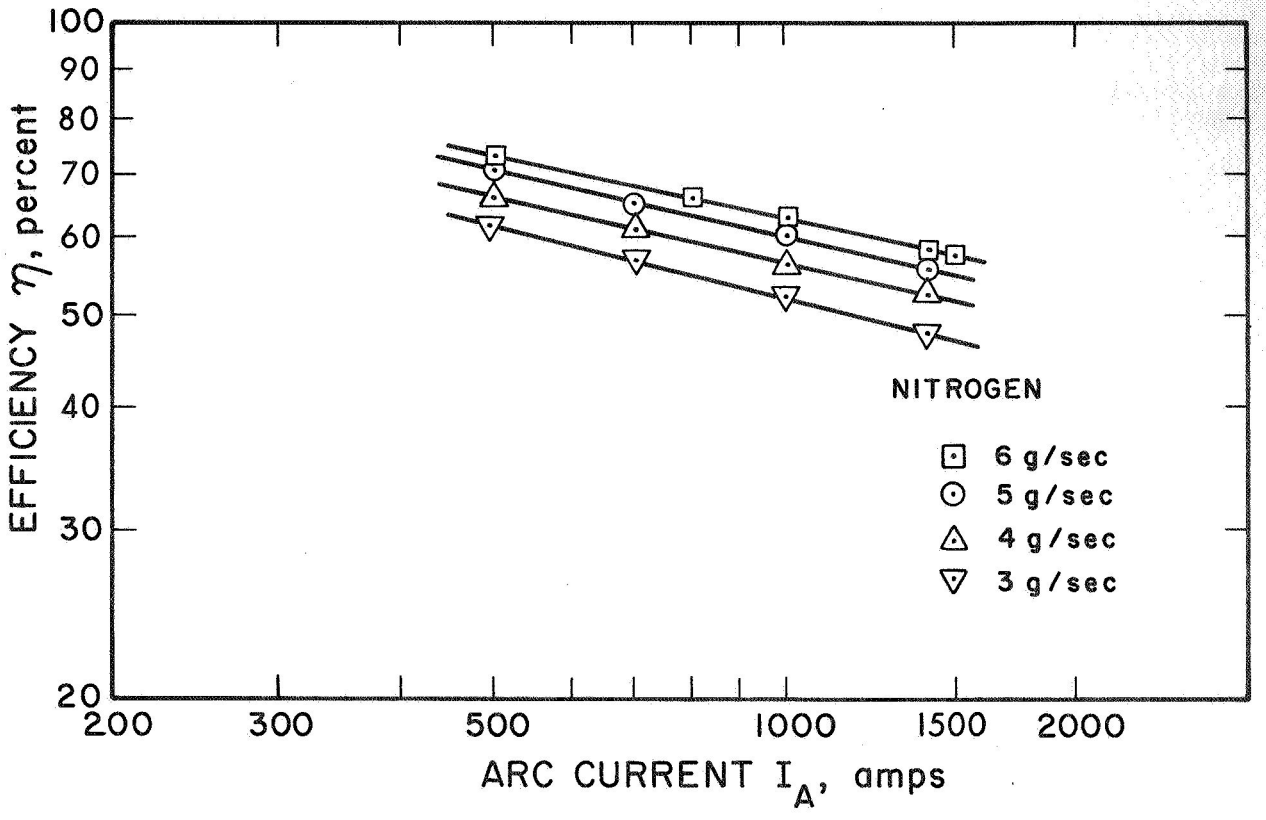

FIG. 4-22 EFFICIENCY OF THE 2-cm-DIAMETER CONSTRICTED ARC HEATER AS A FUNCTION OF ARC CURRENT AND MASS FLOW RATE

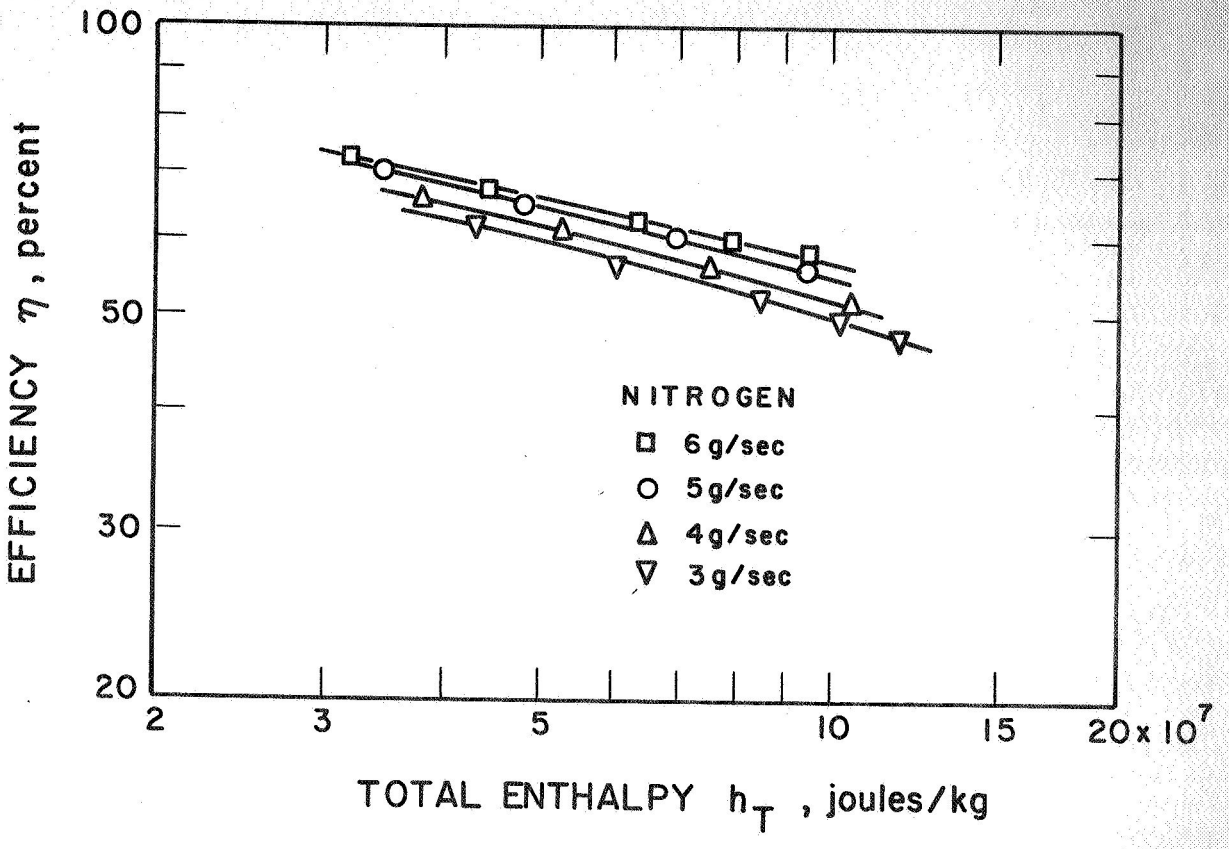

FIG. 4-23 EFFICIENCY OF THE 2-cm-DIAMETER CONSTRICTED ARC HEATER AS A FUNCTION OF TOTAL ENTHALPY AND MASS FLOW RATE

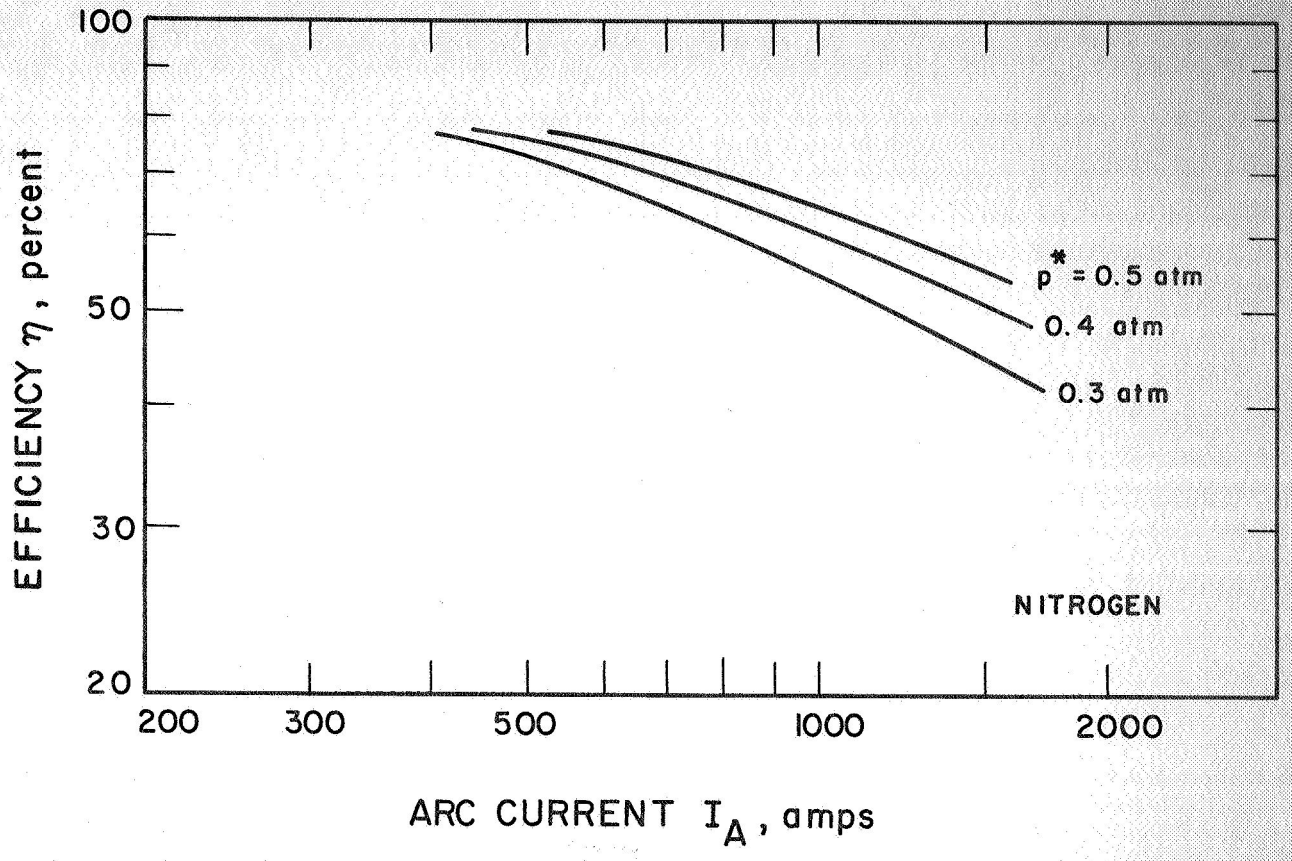

FIG. 4-24 EFFICIENCY OF THE 2-cm-DIAMETER CONSTRICTED ARC HEATER AS A FUNCTION OF ARC CURRENT AND THROAT PRESSURE

73618857

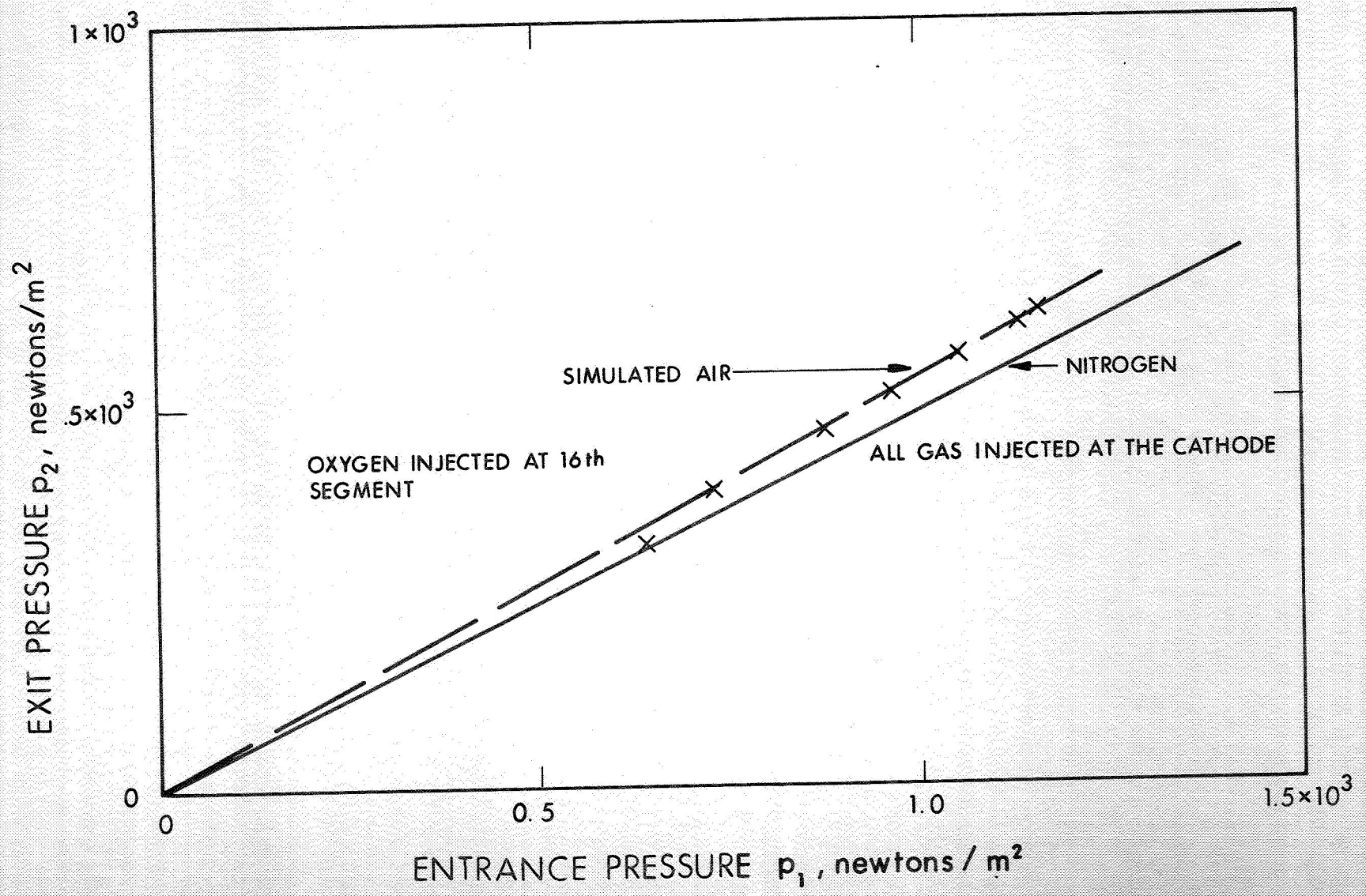

FIG. 4-25 CORRELATION BETWEEN ENTRANCE PRESSURE AND EXIT PRESSURE OF THE 2-cm-DIAMETER CONSTRICTED ARC HEATER OPERATING WITH SIMULATED AIR AT CHOKED EXIT CONDITIONS

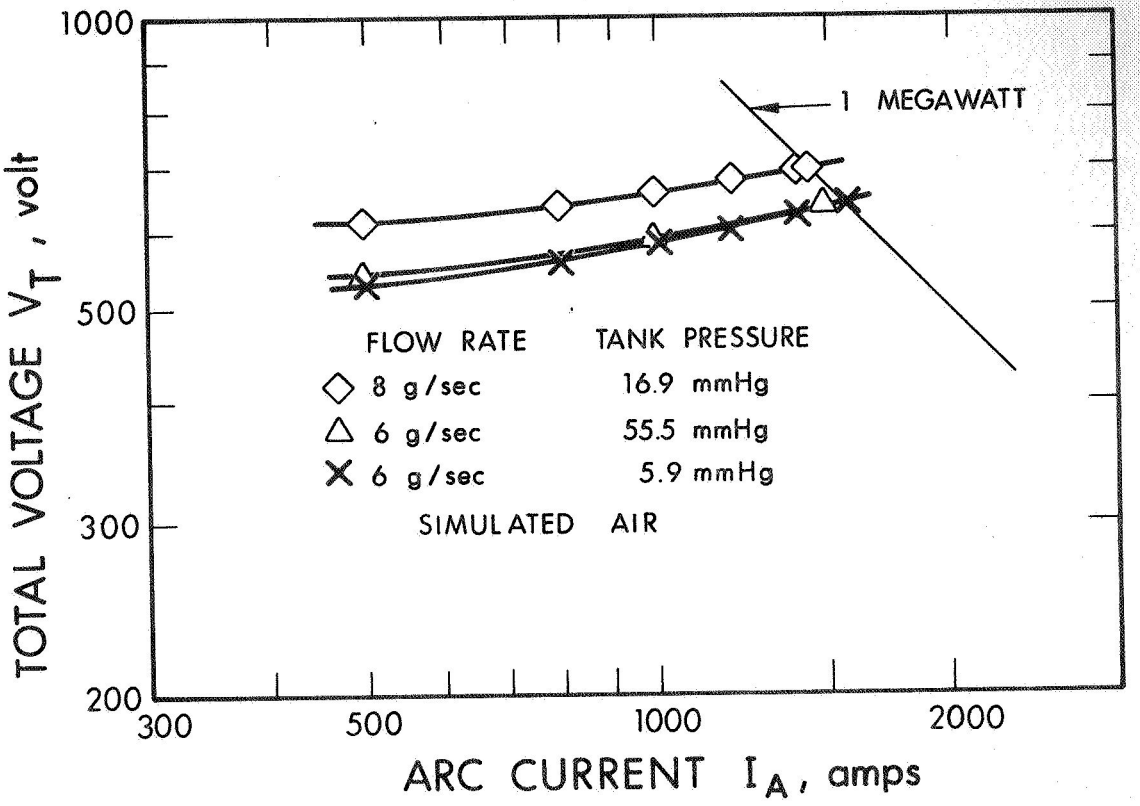

FIG. 4-26 TOTAL VOLTAGE-ARC CURRENT RELATION FOR SIMULATED AIR

5. ONE MEGAWATT MATERIALS TEST HEATER (Materials Test Heater, Model HE-1MW)

5.1 Materials Test Heater, Model HE-1MW, Design

After testing of the laboratory model heater had confirmed all basic design details for the 1-megawatt constricted-arc heater, the Materials Test Heater, Model HE-1MW, was designed. The design of the Materials Test Heater incorporates several improvements which were developed as a result of experience gained with the laboratory model heater. The design also provides for the final installation of the heater at the NASA test facility of the Manned Spacecraft Center in Houston.

A special aluminum support structure was designed, in which the heater itself is mounted. This structure contains the four water manifolds (two inlet manifolds and two outlet manifolds), from which all heater cooling water circuits are supplied. The support structure makes the heater a self-contained unit to which only the electric power and the main water lines have to be attached.

Another feature of the Materials Test Heater design is the segmentation of the heater into two distinct assemblies which can be assembled and disassembled independently of each other. The nozzle and anode assembly is assembled on the front plate of the support structure while the constrictor assembly can be bench-assembled and then mated with the nozzle and anode assembly. The constrictor assembly contains the tungsten cathode, the main and auxiliary gas inlets, the water-cooled copper contrictor column segments, and associated hardware. The nozzle and anode assembly contains the 30 copper anode pin assemblies and the nozzle segments, and provides the mounting plate for installation of the heater on the vacuum test chamber. The complete design of the heater is shown in the assembly

drawing, Fig. 5-1. The assembled heater is shown in Figs. 5-2 and 5-3. An exploded view of the constrictor and nozzle sections is shown in Fig. 5-4.

The Materials Test Heater is shown schematically in Fig. 5-5. The heater is designed for a cooling water supply of 500 psig at a flow rate of 140 gpm, and an inlet temperature of less than 100°F. The water is chemically treated to prevent scaling of the component coolant passages. Coolant flow is provided from the inlet manifolds for the housing cooling segment, the constrictor column and nozzle segments, the cathode, the anode manifold rings, and the mounting plate.

The main gas flow of nonoxidizing or inert gas is introduced into the constrictor section through inlets located a short distance downstream of the cathode. If it is necessary to simulate air, or to otherwise provide oxidizing gases, such gases are introduced into the constrictor through the sixteenth constrictor segment located approximately 10-inches downstream of the cathode. The downstream location of the auxiliary inlets prevents erosion of the tungsten cathode by oxygen or other oxidizing gases. All gases enter the constrictor tangentially at low velocities.

Argon gas is supplied to a plenum in the anode pins support ring from where it flows around each of the 30 anode pins to protect the pins from highly concentrated arc attachment and the affects of oxidizing gases.

Electrical power and coolant requirements, and other operating requirements and characteristics of the heater are given in the following Table 5-1.

5.2 Materials Test Heater, Model HE-1MW, Operation

The operation of the Materials Test Heater is the same as that of the laboratory test heater. The arc is initiated by a voltage breakdown from the cathode to the anode pins in an argon atmosphere.

SECURITY CLASSIFICATION
UNCL.

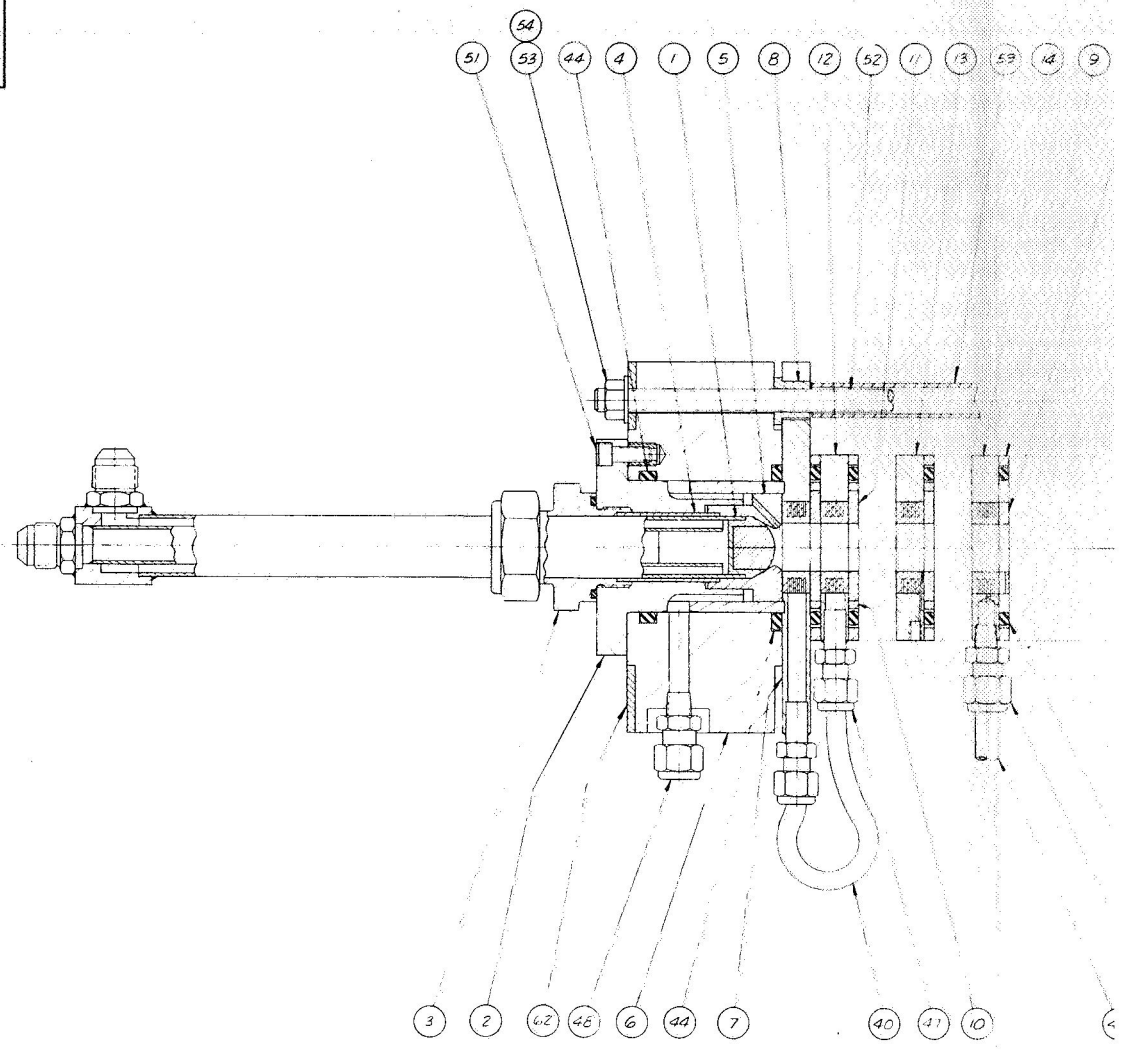

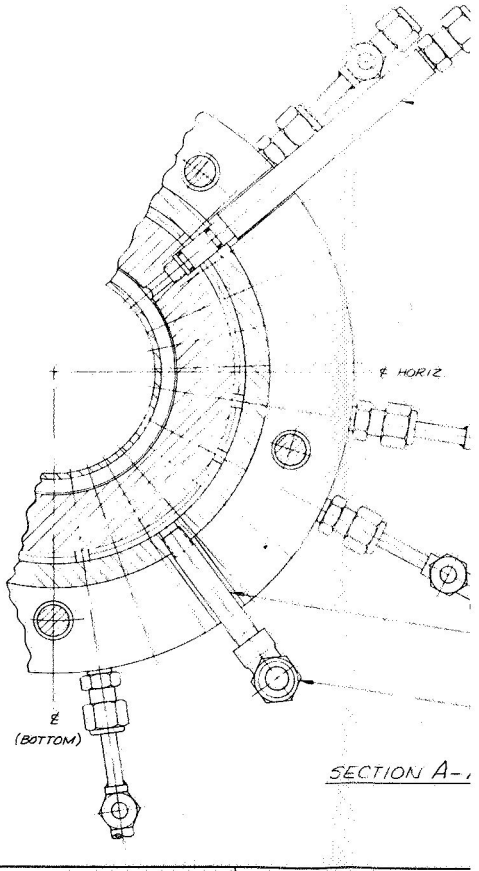

SECTION A-

3 1

C.O.S. FORM NO. 271

REVISIONS					
CHANGE	ZONE	DESCRIPTION	BY	CHECKED	APPROVED	DATE
		RELEASED FOR ASSY	R.S.			8/9/65
A		REVISED ANODE & CATHODE SECTIONS	R.S.			9/14/65

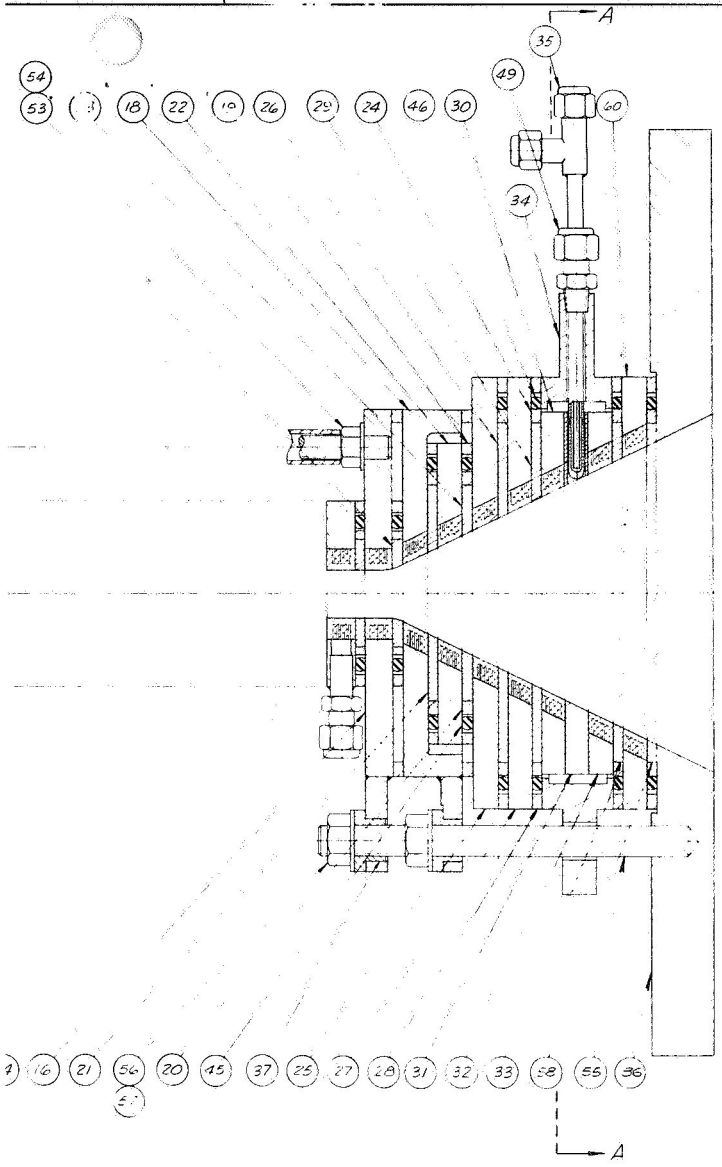

1	62		RING	6.00 O.D. x 3/8 10 x .187 THK	6061-T4 AL ALLOY	
2	61	600-8-2	FEMALE ELBOW	1/2" TUBE TO 1/2 F.P.T.	BRASS	SWAGELOK
1	60	D710-334-6	NOZZLE SEGMENT #7			
5	59		INSULATOR	3.0 O.D. x 1.5 I.D. x .78 LG	NEMA GRADE LE PHENOLIC	
	58	B710-329-7	NOZZLE SEGMENT INSULATOR			
10	57	MS35690-602	NUT, HEX	1/2-13	ALLOY STEEL CAD. PL. FINISH	
10	56		WASHER, FLAT	1/2	ALLOY STEEL	
5	55		STUD, THREADED	1/2-13 x 2 LONG	ALLOY STEEL	
10	54	MS35690-602	NUT, HEX	3/8-16	ALLOY STEEL CAD. PL. FIN	
10	53		WASHER, FLAT	3/8	ALLOY STEEL	
5	52		STUD, THREADED	3/8-16 x 6 1/4 LONG	ALLOY STEEL	
4	51	MS35458-22	SCREW, CAP, HEX. SOC. HEAD	10-32 x 3/16 LONG	ALLOY STEEL CAD. PL. FINISH	
2	50		FITTING, UNION	3/16 TUBE TO 3/16 TUBE	BRASS	SWAGELOK
30	49	ZY400-1-2	FITTING, MALE CONNECTOR	1/4 TUBE TO 1/4 M.P.T.	NYLON	
3	48	600-1-5	FITTING, MALE CONNECTOR	5/16 TUBE TO 1/8 M.P.T.	BRASS	
10	47	500-R-6	FITTING, REDUCER	3/8 F.P.T. BE TO 1/4 TUBE	BRASS	SWAGELOK
4	46	[illegible]-961	O RING	5.975 I.D. x .210 W.	SILICONE RUBBER	PARKER
2	45	MS9068-245		3.975 I.D. x .210 W.		
25	44	MS9068-330	O RING	3.100 I.D. x .210 W.	SILICONE RUBBER	PARKER
4	43		TUBING	5/16 GAGE x .020 WALL	TEFLON	
A/R	42			5/16 O.D. x .135 WALL	COPPER	
A/R	41			1/4 O.D. x .040 WALL	HIGH PRESSURE NYLON	
A/R	40		TUBING	5/16 O.D. x .062 WALL	HIGH PRESSURE NYLON	
1	39		PIPE, THREADED BOTH END	1/8 SCH 40 x 2 1/8 LG.	COPPER	
4	38	C710-339	WATER FEED THRU TUBE			
10	37	B710-336-1	INSULATOR BUSHING			
REF.	36	E710-342	MANIFOLD SUPPORT FRAME			
30	35	C710-338	ANODE PIN ASSY			
1	34	C710-317	ANODE PINS SUPPORT RING			
1	33	B710-329-6	NOZZLE SEGMENT INSULATOR			
1	32	D710-334-5	NOZZLE SEGMENT #6			
1	31	C710-326	ANODE PINS INSULATING RING			
	30	C710-334-4	NOZZLE SEGMENT #5			
	29	B710-329-5	NOZZLE SEGMENT INSULATOR			
4	28	B710-328-7	INSULATOR SPACER RING			
1	27	D710-334-3	NOZZLE SEGMENT #4			
1	26	B710-329-4	NOZZLE SEGMENT INSULATOR			
1	25	D710-334-2	NOZZLE SEGMENT #3			
6	24	C710-326-6	INSULATOR SPACER RING			
1	23	B710-329-3	NOZZLE SEGMENT INSULATOR			
	22	D710-334-1	NOZZLE SEGMENT #2			
	21	B710-329-2	NOZZLE SEGMENT INSULATOR			
2	20	B710-328-6	INSULATOR SPACER RING			
2	19	B710-328-5	INSULATOR SPACER RING			
1	8	D710-319	NOZZLE SEGMENT #1			

E710-320 A

1	17	B710-329-1	NOZZLE SEGMENT INSULATOR			
1	16	C710-323	COLUMN SEGMENT #3			
1	15	B710-321-3	COLUMN SEGMENT INSULATOR			
1	14	C710-322-2	COLUMN SEGMENT #2			
1	13	C710-322-3	COLUMN SEGMENT #3			
1	12	C710-322-1	COLUMN SEGMENT #1			
21	11	B710-321-1	COLUMN SEGMENT INSULATOR			
21	10	B710-328-2	INSULATOR SPACER RING			
22	9	B710-328-1	INSULATOR SPACER RING			
5	8	B710-336-2	INSULATOR BUSHING			
1	7	C710-324	HOUSING COOLING RING			
1	6	C710-285	HOUSING			
1	5	C710-330	CATHODE INSULATOR			
1	4	C710-331	INSULATOR SLEEVE			
1	3	C710-332	REWORKED TUBE FITTING			
1	2	C710-327	CATHODE SUPPORT			
1	1	C710-335	CATHODE			
REQ'D	ITEM	PART NO.	DESCRIPTION	SIZE	MATERIAL	SPECIFICATION

LIST OF MATERIALS

3 (2)

		UNLESS OTHERWISE NOTED: 1. LINEAR DIMENSIONS IN INCHES. 2. TOLERANCES: DECIMAL FRACTIONS ANGULAR .X ± ± .XX ± .XXX ±	DRAWN R. SWOPE 8.19.65 CHECKED DESIGN APPROVED APPROVED RELEASED ACT. WT. CALC. WT.

THIS DRAWING CONTAINS INFORMATION PROPRIETARY TO ELECTRO-OPTICAL SYSTEMS, INC. IT SHOULD NOT BE REPRODUCED, USED OR DISCLOSED TO ANYONE WITHOUT THE PRIOR WRITTEN PERMISSION OF THIS ORGANIZATION.

ORIGINAL APPLICATION

ELECTRO-OPTICAL SYSTEMS, INC., Pasadena, California · MUrray 1-4671, 449-1230

TITLE: HIGH ENTHALPY GAS HEATER ASSEMBLY- MODEL HEGH-2

SECURITY CLASSIFICATION: UNCL | SIZE: E | NUMBER: 710-320 | REV: A | CODE IDENT NO. | SCALE | SHEET 1 OF 1

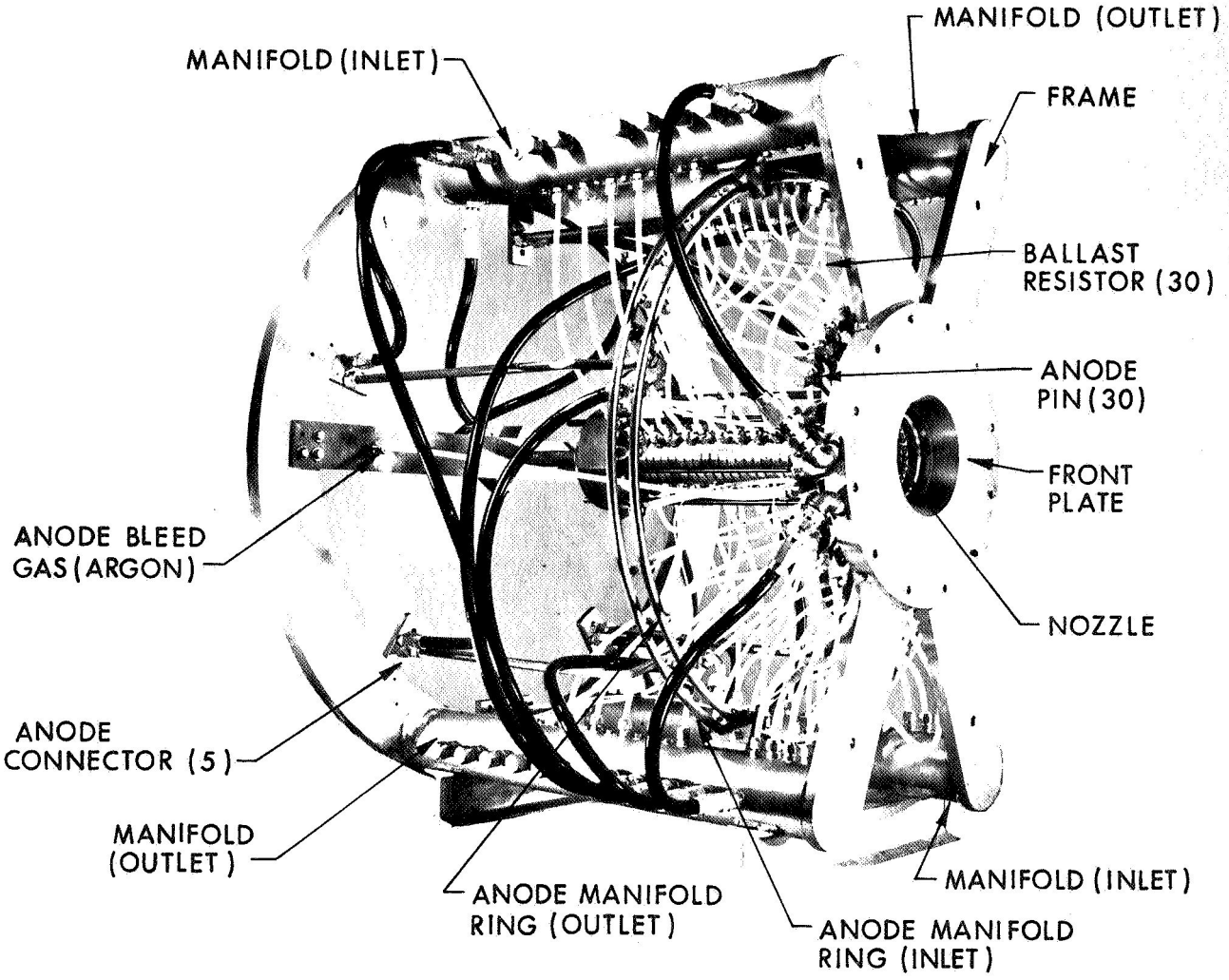

FIG. 5-2 MATERIALS TEST HEATER, MODEL HE-1MW (nozzle view)

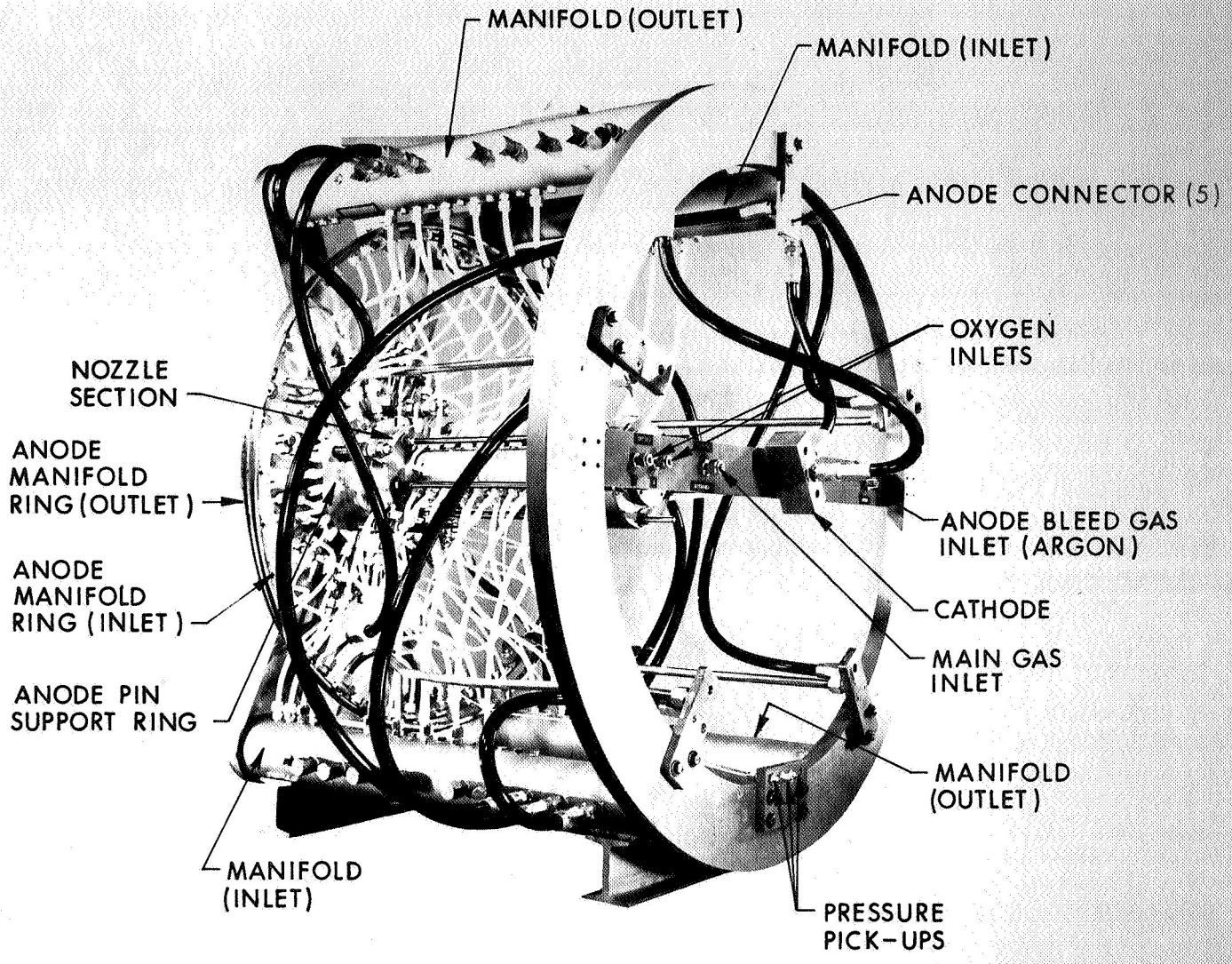

FIG. 5-3 MATERIALS TEST HEATER, MODEL HE-1MW (rear view)

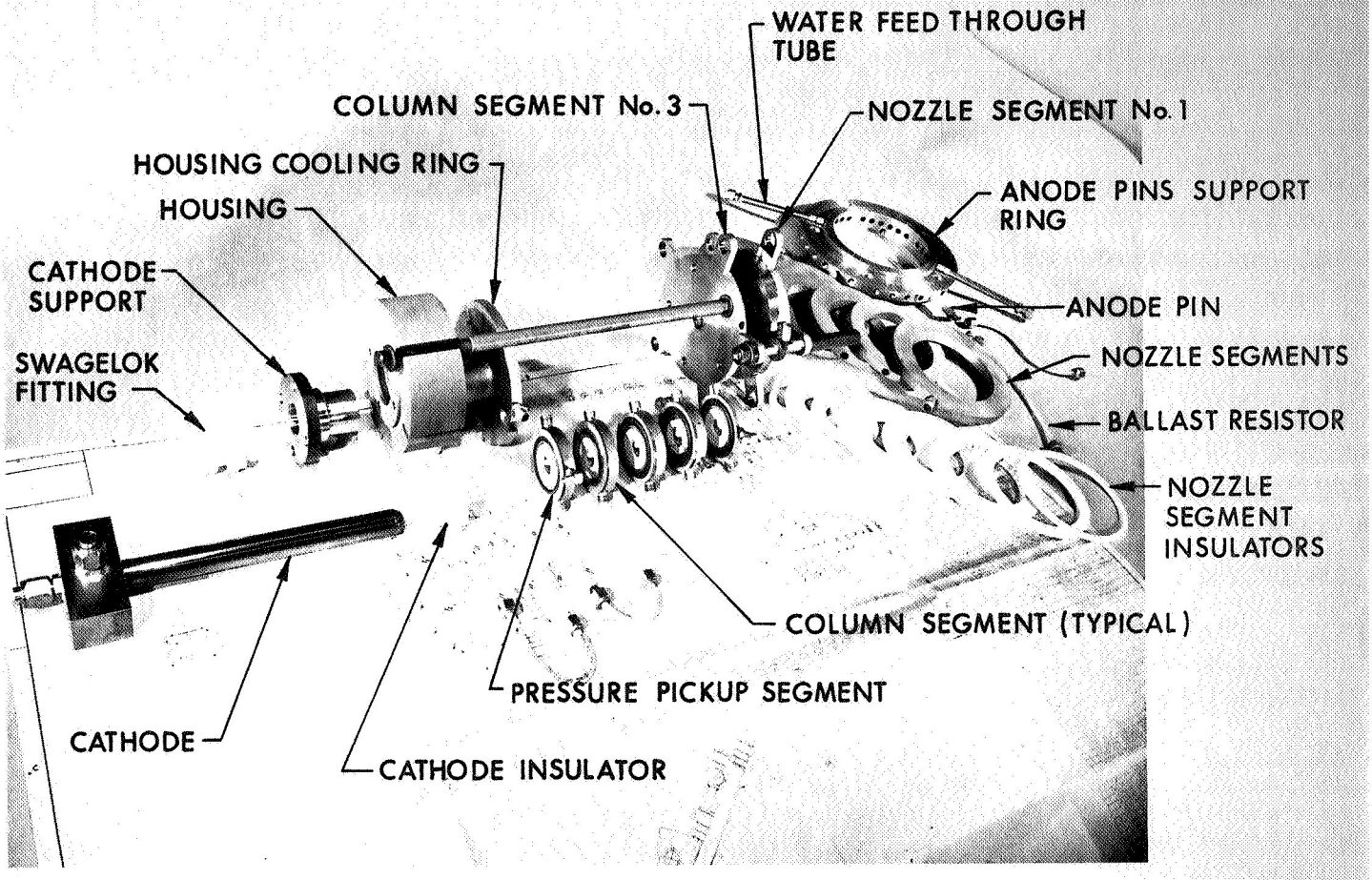

FIG. 5-4 EXPLODED VIEW OF MATERIALS TEST HEATER MODEL HE-1MW

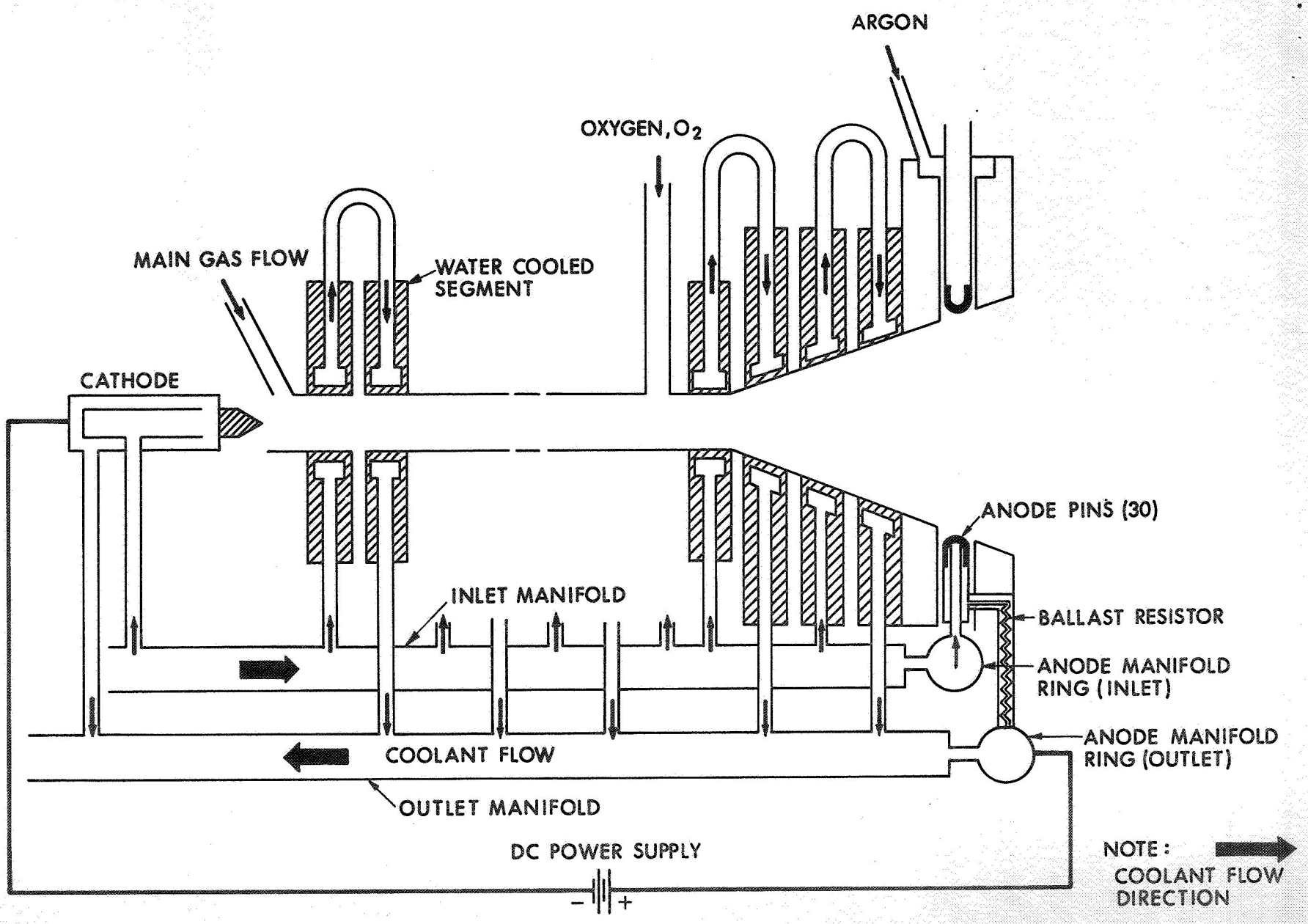

FIG. 5-5 SCHEMATIC OF MATERIALS TEST HEATER, ELECTRICAL SYSTEM, COOLANT, AND GAS FLOW

TABLE 5-1

LEADING PARTICULARS

MATERIALS TEST HEATER, MODEL HE-1MW

Total Electrical Power	1-megawatt
Arc Current	1500 amperes (1600 amperes maximum)
Total Average Enthalpy	9.3×10^7 joules/kg (40,000 Btu/lb)
Gas Flow Rate	6 g/sec
Critical Sonic (Throat) Pressure	0.55×10^5 newtons/m^2 (0.54 atmospheres)
Coolant	Chemically Treated Water
Coolant Flow Rate	140 gpm
Coolant Inlet Temperature	$100^{\circ}F$ maximum
Coolant Inlet Pressure	500 psig minimum at Full Flow
Coolant Outlet Pressure	150 psig maximum at Full Flow
Dimensions, Overall	40 inches diameter x 30 inches
Weight (approximate)	295 lbs
Chamber Mounting Provisions	12 3/4-inch - 16 bolts on circle of 13.625 diameter

The initial breakdown occurs at about 560 volts open circuit voltage with 0.5 g/sec argon flow. The arc, however, cannot be maintained at full nitrogen flow if the onset of current flow causes the supply voltage to drop below 460 volts. This voltage level appeared to be the minimum operating voltage requirement for the heater-power supply combination at the EOS Plasma Laboratory. The full main gas flow is initiated by an automatic starting device, which is activated by the potential difference developed across the anode pin ballast resistor upon starting of the arc.

5.3 Life and Endurance Test of Materials Test Heater, Model HE-1MW

On 1 and 2 November, 1965, the Materials Test Heater, Model HE-1MW was life and endurance tested for a total accumulated time of 5 hours and 3 minutes with 21 starts. During this test, the total voltage and arc current, as well as the temperature rise of the coolant, were recorded for each test point. The total voltage and arc current, and the downstream pressure of the sonic constrictor orifice were recorded continuously on a chart recorder.

Throughout the five hours of operation, the heater performance, i.e., the voltages and heater exit pressures (and hence, the enthalpies and efficiencies) for given values of current and mass flow rates were repeated within the measuring accuracy. There was no cathode "spitting" or "sparking" at any of the current and mass flow levels tested (500 to 1550 amps with N_2, up to 1600 amps with argon, 3 to 12 g/sec mass flow). The jet appeared extremely stable and clean under all conditions covered by the test. Run durations were limited only by tank, window, and power supply cooling limits, which permitted continuous operation at maximum current for 10-minute periods and continuous runs at lower power (below 800 kW) for 30 to 50 minutes. The heater itself showed no signs of overheating and could have been operated continuously for 5 hours or longer.

However, the many starts, stops, and changes in operating conditions, represented a more severe and realistic test of the heater in terms of its intended purpose.

The statistics of the entire test including the operating points covered and the duration for each are compiled in Table 5-2. The performance of the heater during the test is shown in Figs. 5-6 to 5-9. The highest enthalpy at which the heater was tested was 13.4×10^7 joules/kg (58.6×10^3 Btu/lb) with an efficiency of 50.4 percent. At a mass-averaged total enthalpy of 9.3×10^7 joules/kg (40,000 Btu/lb) the efficiency was 59 percent. The heater performance during the test indicated that all design specifications were substantially exceeded.

Following the life test, the heater was carefully inspected and found to be in perfect condition. There was no need for any repair, modification, or cleaning. There was a small rough spot at the center of the cathode, probably the result of the cold starting. In Fig. 5-10 the cathode, the cathode insulator, and one anode pin, which were used during the five hour test are compared with new heater components. This figure provides a graphic demonstration of the excellent condition of the critical parts of the heater. The normal life expectancy of all heater parts can be conservatively estimated to be at least 50 hours.

Starts	Time	Point	Run Duration Minutes	Accumulated Time Minutes	Gas	Current ma	Vol v
S*	14:35*	0*					
		1			N_2	1000	5
	14:52	2			N_2	1200	5
			10	10			
S	15:35	3			N_2	500	5
	15:38	4			N_2	1000	5
	15:40	5			N_2	1200	5
			10	20			
S	17:33	6			N_2	500	5
	17:34	7			N_2	1000	5
	17:35	8			N_2	1200	6
	17:36	9			N_2	1500	6
	17:40	10			N_2	1000	5
	17:43	11			N_2	500	5
	17:50	12			N_2	1500	6
			30	50			
S	19:15	13			N_2	500	5
	19:20	14			N_2	1200	6
	19:21	15			N_2	1500	6
	19:22	16			N_2	1550	6
	19:26	17			N_2	1000	5
	19:32	18			N_2	400	4
			17	67			
S	19:33	19			N_2	1000	5
			14	81			
S	20:55	20			N_2	500	5
	20:58	21			N_2	1000	5
	21:00	22			N_2	1500	6
	21:06	23			N_2	1000	5
	21:15	24			N_2	1200	6
		25			N_2	500	5
			30	111			
S	22:15	26			N_2	500	5
	22:17	27			N_2	1000	5
	22:18	28			N_2	1500	6
		29			N_2	1000	5
S	22:33	30			N_2	500	5

*The times given denote the instant when the readings were taken for each indivi
"S" denotes that a new run was started prior to the given point.

LE 5-2

)F MATERIALS TEST HEATER HEGH-2

:o 2 November 1965

ıge lt	Power kW	Flow Rate g/sec	Throat Pressure mbar	Enthalpy joules/kgx10^{-7}	Efficiency Percent	Tank Press mm Hg
)	570	5.8	430	6.09	62.0	6.0
5	714	5.8	480	7.45	60.5	
3	252	5.8	322	3.32	76.4	5.0
)	570	5.8	434	6.18	62.9	5.2
5	714	5.8	478	7.38	59.9	
9	254	6	329	3.19	75.4	
5	575	6	443	6.00	62.6	
0	720	6	491	7.20	60.0	
9	958	6	551	9.35	58.6	
9	579	6	450	6.12	63.4	5.2
9	254	6	331	3.30	78.0	5.0
5	951	6	551	9.35	59.0	
9	254	6	325	3.10	73.2	5.0
0	720	6	489	7.10	59.2	
5	951	6	551	9.35	59.0	5.3
2	1 [illegible]	6	560	9.61	57.1	
5	575	6	443	6.00	62.6	
2	197	6	297	2.35	71.6	
8	578	6	441	5.95	61.8	
1	256	6	331	3.30	77.3	5.1
0	580	6	448	6.08	62.9	5.3
0	960	6	555	9.45	59.0	5.4
0	580	6	450	6.13	63.4	5.2
3	724	6	493	7.27	60.2	5.5
9	254	6	331	3.30	78.0	5.1
9	254	6	327	3.13	73.9	5.0
0	580	6	448	6.08	62.9	5.2
9	958	6	556	9.46	59.2	5.4
0	580	6	446	6.07	62.9	23.0
2	266	6	329	3.28	74.0	23.0

al point.

TABL

ENDURANCE AND LIFE TEST O

1 Novembe

Starts	Time	Point	Run Duration Minutes	Accumulated Time Minutes	Gas	Current amp	Volt v
			20	131			
S	22:40	31			N_2	500	50
	22:42	32			N_2	500	56
	22:43	33			N_2	1000	63
	22:46	34			N_2	500	56
	22:48	35			N_2	500	58
	22:51	36			N_2	1000	66
	22:54	37			N_2	500	48
			22	153			
S	23:18	38			N_2	500	47
	23:20	39			N_2	1000	54
	23:21	40			N_2	1500	60
	23:23	41			N_2	500	44
	23:24	42			N_2	1000	50
	23:25	43			N_2	1500	56
	23:27	44			N_2	500	40
	23:28	45			N_2	1000	47
	23:29	46			N_2	1500	53
	23:39	47			N_2	1000	46
	23:55	48			N_2	1500	53
			45	198			
S	00:27	49			N_2	500	64
	00:28	50			N_2	1000	71
		51			N_2	1320	5
			10	208			
S	00:56	52			A	500	2
		53			A	1000	3
		54			A	1200	42
		55			A	1500	4
S		56			A	1600	4
	01:10	57			A	500	2
	01:11	58			A	500	3
	01:13	59			A	1000	2
	01:15	60			A	1000	3
9 Starts		61	25	233		1500	4
		62				1550	65
		63			N_2	1000	5
		64			N_2	1550	65
		65			N_2	1500	63
		66			N_2	1000	57
			70	303			

Totals: 21 starts, 303 minutes running time

5-2

ATERIALS TEST HEATER HEGH-2 (contd)

:o 2 November 1965

Power kW	Flow Rate g/sec	Throat Pressure mbar	Enthalpy joules/kgx10^{-7}	Efficiency Percent	Tank Press mm Hg
254	6	320	2.8	66.1	23.0
284	8	407	2.54	71.5	15.05
639	8	551	5.33	66.7	15.0
282	8	410	2.60	73.8	15.0
290	8.85	438	2.40	73.2	15.0
662	8.85	601	5.35	71.5	11.0
240	5	286	3.65	76.0	4.5
239	5	277	3.37	70.5	
540	5	377	6.15	56.9	
900	5	478	10.2	56.7	
221	4	233	3.82	69.1	3.9
509	4	331	7.35	57.8	3.9
854	4	407	11.8	55.3	3.9
200	3	189	4.50	67.5	
470	3	267	8.70	55.5	3.2
789	3	320	13.4	50.4	3.2
468	3	267	8.7	55.8	3.2
796	3	320	13.4	50.5	3.2
320	10	483	2.22	79.4	34.0
710	10	686	4.70	66.2	34.0
990	10	781	6.50	65.7	34.0
141	8	400			6.0
3[illegible]3	8	480			6.0
504	8	514			6.0
7[illegible]3	8	564			6.0
7[illegible]9	8	578			6.0
1[illegible]6	1[illegible]	468			14.6
1[illegible]	12	[illegible]			16.6
4[illegible]	12	6[illegible]8			16.6
7[illegible]	12	7[illegible]			[illegible]
9[illegible]0	[illegible] 6.2	571			[illegible]
[illegible]0[illegible]0	[illegible] 6.2	583			5.8
595	[illegible] 6.2	468			5.5
1010	[illegible] 6.2	587			5.8
953	[illegible] 6.2	547			5.3
578	[illegible] 6.2				5.2

2

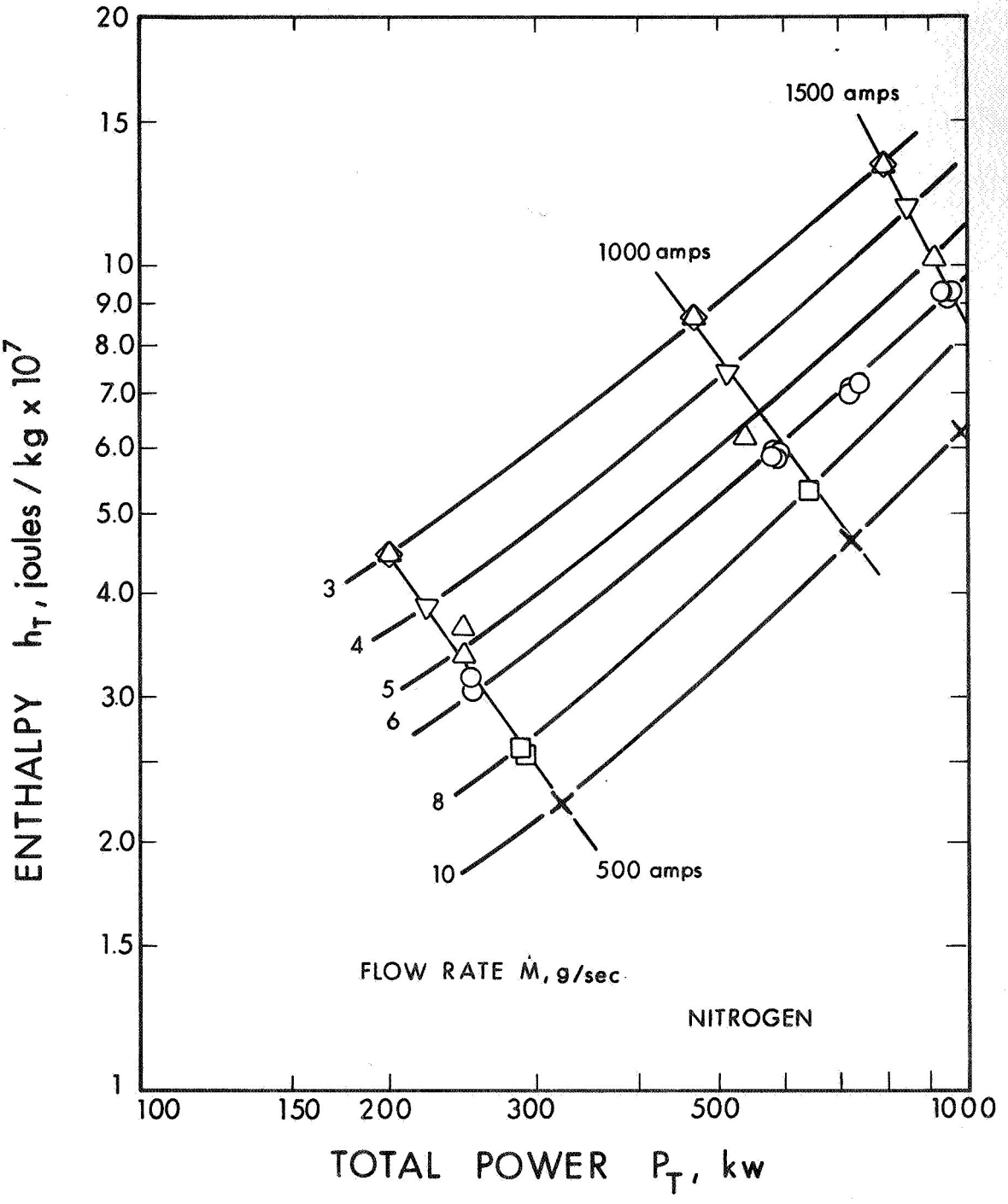

FIG. 5-6 PERFORMANCE CHART FOR MATERIALS TEST HEATER MODEL HE-1MW (Enthalpy vs Total Power)

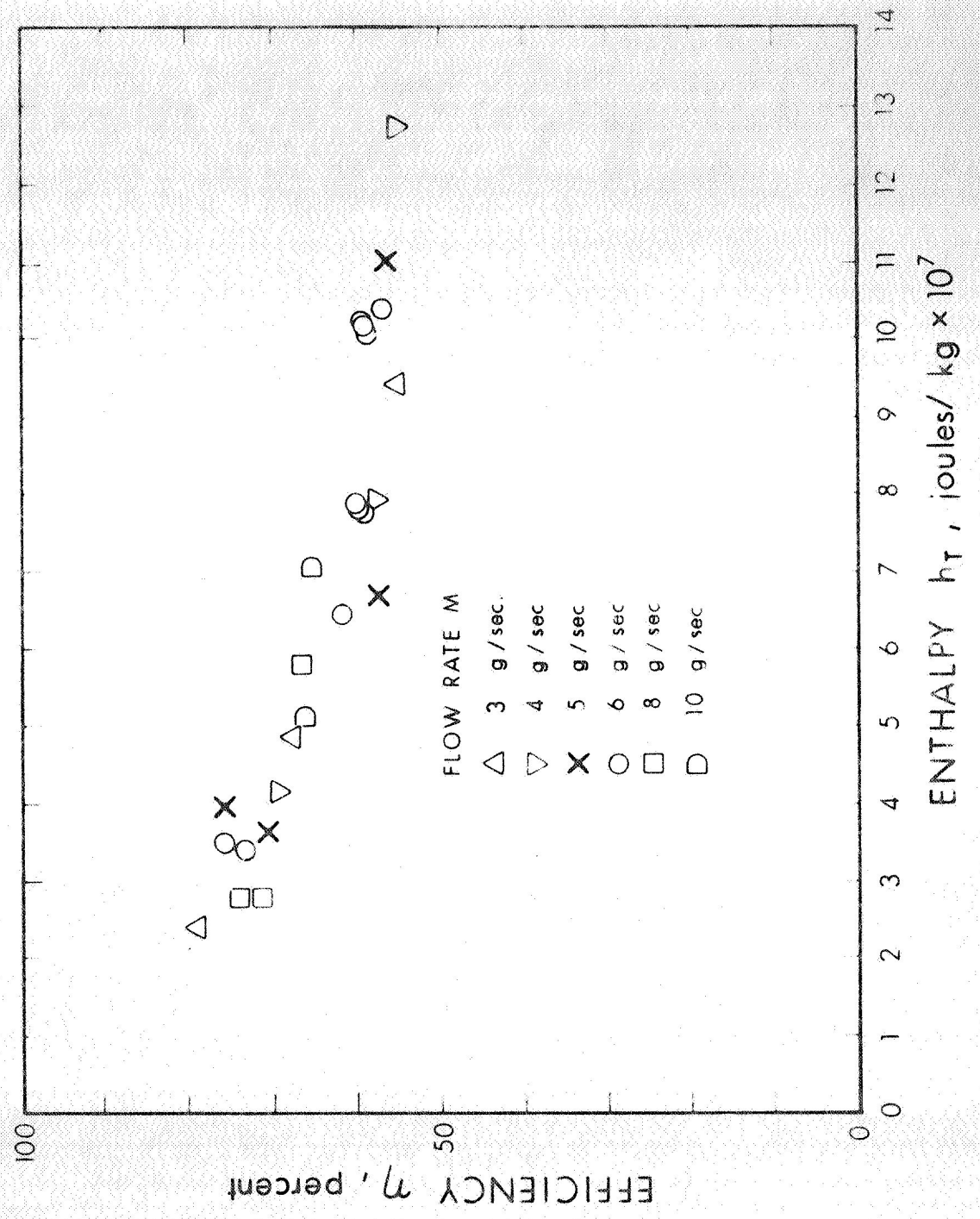

FIG. 5-7 EFFICIENCY OF MATERIALS TEST HEATER MODEL HE-1MW AT LIFE TEST OPERATING POINTS

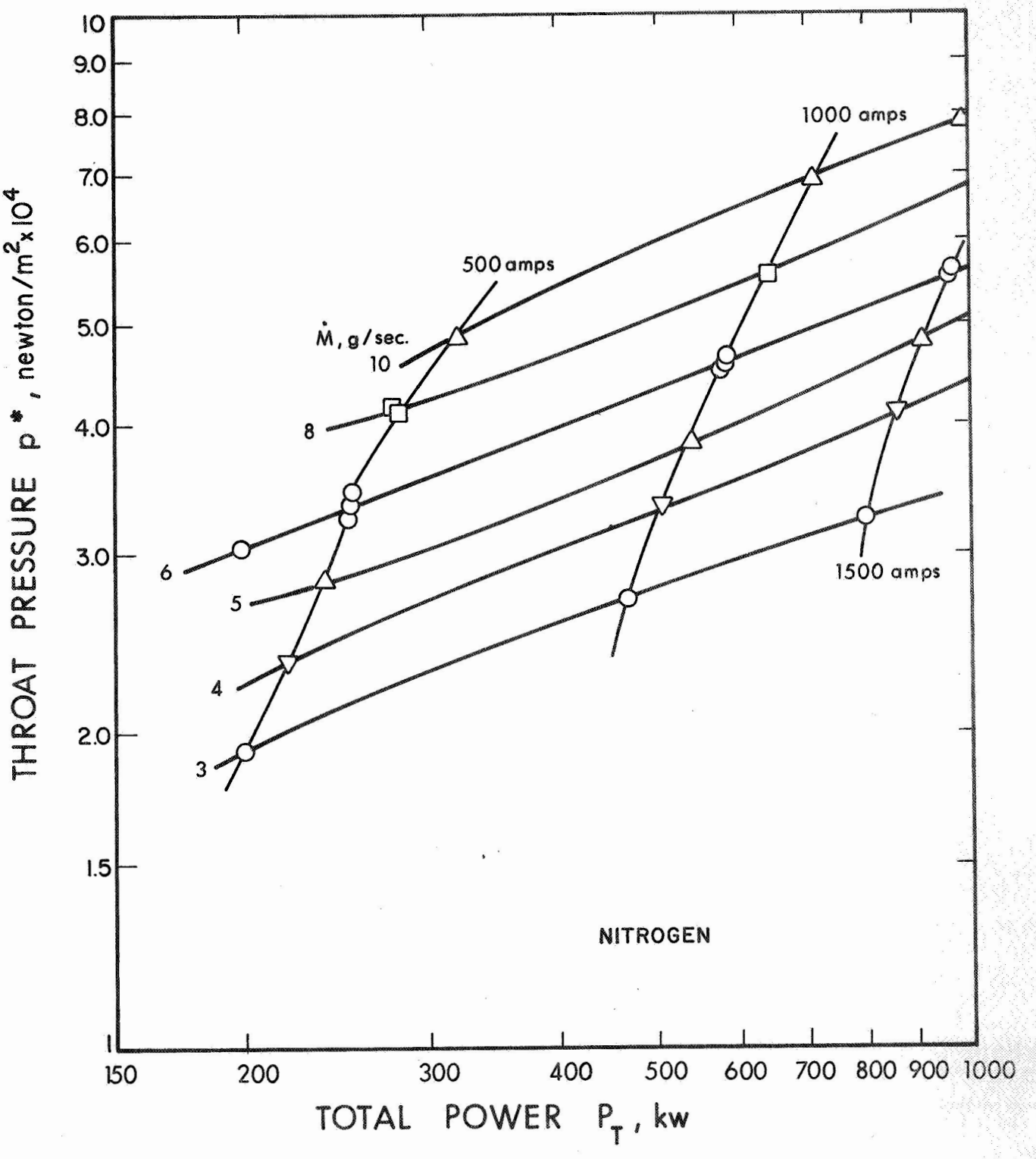

FIG. 5-8 PERFORMANCE CHART FOR MATERIALS TEST HEATER MODEL HE-1MW
(Throat Pressure versus Total Power)

3620177

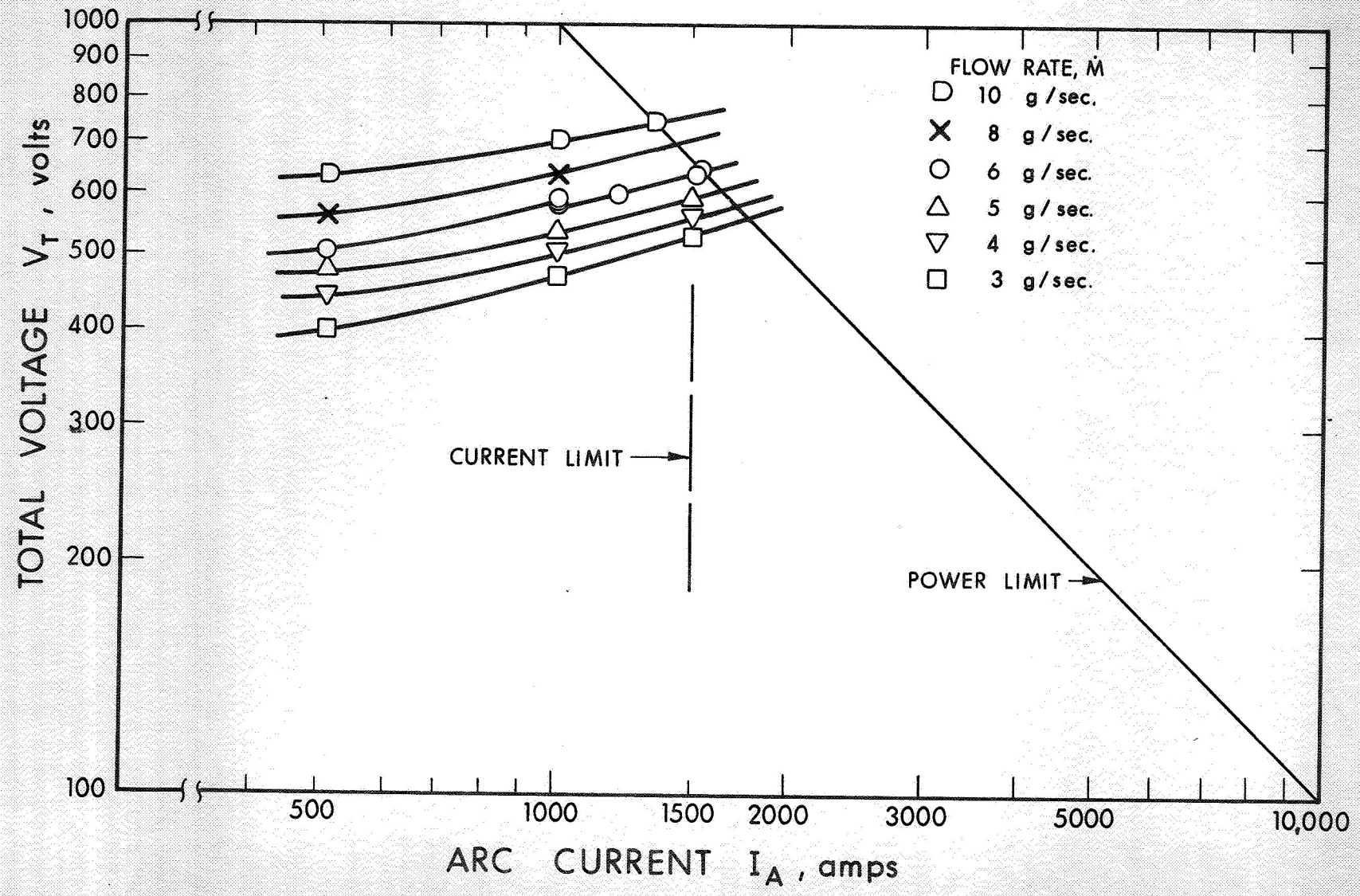

FIG. 5-9 TOTAL VOLTAGE - ARC CURRENT CHARACTERISTICS OF MATERIALS TEST HEATER MODEL HE-1MW

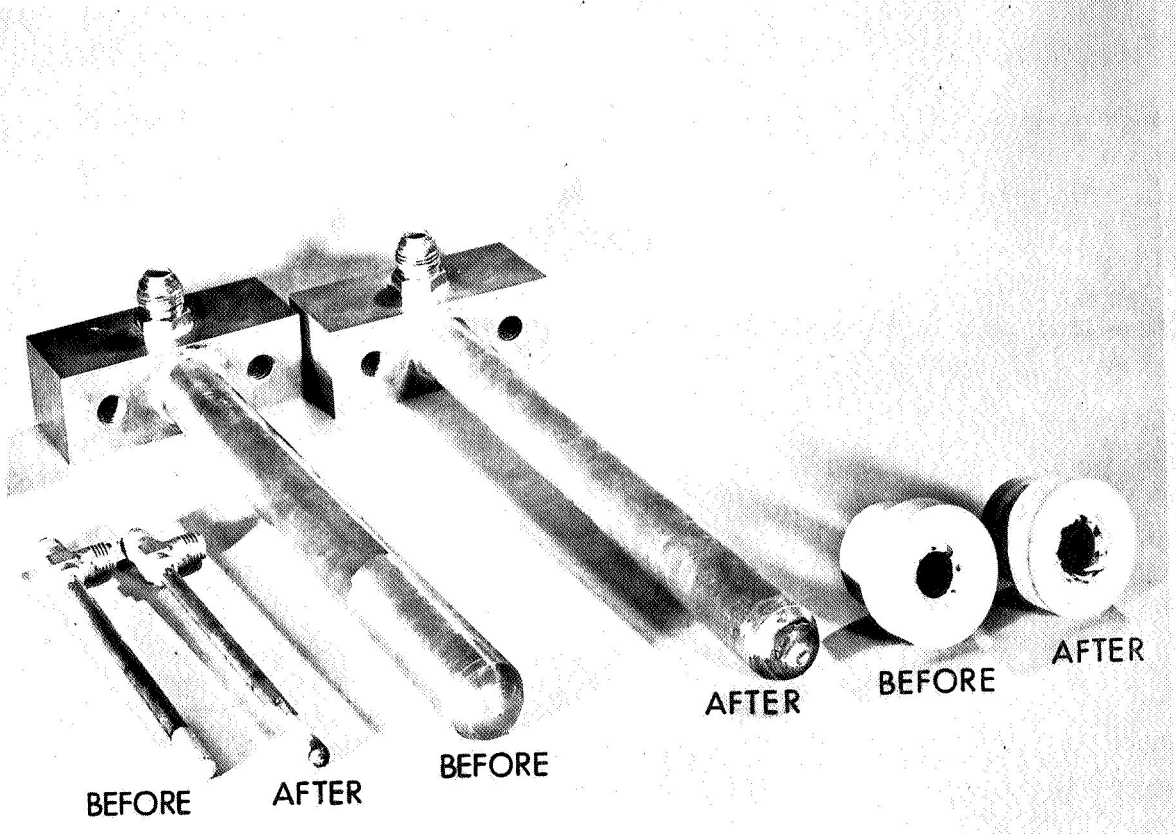

FIG. 5-10 COMPARISON OF VITAL HEATER COMPONENTS (ANODE PINS, CATHODE, AND CATHODE INSULATOR) BEFORE AND AFTER LIFE TEST

6. EXTRAPOLATION TO LARGE-SIZE CONSTRICTED-ARC HEATERS

The test results and the empirical relations presented in Section 4 between all operating parameters for the 2-cm diameter constricted-arc heater enable EOS to design constricted-arc heaters of this size for a broad range of operating conditions and to accurately predict their performance characteristics. The test results have furnished two "constants" for the 2-cm diameter heater which must be assumed to be functions of the constrictor radius: the heat loss constant K_A, and the electric field constant K_E.

The choked flow relations discussed in Subsection 4.1 are considered valid and sufficiently accurate for use in the design of heaters of any contemplated size. These relations will determine the proper constrictor size for a given mass flow, enthalpy, and throat pressure.

Two additional relations are needed to complete design calculations and performance predictions for heaters large than 1 MW; namely, one for the electric field along the constrictor, and one for the heat loss to the wall. With these two relations determined, all necessary design and performance information can be obtained, including:

1. Constrictor length and total voltage versus arc current, for given outlet gas conditions
2. Constrictor wall heat load distribution, and heating efficiency versus current

From these relations, all other necessary heater calculations can be made except those for the electrodes which are still in the experimental stage.

To obtain the necessary electric field and constrictor wall heat load relations, the rules must be found by which the corresponding relations will scale in relation to size. Based on experience, it is

reasonable to postulate that the dependence of the electric field on pressure and of the wall heat loss on current will remain valid, so that only the factors K_A (R) and K_E (R) will be size dependent. This amounts to a "separation of variables" concept which is justified, at least to first order, from the nature of the pertinent equations. Thus, it is postulated that expressions of the form

$$\dot{q}_A \doteq K_A (R) \times f_A (I)$$

and

$$E = K_E (R) \times f_E (p)$$

will be adequate for scaling, where f_A and f_E will be the same as those found for the 1 MW heater. The validity of this postulation is based on the assumptions that the 1 MW and the 10 MW heaters are in the same energy transfer regime, namely, predominantly governed by radiation rather than thermal conduction. Because of this, it is assumed that $f_A = f_A$ (I only) and $f_E = f_E$ (p only) as indicated above, because these dependencies were found to hold for the 1 MW heater over the range tested. The validity of this approach will be checked by resorting to the rather general, though complicated, scaling rules of Ref. 3.

The essential assumption made here is that the theoretical arc column results should give sufficiently accurate size and pressure dependencies although these results do not yet yield absolute values. In the past, this has been the case, insofar as the assumption has been tested.

Eventually, research tests with several heaters larger than 1 MW and operating over a wide range of pressures will have to be carried out and the results compared with more theoretical calculations. This would permit verification of the scaling rules and enhance the understanding of high-powered arcs.

6.1 A Combined Analytical and Experimental Approach to the Design of Large-Diameter Constricted-Arc Heaters

The lack of experimental data from large diameter constricted arcs and of a complete analysis of the constricted arc column for this size regime makes it necessary that the approximate dependency of the "constants" K_A and K_E on the constrictor size be determined from the analytical considerations given in Ref. 3. The results of Ref. 3 provide scaling rules which correlate the numerical arc column integrations of Yos (Ref. 1) and it is assumed that these rules will also be valid for constricted-arc heaters.

In Fig. 11 of Ref. 3 it is shown that for high currents the electric field is a very weak function of the arc current and can, therefore, be expressed by

$$\frac{E\,R}{(1+\xi)^{\frac{1}{2}}}\,p^{s/2} \approx C_1 \tag{6.1}$$

where from Fig. 13 of the same reference the relation for the function ξ can be found to be

$$\xi \approx C_2\,R^2\,p^t = \frac{\text{radiative heat loss}}{\text{conductive heat loss}} \tag{6.2}$$

For large diameters

$$\xi \gg 1$$

so that

$$1 + \xi \approx \xi$$

Inserting relation 6.2 into Eq. 6.1, one can find

$$\frac{E\,R\,p^{s/2}}{C_2^{\frac{1}{2}}\,R\,p^{t/2}} = C_1 \tag{6.3}$$

or

$$E = C_E\,p^{(t/2 - s/2)} \tag{6.4}$$

From Fig. 16 of Ref. 3

$$t \approx 1.31$$
$$s \approx 0.31$$

which finally results in an electric field dependency of

$$E \approx C_E\, p^{\frac{1}{2}} \tag{6.5}$$

Thus, the scaling rules of Ref. 3 agree at least in this important respect with both the 1 MW experimental data and with open arc experience. All the evidence, therefore, indicates that, in the high-powered arc regime, the potential gradient E should be independent of either the radius R and the current, and depend substantially only on the pressure and gas type. The evidence also indicates that, in this respect, the 1 MW heater falls well within the regime analyzed in Ref. 3, a matter which was previously open to question.

Next, it is desired to find the scaling rule which applies to the wall heat loss calculation. From Fig. 14 of Ref. 3

$$\frac{\dot{q}_A\, R}{(1+\xi)} = f\left(\frac{I}{R(1+\xi)^{\frac{1}{2}}\, p^{\,s/2}}\right) \tag{6.6}$$

But from the 1 MW experimental results it was established that for a fixed radius of 1 cm

$$\dot{q}_A = K_A\, I^n \tag{6.7}$$

Combining these two results gives

$$\frac{\dot{q}_A\, R}{1+\xi} = C_3\, \frac{I^n}{R^n (1+\xi)^{n/2}\, p^{ns/2}} \tag{6.8}$$

If it is again assumed that $\xi \gg 1$ and remains roughly constant over a range, then

$$\dot{q}_A = C_3 I^n \frac{\left(C_2 R^2 p^t\right)^{1-n/2}}{\left(R^{n+1}\right) \times p^{ns/2}}$$

$$= C_3 C_2^{(1-n/2)} \frac{I^n}{R^{2n-1}} \times p^{t(1-n/2)-ns/2} \qquad (6.9)$$

From the 1 MW experimental results, the exponent on the current dependence was

$$n = 1.617$$

so that, for $t \approx 1.31$ and $s \approx 0.31$, the exponent on the pressure becomes

$$t(1-n/2) - ns/2 = 1.31 \times 0.1915 - \frac{1.617 \times 0.31}{2} = \underline{0}$$

and the exponent of the radius R

$$2n-1 = \underline{2.234}$$

The complete relation for the energy transfer $\dot{q}_A$ is then

$$\dot{q}_A \doteq C_Q \frac{I^{1.617}}{R^{2.234}} \left[W/m^2 \right] \qquad (6.10)$$

Again, a good agreement between test data and the derived approximation is found with this relation. The analytical relations indicate that there should be no dependence between energy transfer to the constrictor wall and the pressure. This analytically determined independence is in agreement with test results. The interesting fact is that in relation 6.10 the constrictor radius exponent is actually solely determined by the experimentally found value of n. Comparing relation 6.7

with relation 6.10, the factor K_A is found to be the following function of the constrictor radius

$$K_A(R) = \frac{C_Q}{R^{2.234}} \tag{6.11}$$

where C_Q is a function of the gas.

From the test results for nitrogen it is concluded that

$$C_{Q_{N_2}} = 3.38 \times 10^{-3} \quad \left[\text{MkS}\right] \tag{6.12}$$

Relations have now been established between the operating parameters and the physical parameters of constricted arcs in nitrogen. These relations are based on combinations of analytical and experimental correlations and can now be used in the design of constricted-arc heaters of larger size. The procedure for this design and performance prediction is outlined in the next subsection.

6.2 Design and Performance Calculations for a 10-Megawatt Constricted-Arc Heater

The following procedure may be used in designing any constricted-arc heater in the megawatt size range. From what has been said previously, it is clear that there exists no unique design for any particular size heater. The design of a heater will generally be governed by several factors, the importance of which will depend upon the particular design in question. Some of these factors are: the required enthalpy-pressure envelope; the maximum power; current and voltage envelope available; the required jet size and, hence, lowest allowable efficiency; the maximum heat load on the constrictor wall; the test gases to be used; and the required service life between overhauls.

For the 10 MW constricted-arc heater, the following design limits have been tentatively established.

Total input power P_T	10 Megawatt
Constrictor-Exit pressure p*	0.5 atm
Gas	Air (Nitrogen)
Ballast resistance voltage drop V_B (if used)	70 volt

With these considerations given, the following relations can be used to prepare design charts from which a specific design can be selected. From the relations:

$$V_T = V_A + V_a + V_c + V_B \tag{6.13}$$

and

$$V_T = P_T \Big/ I_A$$

and the arc voltage relation

$$V_A = L \left[1.239\, k_E \left(\frac{p^*}{p_a}\right)^{\frac{1}{2}}\right] \tag{6.14}$$

a correlation between arc current I_A and constrictor length L is obtained which will result in a heater length of the chosen input power:

$$L = \left\{\frac{P_T}{I_A} - V_a + V_c + V_B\right\} \Big/ \left\{1.239\, k_E \left(\frac{p^*}{p_a}\right)^{\frac{1}{2}}\right\} \tag{6.15}$$

This correlation is shown in Fig. 6-1.

With the energy transfer coefficient, which is given by Eq. 6.11, and the constant given by relation 6.12, inserted into Eq. 6.15, the efficiency is found to be

$$\eta = 1 - \frac{\dfrac{C_{Q_{N_2}}}{R^{1.234}}\, I_A^{0.617} \times 10^{+3} + \dfrac{V_a + V_c + V_B}{L}}{1.239\, k_E \left(p^*/p_a\right)^{\frac{1}{2}} + \dfrac{V_a + V_c + V_B}{L}} \tag{6.16}$$

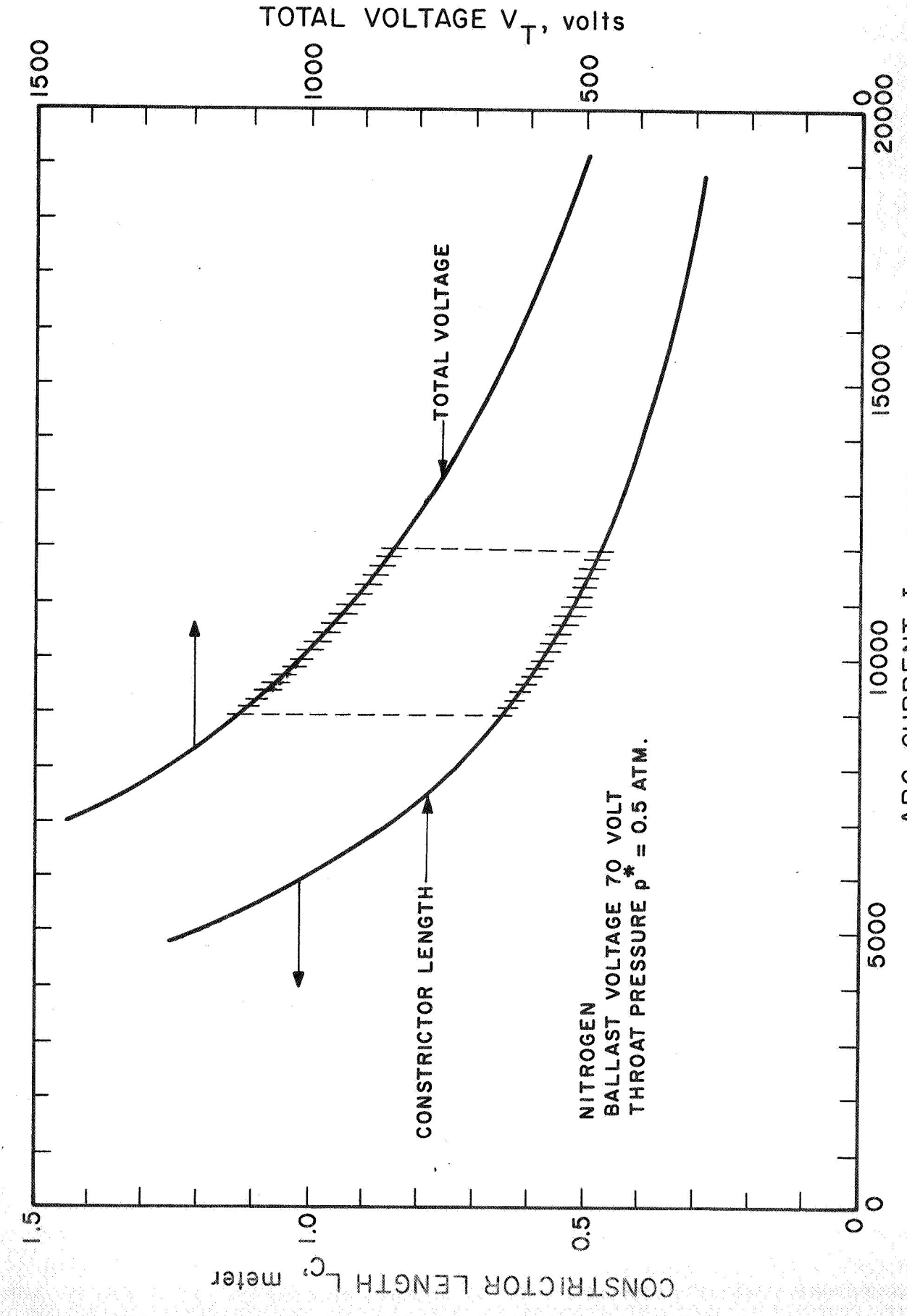

FIG. 6-1 CORRELATION BETWEEN ARC CURRENT, TOTAL VOLTAGE, AND CONSTRICTOR LENGTH FOR A 10 MEGAWATT CONSTRICTED ARC HEATER

The efficiency can then be plotted by substituting Eq. 6.15 in Eq. 6.16 to eliminate the length parameter. This plot is shown in Fig. 6-2. The third design chart is constructed from the relation between the total enthalpy and critical flow parameters,

$$h_T = f\left(\frac{\dot{M}}{\pi R^2 p^*}\right)$$

which is given in Fig. 6-1, and the simple efficiency relation

$$\eta P_T = \dot{M} h_T .$$

This plot is shown in Fig. 6-3. The final design chart correlates the heat load on the constrictor wall, $\dot{q}_A$, with the arc current, I_A, and the constrictor radius R_c (Fig. 6-4).

Because boron nitride is used in the constrictor, the general philosophy for the 10 MW heater design should be to limit the constrictor wall heat load to a minimum. Figure 6-4 indicates a low current and large constrictor diameter design should be chosen for this purpose. From Fig. 6-1, indications are that the arc current should fall into a range between 9000 to 12,000 amps. From Fig. 6-2, one can expect a heater efficiency of 65 to 72 percent. For a total enthalpy between 9.3×10^7 to 10×10^7 joules/kg, a flow rate of 69.0 to 77.5 g/sec and a constrictor radius, R, of 3.525 cm to 3.65 cm are found from Fig. 6-3. Figure 6-4 indicates that the heater can be designed for a constrictor wall heat load between 1.2 and 2.4 kW/cm^2. The constrictor length for such a design would be between 47 and 65 cm. The design areas determined by the above limits for the 10 MW constricted-arc heater design have been indicated on Figs. 6-1 through 6-4. Of course, the operating point can be shifted to a lower current if power equipment considerations so indicate.

The new design results and performance predictions make the 10 MW high enthalpy heater much more feasible and promising. The

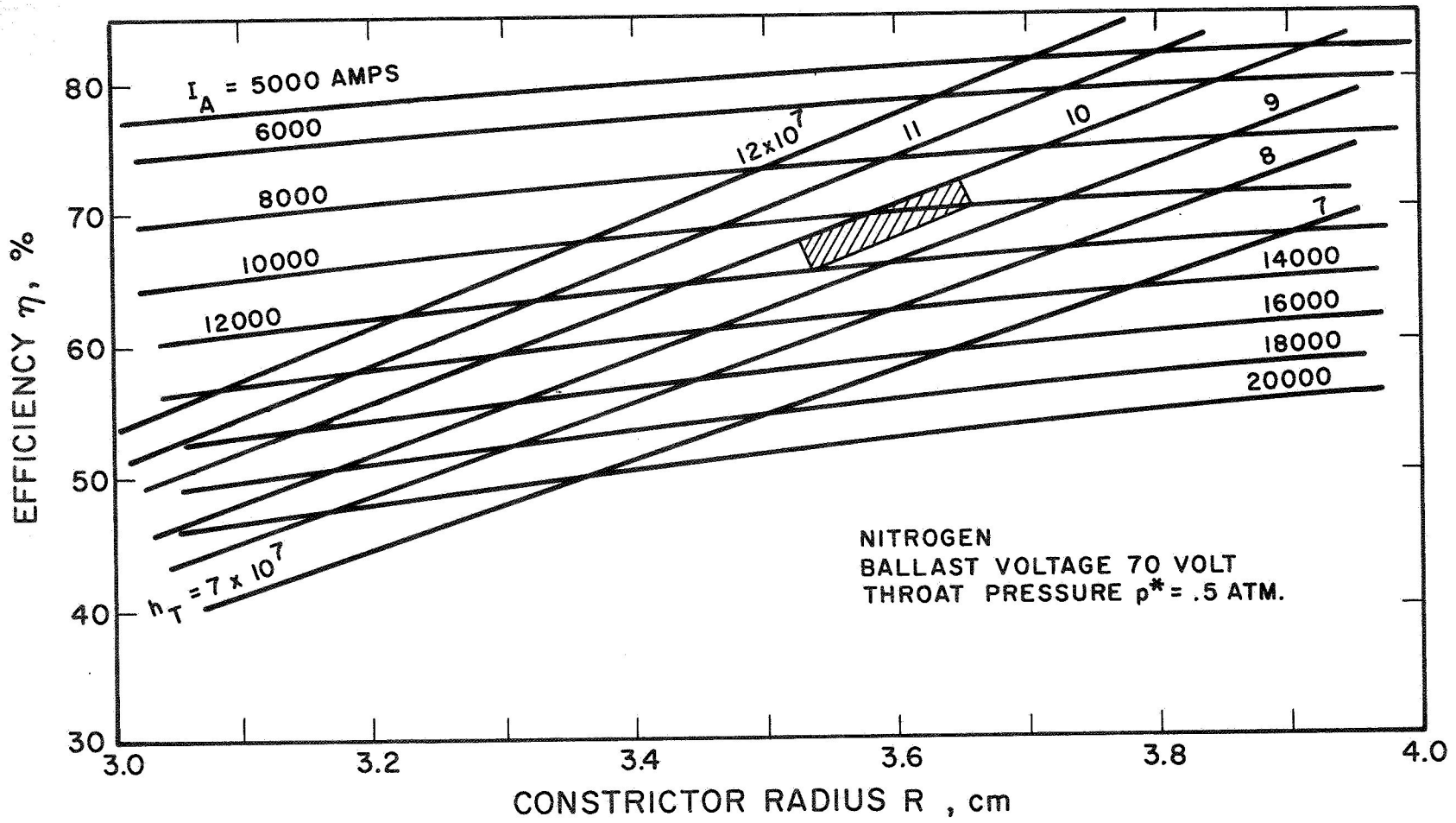

FIG. 6-2 DESIGN CHART FOR A 10 MEGAWATT CONSTRICTED ARC HEATER
(Efficiency, Constrictor Radius, and Arc Current)

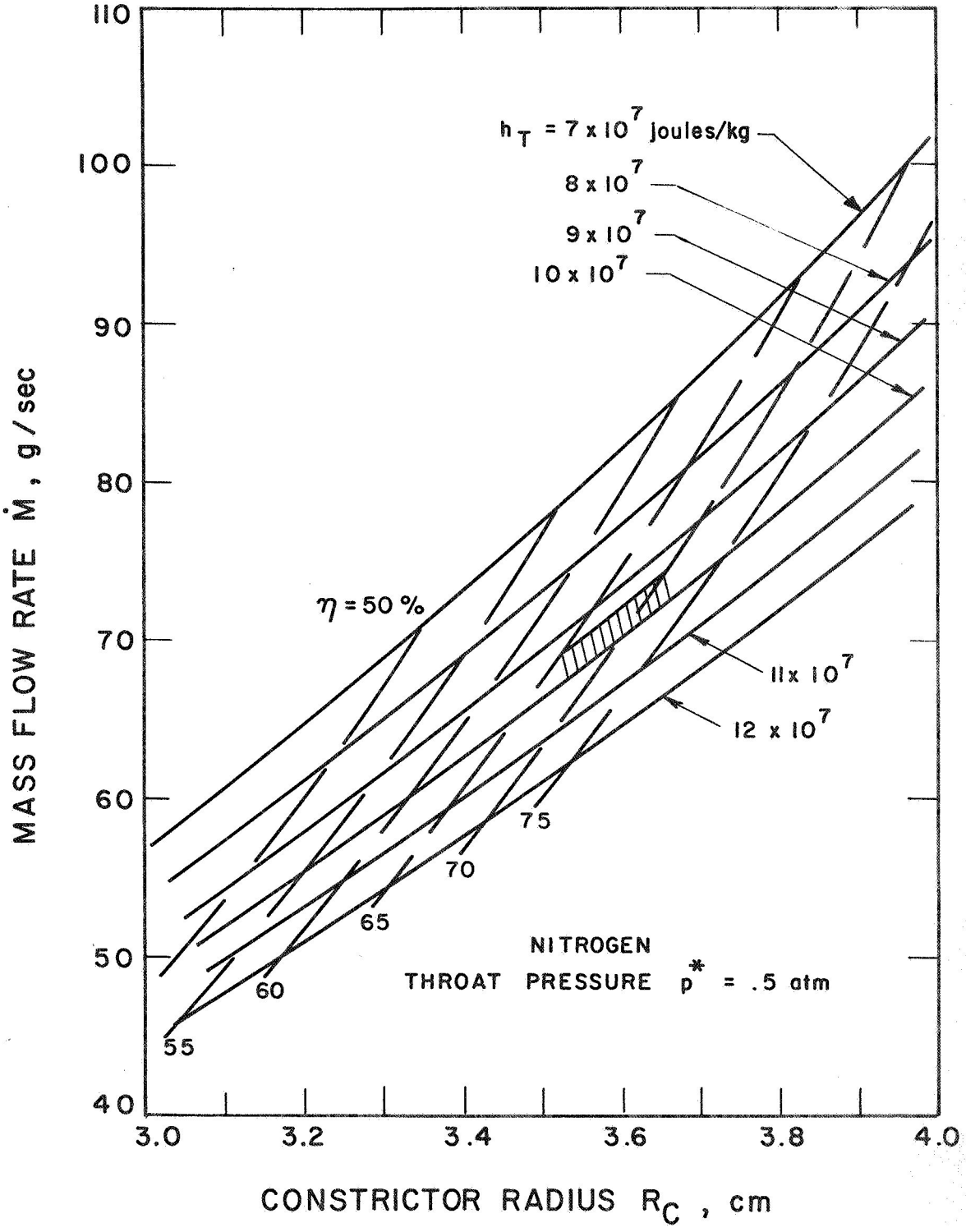

FIG. 6-3 DESIGN CHART FOR A 10 MEGAWATT CONSTRICTED ARC HEATER (Mass Flow Rate, Constrictor Radius, Total Enthalpy, and Efficiency)

73618860

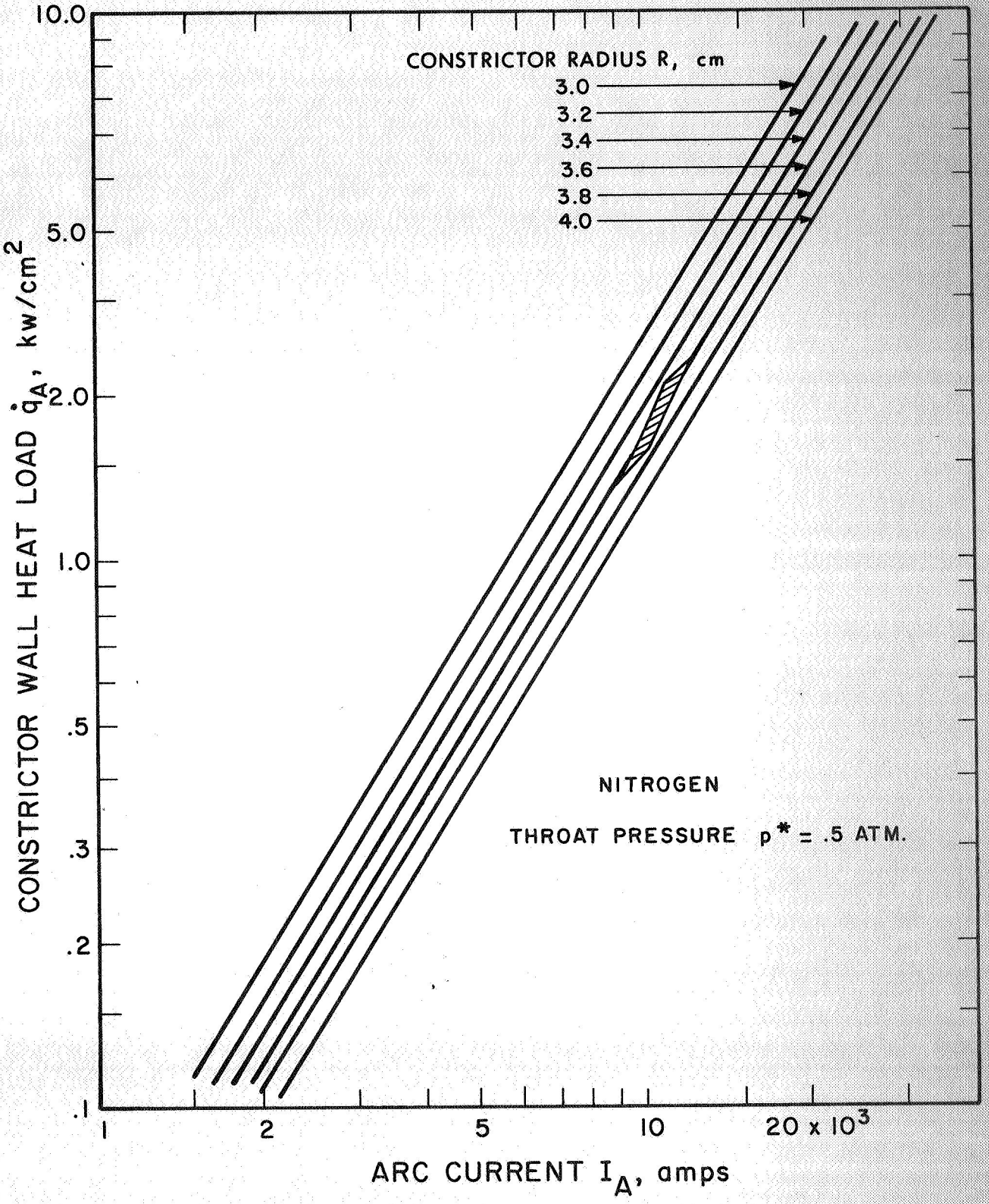

FIG. 6-4 DESIGN CHART FOR A 10 MEGAWATT CONSTRICTED ARC HEATER (Constrictor Wall Heat Load, Arc Current, and Constrictor Radius)

constrictor wall heat loads of about 2 kW/cm^2 should present no severe problems for either the segments or the insulators, even in regions where there is a high oxygen concentration. Neither should the anodes present insurmountable problems, since they can be scaled to higher currents and can also be subdivided. Only at much higher pressures will the anode problem become a critical one.

The cathode, however, does present a definite problem for the 10,000+ ampere regime. Here, the pressure must be at least on the order of one atmosphere, and subdividing is generally more difficult than with the anodes. However, designing a 10,000-ampere cathode for operation in the 1 to 2 atmosphere pressure range should not be impossible. Also, it can be hoped that cathode studies, now in progress in several laboratories, will contribute to the solution of this problem.

It is concluded that the development of an efficient, 10 MW high-enthalpy, constricted-arc type heater is practicable and may be undertaken with an excellent probability of success.

7. AXISYMMETRIC MHD ACCELERATOR

7.1 Purpose

The inclusion of an ultra-high enthalpy axisymmetric MHD accelerator into the high enthalpy heater program was intended to demonstrate the feasibility and the potential suitability of a Hall-current type accelerator device for structural testing applications. Such a device was expected to achieve mass-averaged enthalpies in excess of the enthalpies that were believed attainable with constricted-arc heaters in the near future. It was thus considered as a backup to the high-enthalpy constricted-arc heaters. In addition, it is believed that the accelerators can achieve higher gas velocities than the constricted-arc heaters with expansion nozzles. The work to be performed was limited in scope and was to provide a foundation for possible future development of such a device.

7.2 Design of the Axisymmetric MHD Accelerator

Very little background material was available for use in the design of the accelerator, particularly in terms of the power, tank pressure regimes and type of gas of interest here. Most of the work on Hall-current devices had been done on propulsion devices for which the total thrust in a high-vacuum tank had been measured. Flow, density, enthalpy, and pitot pressure distributions were not available for design purposes.

The design of the accelerator had only one basic design criterion. This was the estimated arc current of 2000 amps minimum to be carried by a tungsten-tipped cathode and copper anode in order to reach a power level of at least 200 kW. The copper anode size was determined by the inner diameter of a magnetic field coil which was to be made available from another project. The design was, in general,

a scaled-up version of the Hall accelerator thrustors which had been operated up to an arc power of approximately 90 kW. However, a much larger and stronger coil was used to permit a sufficiently high Hall parameter at tank pressures much higher than those used for propulsion work (say 2 to 10 mm Hg or higher).

The accelerator design that evolved from these considerations is shown in Fig. 7-1. In Figs. 7-2 and 7-3 the accelerator is shown mounted on the vacuum door flange with the field magnet in place.

The field magnet was a coil with the capability of developing axial field strengths of 24,660 gauss at its center, and 27,000 gauss at its inside diameter, with a current of 3000 amps. Under these conditions, the total power in the coil would be 612 kW. The accelerator was mounted with the coil in such a position that the anode remained 1-inch inside the coil. At this point, the axial magnetic field strength on the centerline was 6.7 gauss/amp or 81.7 percent of the maximum axial field strength.

7.3 Testing of the Axisymmetric MHD Accelerator

Testing of the accelerator was initiated to determine a regime of stable and safe operating conditions. The accelerator was started with a small flow of argon at a tank pressure of approximately 1.6 mm Hg. After ignition, the main nitrogen flow was started and the argon flow turned off. Since the start of the arc occurred at an open voltage of less than 200 volts, no special precautions against high starting currents were indicated.

The initial test was run with a magnet current of 500 amps. This magnet current appeared to be insufficient to move the arc attachment point on the anode. When the magnet coil current was raised to 1000 amps, the arc attachment points on the cathode as well as on the anode appeared diffuse. At this point, the noise on the recorded magnet current trace disappeared, indicating that the previously present small arcs to the coil had also been eliminated by the stronger field.

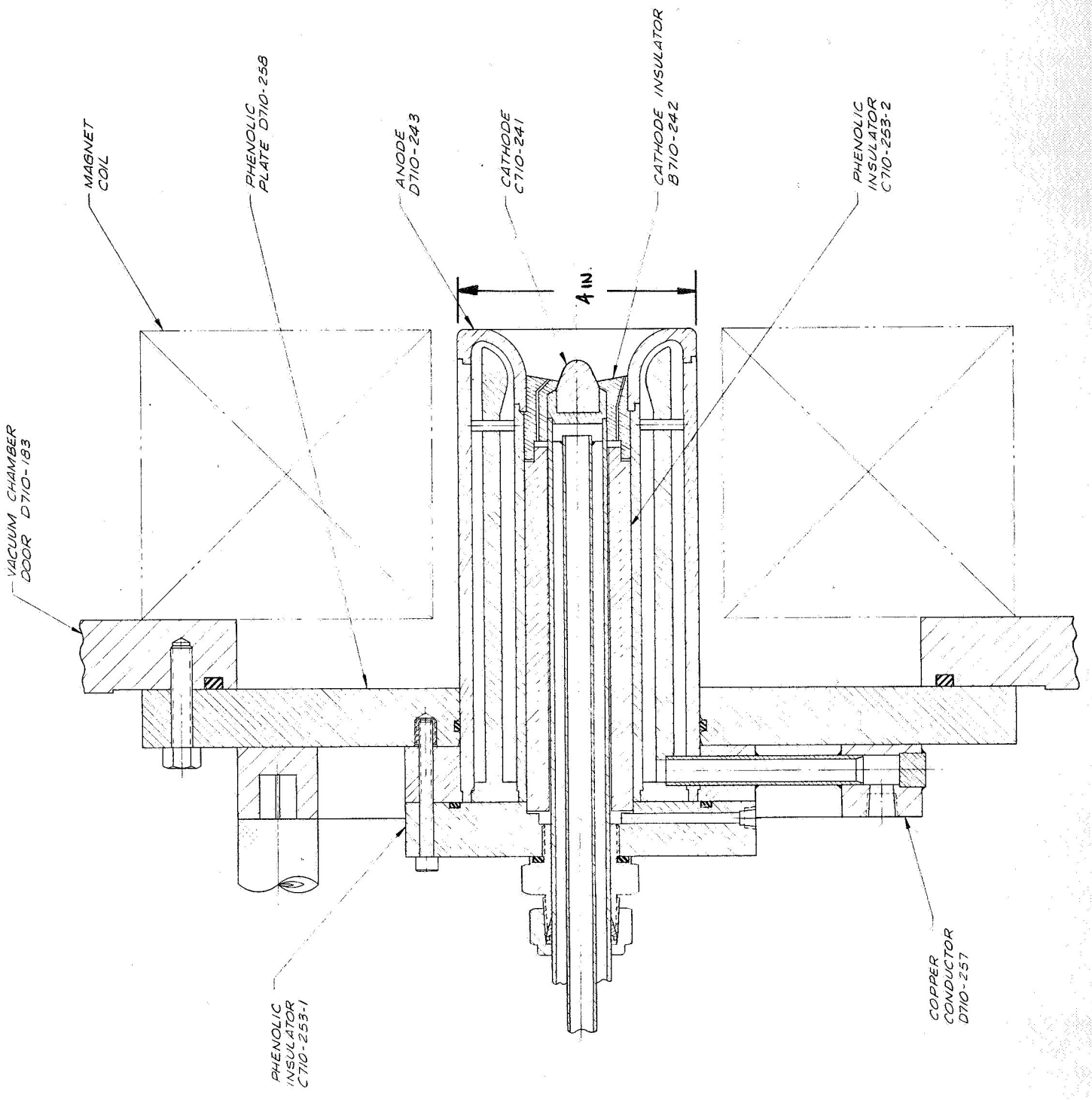

FIG. 7-1 HALL CURRENT ACCELERATOR ASSEMBLY

FIG. 7-2 HALL CURRENT ACCELERATOR INSTALLATION ON VACUUM TANK LID

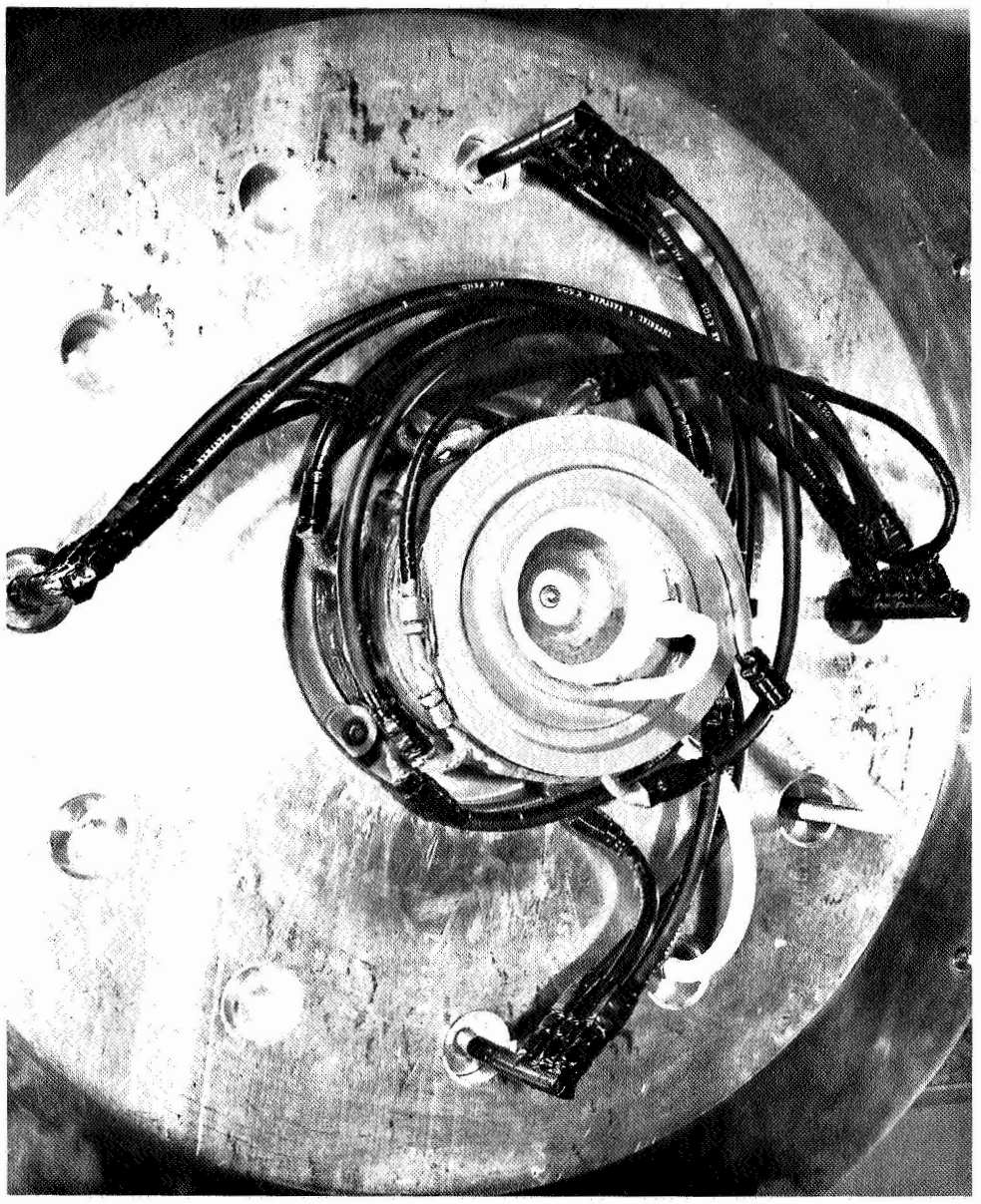

FIG. 7-3 HALL CURRENT ACCELERATOR WITH MAGNETIC FIELD COIL

The initial tests proved the design of the accelerator to be adequate for the intended future investigations. Run durations were not limited as far as the accelerator was concerned. Ten to twenty minute runs were typical.

7.4 Measurements

The principal measurements to be taken were the pitot pressures in the accelerator jet. These proved to be rather difficult to obtain because of the nature of the Hall accelerator jet. By the interaction of the applied magnetic field and the arc current, the arc is extended into the jet. The extension of the arc is a function of the magnetic field strength and the arc current. This "looped" arc produces an electric field in the jet that leads to undesirable arc attachments on any probes brought into the jet. The arc attachments result not only in electrical noise problems superimposed on the quantity to be measured but also, occasionally, in destructive puncturing of water-cooled instruments. In addition, such arc attachments must distort the jet itself which might invalidate the measurement.

After several failures of pitot probes complete electric insulation of the probe was achieved. The second problem was the sharp gradients in pitot pressure across the accelerator jet. This peculiarity, together with a desirable fast traverse of the jet, made the use of an X-Y recorder difficult. Normally the X-Y recorder would be the most convenient means for directly plotting pitot pressure-versus radial position. The pitot pressures and the probe positions were finally successfully recorded on a chart recorder without further difficulty.

7.5 Results

Some typical results of pitot pressure traverses are shown in Figs. 7-4 and 7-5. These results were obtained at tank pressures substantially higher than those in which Hall accelerators had previously been operated. The tests were conducted with nitrogen mass-flow rates of 6 and 4g/sec. The distinct increase in pitot pressure

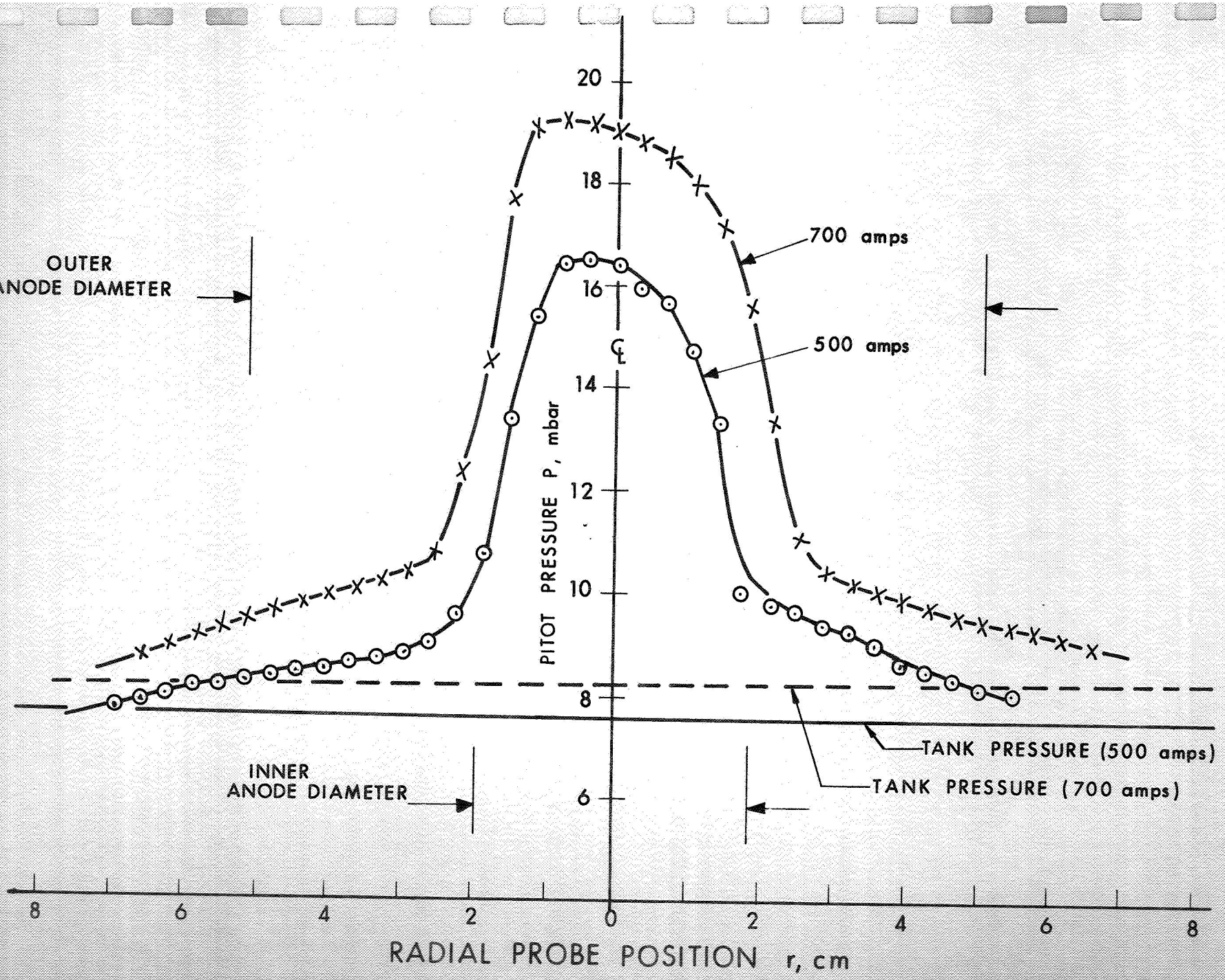

FIG. 7-4 PITOT PRESSURE DISTRIBUTION OF HALL CURRENT ACCELERATOR OPERATING WITH 6 g/sec NITROGEN (Magnet Current 1000 amps)

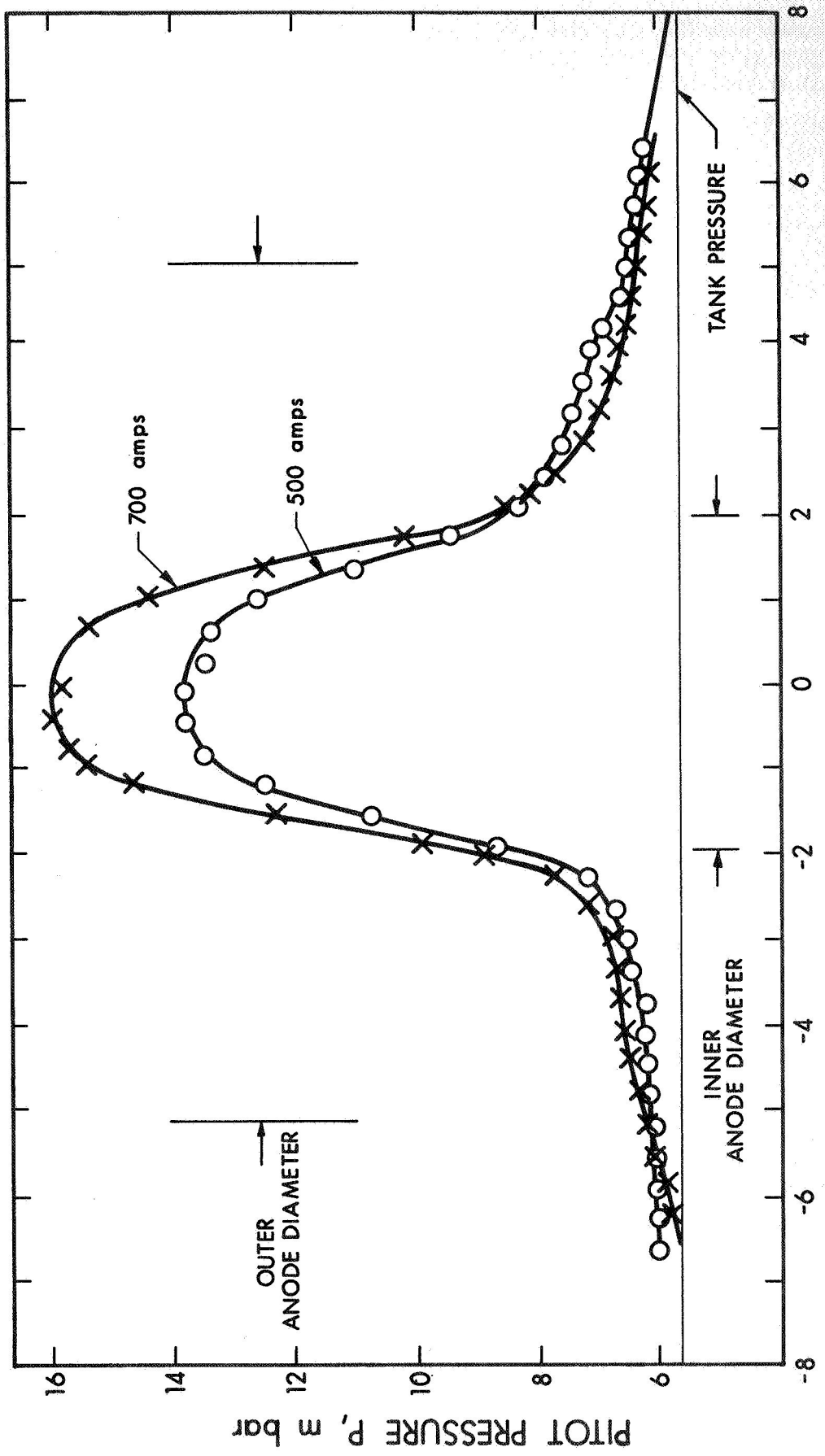

FIG. 7-5 PITOT PRESSURE DISTRIBUTION OF HALL CURRENT ACCELERATOR OPERATING WITH 4 g/sec NITROGEN (Magnet Current 1000 amps)

73620304

across the jet is a good indication that the MHD effect, which leads to the acceleration of the gas, has not been eliminated by the higher tank pressures and that the desired stagnation pressures for the entry simulation application could be reached.

Complete evaluation of the test results and their extrapolation indicate that the mass-flow rate should have been lowered to 1-2 g/sec. At 4 to 6 gm/sec the arc power was not sufficient to dissociate and strongly ionize the gas. Further, the test results and concurrent calculations seemed to show that, for the intended total arc power, ~ 200 kW, the anode diameter should be decreased if really interesting pitot pressures (say 1/10 atmosphere or higher) are to be obtained. For the given accelerator all results pointed in the direction of stronger fields (for higher arc voltage), higher arc current and reduced mass flow through the accelerator, but with the tank pressure held as high or higher than before.

While the mean jet velocities achieved to date with this accelerator (estimated from the pitot pressures) were not yet spectacular (~ 1600 m/sec) some useful information was gained from the tests. First, the pitot pressure profiles are uniform across the jet, and they indicate a well defined jet size. This jet diameter was roughly equal to the inner anode diameter, at the axial station where most of the surveys were made.

Second, the pitot pressures increased steeply with increased current. Thus one can estimate the current regime required for desired pitot pressures and gas velocities.

The successful operation of the axisymmetric (ultra-high enthalpy) accelerator with nitrogen was demonstrated. The accelerator was run for extended periods over a range of operating conditions that permitted good pitot pressure surveys and some initial correlations and evaluations of the device. The test data are not yet sufficient or in the right regime to permit the full evaluation of the device for high-speed entry simulation. However, the initial results

were encouraging in showing a well defined and only slightly diverging jet which may become suitable for structural testing at very high enthalpies.

8. SUMMARY AND CONCLUSIONS

8.1 Objectives

The primary objective of this program was the development and delivery of a 1MW Constricted Arc Heater suitable for materials testing at the NASA-MSC facility and meeting the following performance goals:

Total enthalpy, in useable part of the test jet	9.3×10^7 j/kg (40,000 Btu/lb)
Heater efficiency at design enthalpy - at least	50 percent
Rated input power	1MW
Stagnation pressure range (approximate)	0.5 - 2.0 atm
Minimum life (without maintenance)	5 hours

Secondary objectives of the program were:

1. The presentation of arc heater design information, and design estimates for 10 MW-class high enthalpy heaters.
2. The feasibility demonstration of an axisymmetric (Hall arc-jet type) MHD accelerator for future entry environment simulation testing at still higher enthalpies.

In general, the above objectives were all met, and the heater performance goals were exceeded by comfortable margins. The heater was delivered on schedule.

8.2 Discussion of Results

The basic design configuration chosen was that previously proven out by Shepard et al, at Ames. It consists of a simple up-stream cathode, a highly segmented constant diameter constrictor, and multiple anode pins located in the supersonic expansion nozzle.

This configuration proved entirely satisfactory for the primary purpose of the heater, namely for supersonic jet type testing in a vacuum tank. For later testing at pressures near 1-atm (subsonic jet testing) the anode design has to be modified.

A characteristic of this type of heater is that it can operate in only one single arc mode. The arc as well as the jet, therefore, exhibits an unusual steadiness and stability over the entire range of operating parameters. The jet is completely free from rotation and contamination. Its performance is completely predictable and repeatable for each current and flow rate.

The heater reaches the design mass averaged enthalpy (9.3×10^7 j/kg) at about 1.2 atm stagnation pressure, with an efficiency of 59 percent, and a mass flow rate of 6.4 g/sec. This is achieved at 1540 amp and 650 volt. At different mass flow rates and current values a broad range of enthalpies and stagnation pressures is accessible. Enthalpies up to 1.32×10^8 j/kg (57,000 Btu/lb) and stagnation pressures between 0.5 and 2.0 atm were reached experimentally, but these do not constitute limiting values for this heater.

The 5-hour life was demonstrated in a test sequence covering 31 starts, frequent cycling through the full current range, and several long runs at currents up to 1600 amp. Throughout this demonstration all performance points were repeated within measuring accuracy. After this test series the heater showed no deterioration or wear except for a small rough area in the center of the tungsten cathode.

As a result of this test, a maintenance-free service life of many times the 5 hour test duration may be projected. Excluding possible cathode replacement, all heater components should last for very long periods. No recalibration of the heater test jet should be necessary except after major overhauls or intentional changes of the constrictor length.

For the design of future constricted arc heaters in the 1-10MW regime and for moderate pressures (below ~ 10 atm) the constrictor wall heat loads and performance appears to be quite well predictable by semi-empirical design and scaling rules given in this report. The purely theoretical computer solutions of the laminar flow arc by Watsons program agree qualitatively with experimental results, but important unresolved uncertainties in the theory and the input gas properties prevent reliance on the theory alone at present. Both the theoretical and the semi-empirical predictions make a 10MW heater for the same enthalpy and pressure range as the 1MW Model seem entirely feasible and promising, with currents of ~ 8000 amp and constrictor wall heat loads of the order of 2 kW/cm^2.

The electrode design of these arc heaters is still almost entirely empirical and intuitive, except for a few simple heat flow calculations. In the present heater the low pressure anode pins were virtually trouble-free from the start. The cathode first presented erosion problems, which were corrected by redesign (better heat flow distributions) and by changing the gas flow near the cathode.

The axisymmetric (Hall-arc-jet type) gas accelerator was operated successfully and for extended periods on nitrogen, at tank pressure and power levels appreciably above those previously achieved (in plasma propulsion work). The velocity increments so far achieved were still low, on the order of 1500 m/sec, but they increased consistently with increasing current. Gas velocities and pitot pressures in the range of greatest interest for high-speed entry simulation appear feasible with extensive future development. The pitot pressure surveys indicate that the resulting jets could be suitable for structure testing.

Constricted arc test heaters of the 10MW class should be capable of eventually reaching any enthalpy level which is presently anticipated as an entry simulation requirement. To facilitate their development, continued research on large flow arcs, and incisive new research on electrodes appear indicated.

APPENDIX A

ARC COLUMN MEASUREMENTS WITH THE 0.5-CM I.D. CASCADE APPARATUS

APPENDIX A

ARC COLUMN MEASUREMENTS WITH THE 0.5-CM I.D. CASCADE APPARATUS

1. BACKGROUND AND OBJECTIVES

Testing of the 0.5-cm I.D. cascade apparatus was performed at the beginning of the project. This work had three general objectives. The first objective was to generate test data which could be used for comparison with existing, approximate constricted arc theories. The purpose of this comparison was to determine the accuracy of these theories, the reliability of the available transport properties of nitrogen, and the usefulness of such theories for the design of the 1-megawatt, 2-cm diameter, constricted arc heater.

The second objective was to generate empirical heat transfer data needed for the design of the 2-cm diameter constrictor segments. The third objective was to obtain general correlations of parameters with a 0.5-cm diameter constrictor which could be used later with test data from the 2-cm diameter constrictor for the development of semi-empirical scaling rules and design charts.

Besides these three general objectives, a specific question to be settled by the experiments with the arc cascade apparatus was the optimum segment and insulator thicknesses for the 2-cm diameter heater. It was first stated by Maecker, and accepted by other investigators, that arc attachment to the cascade constrictor wall, i.e., secondary arcs between the segments, could be reliably avoided only if the electrical potential across each metal segment was held lower than the voltage drop required for a secondary arc. Unfortunately, this voltage drop is not a fixed quantity. There are indications that it decreases considerably with increasing temperature of the arc plasma near the wall, since the anode fall potential can approach zero under

these conditions. In recent experiments with nitrogen at very high temperatures, Maecker found it necessary to reduce the segment thickness from the usual 5 mm to 2 mm in his 5-mm diameter cascade channel. This would correspond to ~ 14V per segment. Using this criterion, a segment thickness of about 8 mm was indicated for the 1-MW heater.

The use of thicker boron nitride insulators is desirable for two reasons. The first one is that they are less fragile. The second reason is that the thinner insulators are more easily "shorted out" by small tungsten particles from the cathode which can deposit on them. Thus, the shorting of segments and subsequent arc attachment becomes less likely. These tests proved that the thicker insulators (up to 3 mm) could withstand the constrictor heat loads.

2. TEST SETUP

The 0.5-cm diameter arc column cascade apparatus consists of ten water-cooled copper segments which are isolated from each other by boron nitride insulator segments (Fig. A-1). The arc is drawn through the cascade from the center cathode located at the entrance of the constrictor to the anode at the exit of the cascade. The anode is separated from the last column segment by a 0.71-cm thick insulator.

The cascade apparatus is operated with varying gas flow rates and currents, but with a constant pressure of 1 atm in the anode region. This pressure is regulated by bleeding additional gas into the anode chamber. In this investigation, the working gas and the bleed gas were nitrogen for all tests.

During each test the following measurements were taken:

1. Potential difference between adjacent metal segments
2. Water flow rate through each metal segment
3. Temperature rise of cooling water in each individual segment
4. Total arc current
5. Total arc voltage
6. Gas flow rate

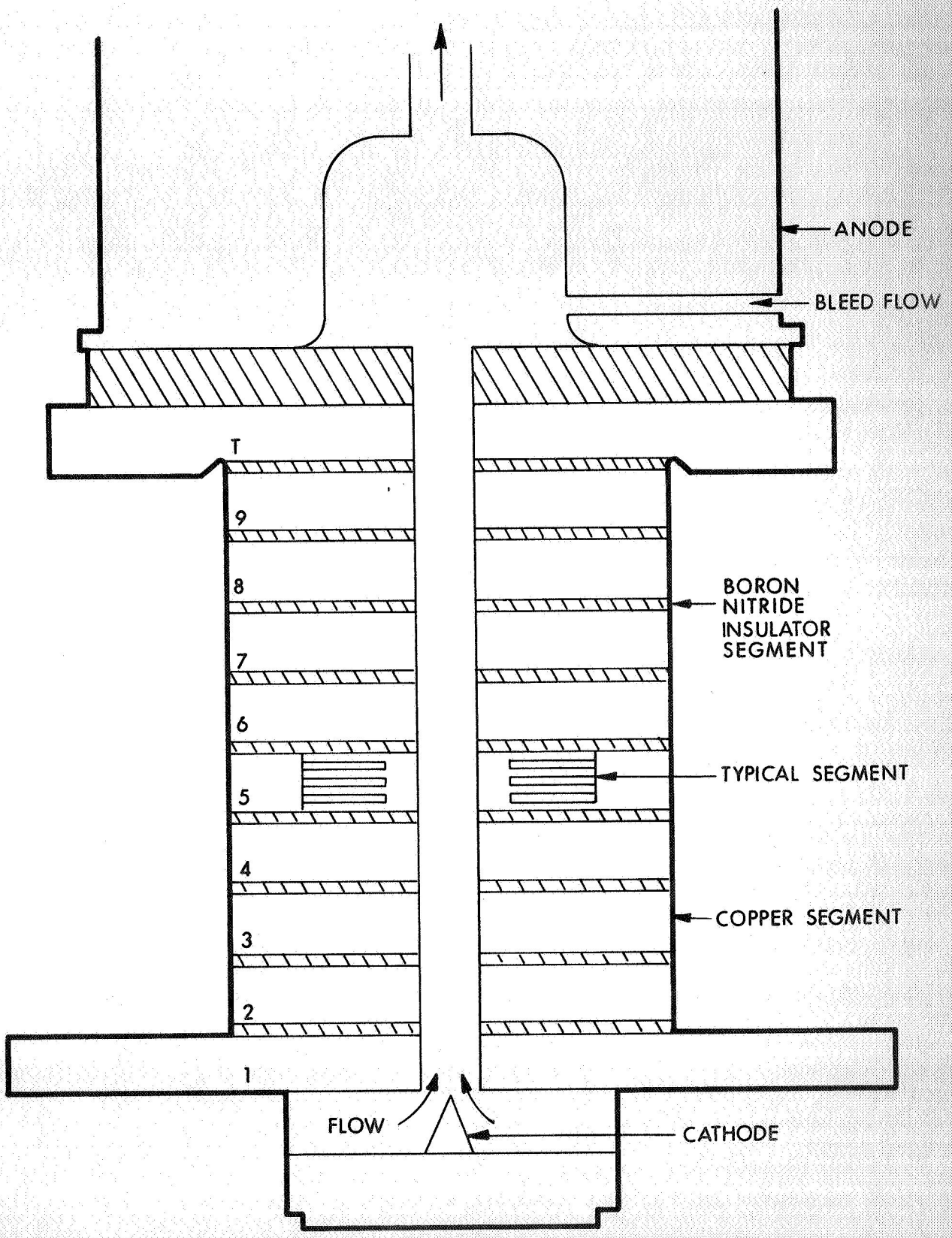

FIG. A-1 0.5 CM DIAMETER CONSTRICTED ARC COLUMN APPARATUS

3620252

3. TESTING OF THE ARC COLUMN WITH VARIOUS INSULATOR AND METAL SEGMENTS

Four configurations were tested, which differed from each other by the thickness and the arrangement of several metal segments and insulator segments in the constrictor. In configuration 1, all insulator segments were 1 mm thick and all water-cooled copper segments 5 mm thick. In configuration 2, three insulators of 3 mm thickness were placed in the exit region of the constrictor. In configuration 3, the 3-mm thick insulator segments were placed into the entrance region of the channel. In configuration 4, the first five water-cooled copper segments were only 0.25 cm thick while all insulator segments were 1 mm thick (see Figs. 1 and 2 and the lower scales of the graphs).

3.1 Potential Gradients

The electric field was determined by measuring the potential differences between the metal segments as shown in Figs. A-2 through A-6. By comparing the electric field measured in the constrictor of uniform segment arrangement (Test 1) with the electric fields of configurations 2 through 4, the locally measured electrical potential appears to be affected by the change in the metal length to insulator length ratio in the constrictor. The apparent electric field seems always to increase at the beginning of the region in which the metal length to insulator length ratio has been increased. It drops, however, at the end of that region by such an amount that the effect of the change in the segment thicknesses on the average electric field for the entire column becomes negligible. This is true whether this effect has been created by thicker insulator segments (configurations 2 and 3) or by thinner metal segments (configuration 4). This indicates that the apparent electric field change is really a shift in the mean potential which individual segments assume at the point where the spacing changes; i.e., this is simply an experimental uncertainty.

3.2 Enthalpy Distribution

For the calculation of the enthalpy distribution along the constrictor, it was assumed that the energy in the gas is equal to the

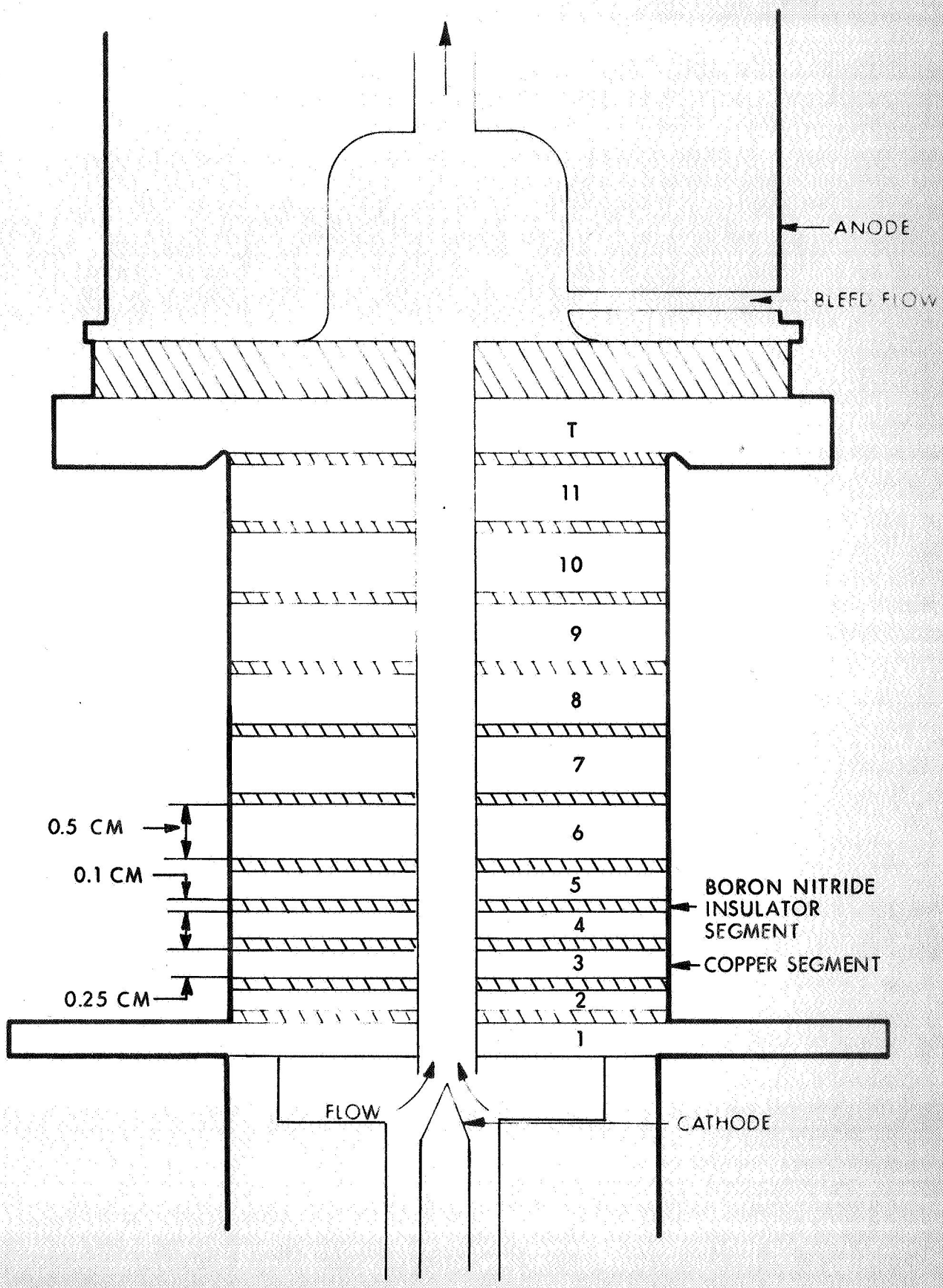

FIG. A-2 0.5 CM DIAMETER CONSTRICTED ARC COLUMN APPARATUS
(segment arrangements for Test 4)

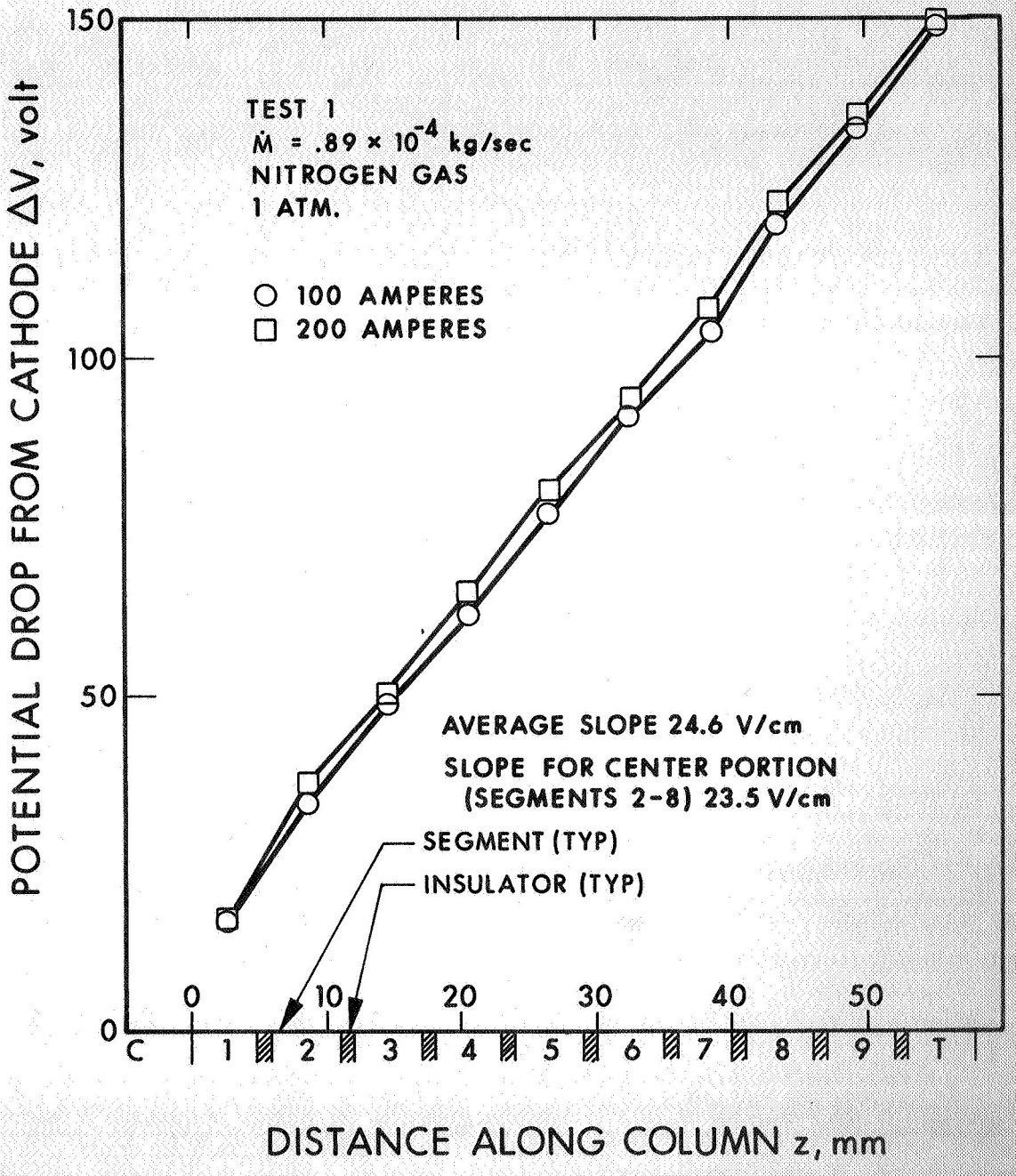

FIG. A-3 POTENTIAL DROP ALONG A 0.5 CM DIAMETER CONSTRICTED ARC COLUMN

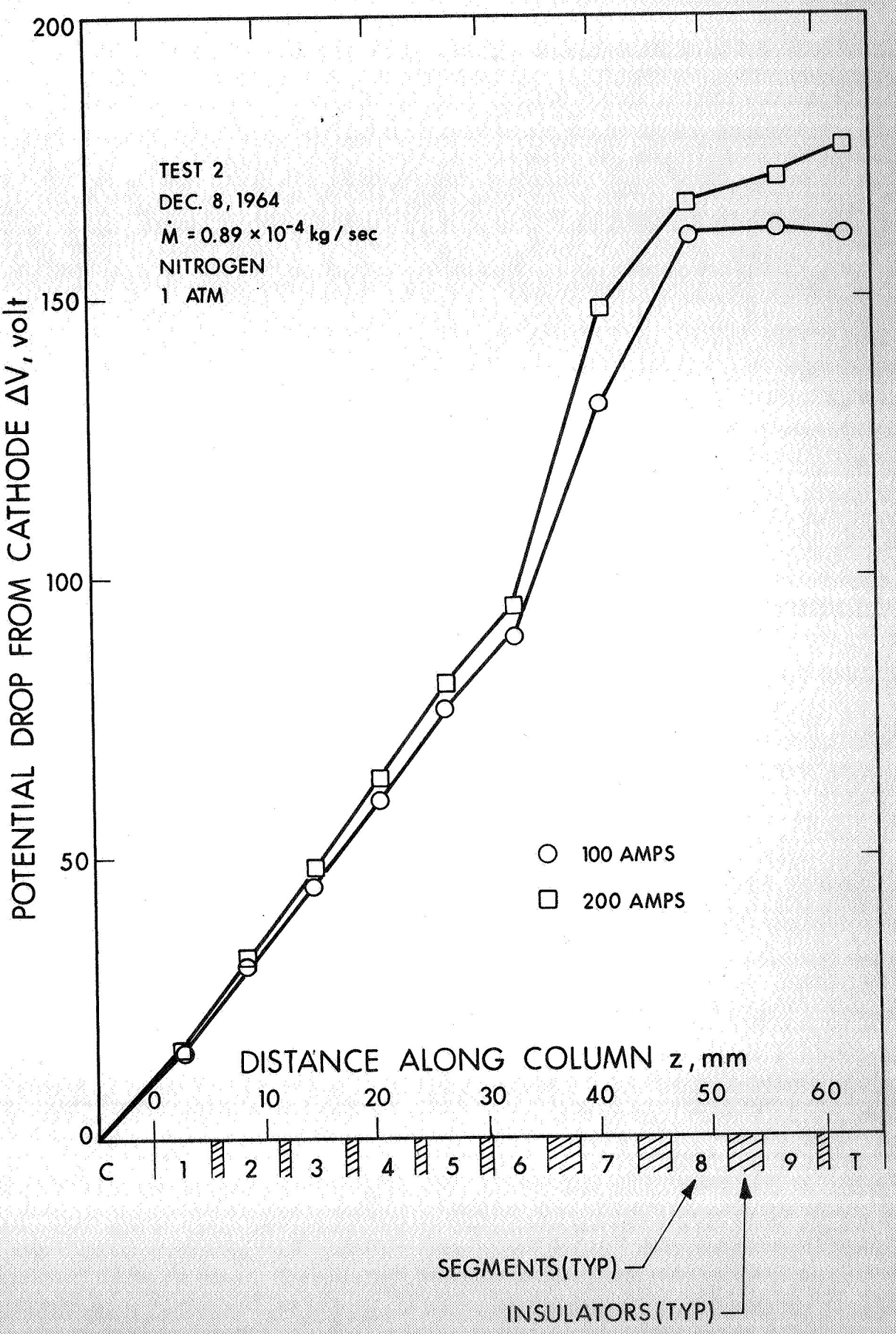

FIG. A-4 POTENTIAL DROP ALONG 0.5-cm-DIAMETER ARC COLUMN

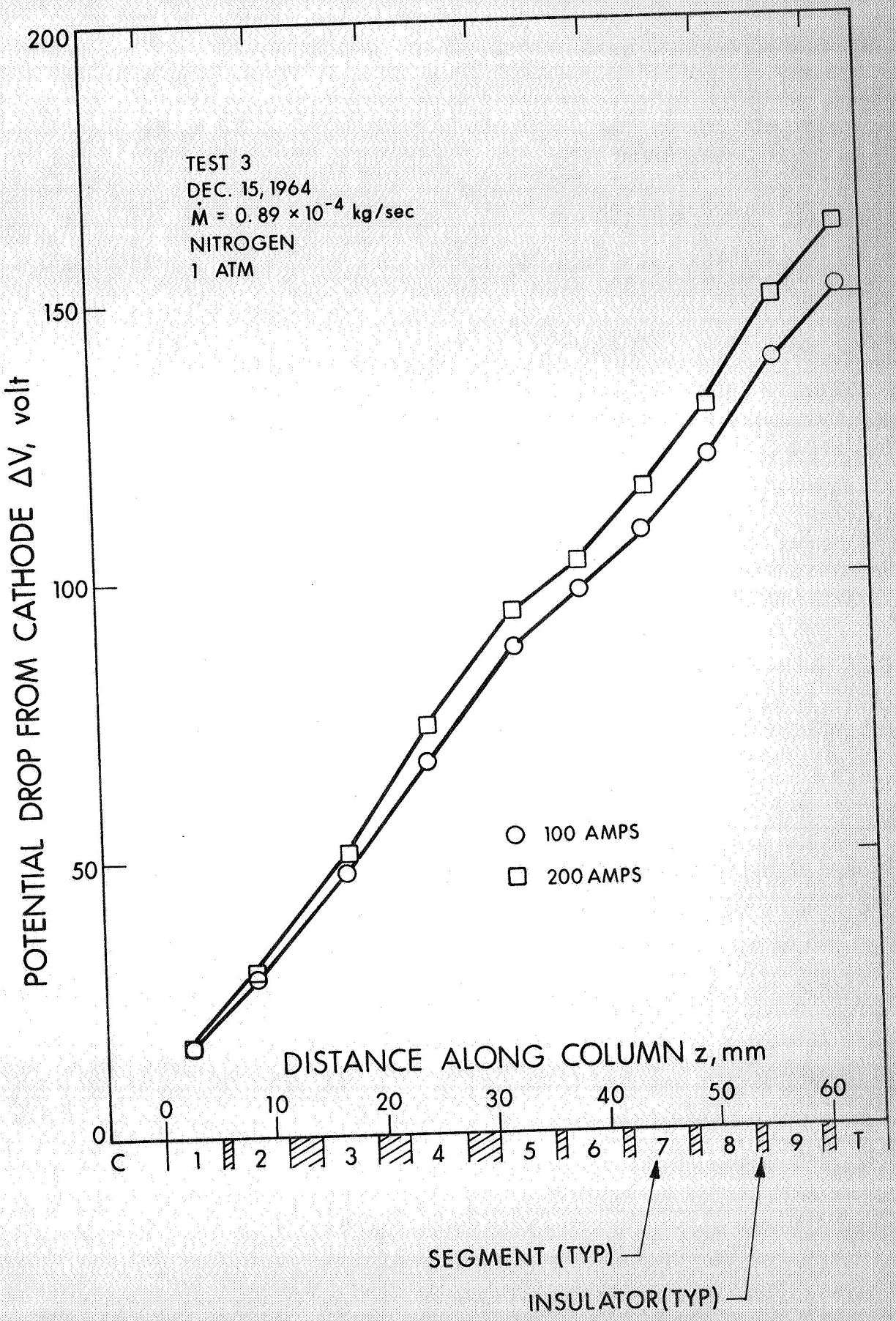

FIG. A-5 POTENTIAL DROP ALONG A 0.5-cm-DIAMETER ARC COLUMN WITH VARYING METAL-TO-INSULATOR RATIO

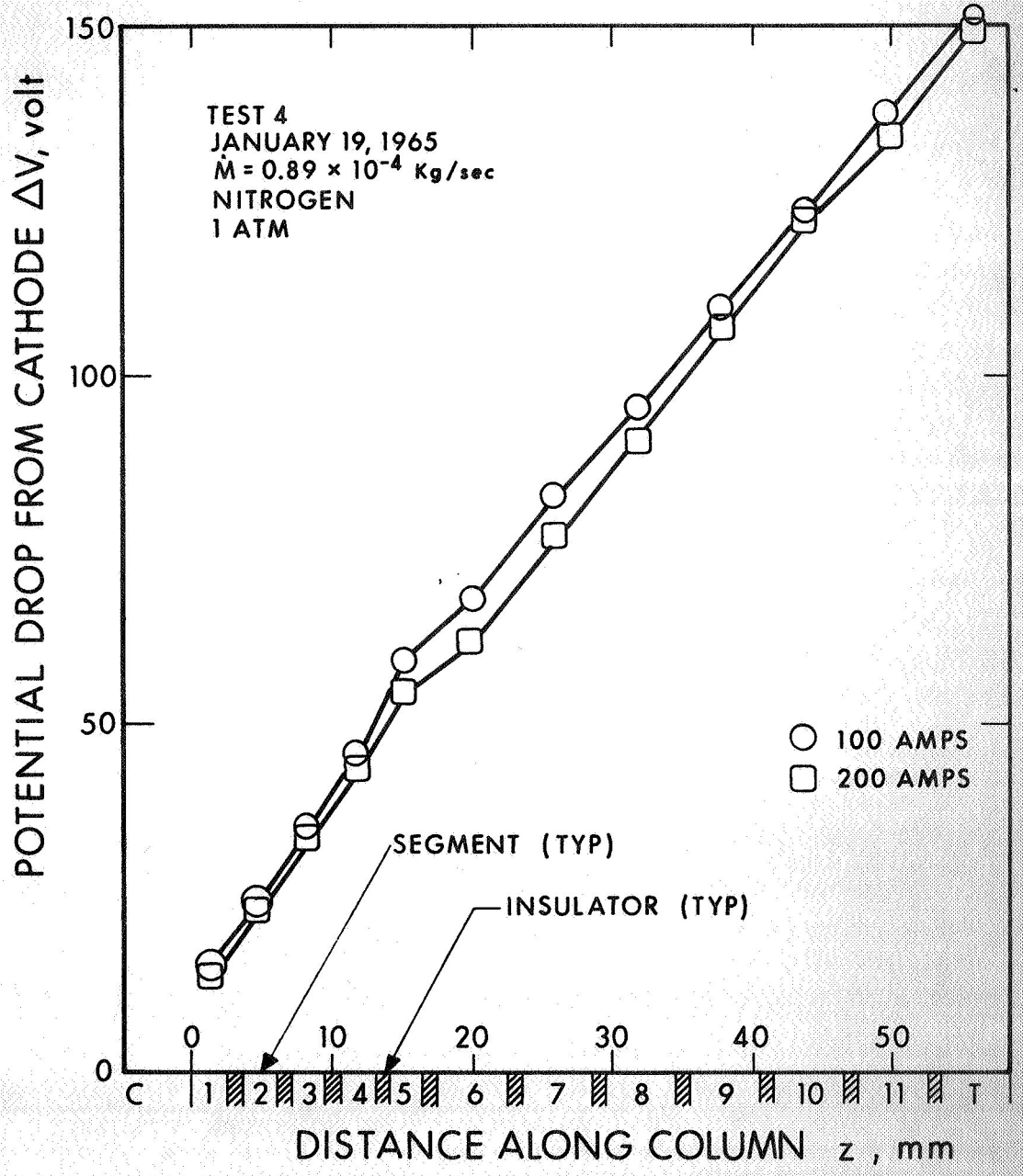

FIG. A-6 POTENTIAL DROP ALONG A 0.5-cm-DIAMETER ARC COLUMN WITH VARYING COOLED COPPER SEGMENT THICKNESSES

20253

potential drop times the arc current, minus the heat flux into the constrictor wall, as measured by the coolant flow rate and the coolant temperature rise. The enthalpies determined from these measurements are shown in Figs. A-7 and A-8. The final enthalpy of configuration 2 with the thicker insulator at the end of the column seems to be slightly higher than the final enthalpies of configurations 1 and 4. But the final enthalpy of configuration 3 is lower. This result seems to be inconsistent with the results of configurations 1, 2, and 4. No explanation can be given. It might have to be attributed to the combined errors in the water flow and temperature measurements.

3.3 Energy Transfer

In Fig. A-9, the energy transfer to the constrictor wall is plotted against the total enthalpy which was calculated by the method described above. Before the test results from the 2-cm diameter constrictor were available, it had been thought that the energy transfer in the 0.5-cm diameter constrictor would be convection dominated. The heat transfer to the constrictor was therefore expected to be predominantly a function of the total enthalpy. This assumption was supported by the results from some numerical calculations and by the presentation of numerical data presented in Ref. 7. When plotting the experimental data there seemed to be a correlation between energy transfer and total enthalpy indicated. The difficulty in discovering the additional dependence of the energy transfer on the arc current from the tests was brought about by the fact that the lower enthalpies and the lower heat transfer values were almost entirely obtained with an arc current of 100 amps, while the higher enthalpy and heat transfer regime belonged exclusively to the 200 amp arc operation. For this reason, the effect of current on the energy transfer was not evident.

Only after the correlation between energy transfer and arc current had been established, from the results of the 2-cm diameter constrictor (laboratory model heater) as expressed by relation 6-10, could the heat transfer data of the small cascade tests be correctly

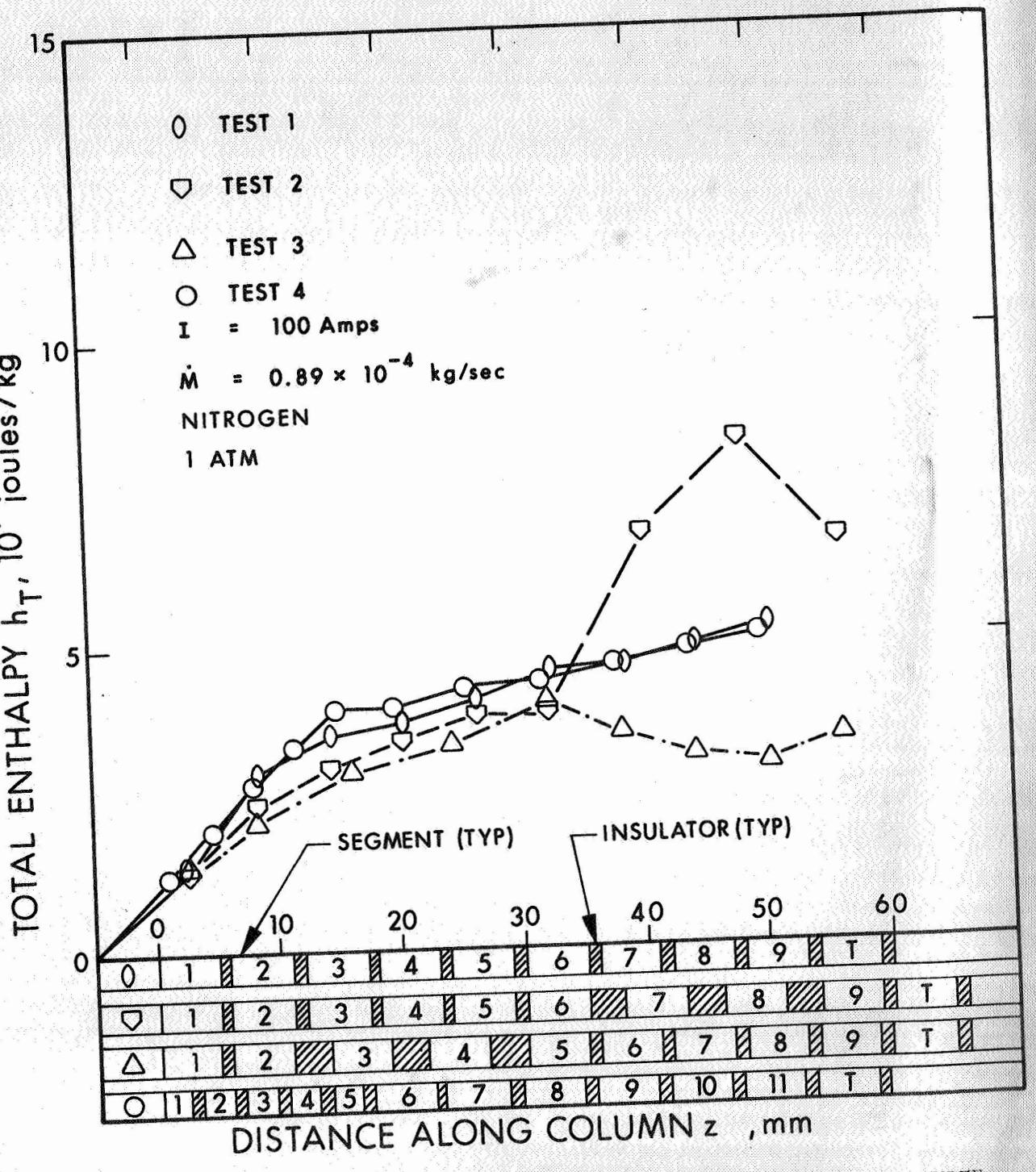

FIG. A-7 TOTAL ENTHALPY ALONG A 0.5 CM DIAMETER ARC COLUMN FOR THREE DIFFERENT CASCADE BUILD-UPS

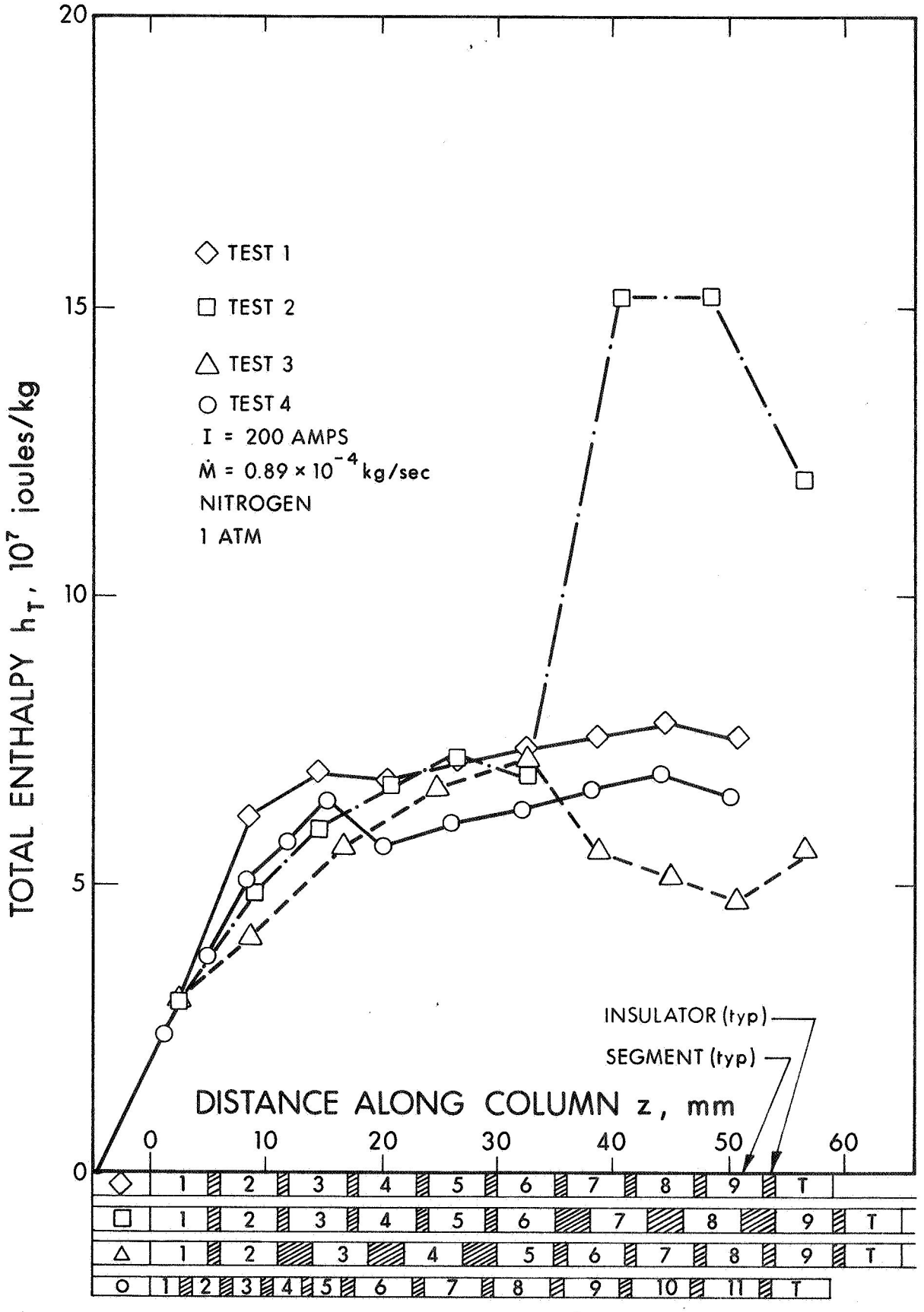

FIG. A-8 TOTAL ENTHALPY ALONG A 0.5 CM DIAMETER ARC COLUMN FOR THREE DIFFERENT CASCADE BUILD-UPS

interpreted. By now, applying relation 6-10, as found from the semi-empirical approach, the heat transfer data from the 0.5-cm diameter constrictor tests are found to be consistent. They actually confirm the semi-empirical results which were presented in Section 6 of this report.

4. CONCLUSION AND SUMMARY

In retrospect, and after the test results from the laboratory model heater were available, it may be noted that the measurements made with 0.5-cm I.D. cascade apparatus contributed initially very little to the design of the 1-megawatt 2-cm diameter constricted arc heater. The test had been conceived because there had been indications that the 2-cm diameter constrictor would operate between the convection and radiation dominated regime; i.e., with a mixed energy transfer to the constrictor wall. This is shown in Appendix B where computer calculations for the 2-cm diameter constrictor are presented. The experimental results have later proved that the 2-cm constrictor operates in the radiation dominated regime, while the 0.5-cm constrictor already operates at 200 amps in the mixed energy transfer regime. That meant, necessarily, that test results from the small cascade were not applicable to the larger heater design.

The test results of the 0.5-cm diameter cascade permitted, however, the evaluation of the transport properties and the theories that were to be used for the design of the 2-cm diameter constrictor. This evaluation pointed early in the program to the need of relying more on empirical correlations for design charts and scaling. The small scale cascade results proved useful in the following manner: By comparison of the small scale heat transfer data with the 2 cm results, it was possible to more clearly separate the relative contributions of the convective and the radiative transfer for both sizes. Thus, the semi-empirical radiation heat transfer relation (Section 6, Eq. 6-10) was verified for a different size by the small-scale results.

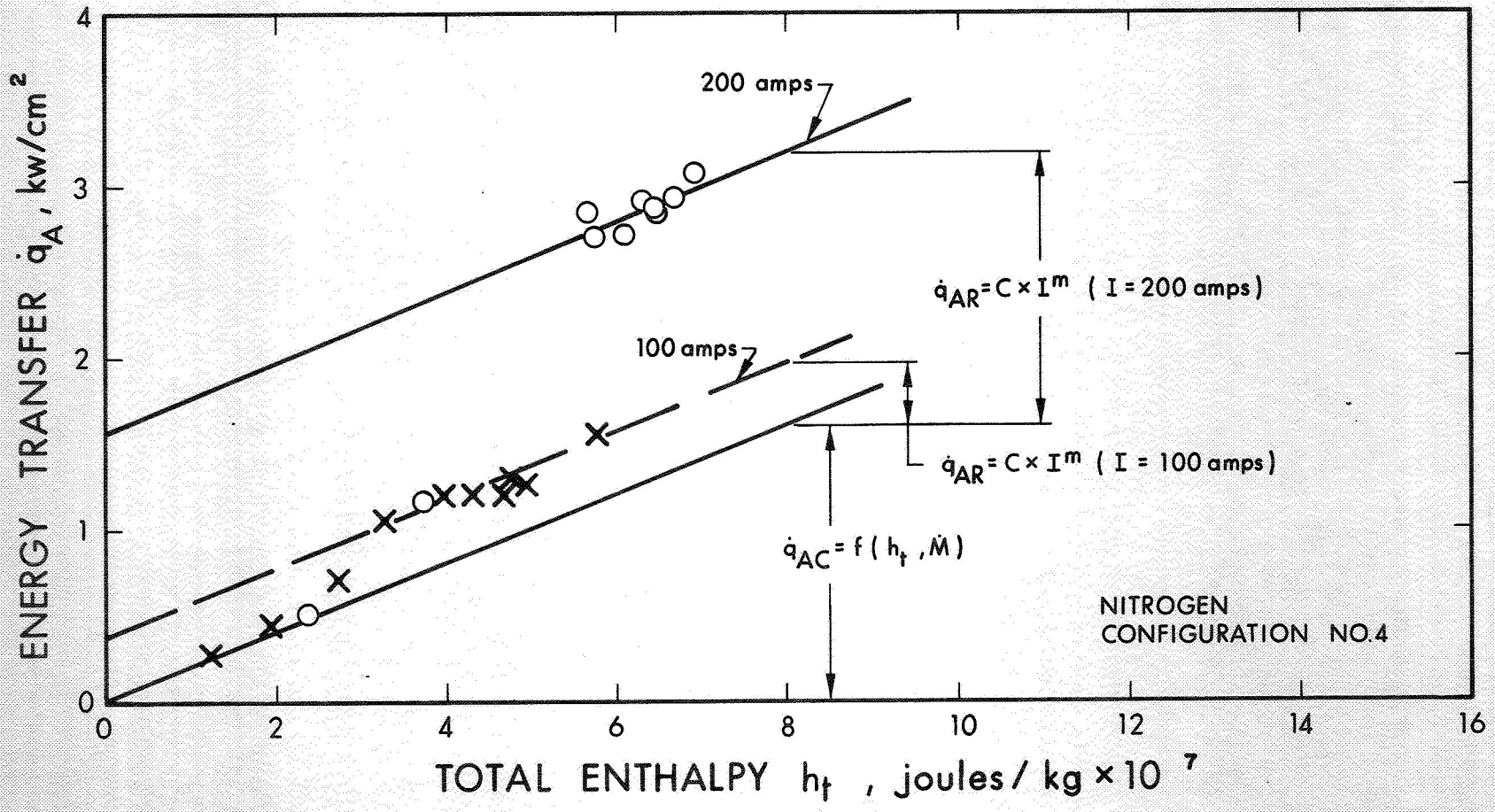

FIG. A-9 ENERGY TRANSFER TO CONSTRICTOR WALL A FUNCTION OF TOTAL ENTHALPY AND ARC CURRENT

APPENDIX B

COMPUTER CALCULATIONS

APPENDIX B
COMPUTER CALCULATIONS

Dr. G. Marlotte

Computer calculations were carried out by Velvin R. Watson of the Magnetoplasmadynamics Branch, Thermal and Gas Dynamics Division, NASA/Ames Research Center. The Stine-Watson arc heater calculation program was used, as reported in Ref. 4 and discussed further in Ref. 10. Various cases defined by current, I, mass-flow, $\dot{M}$, constrictor radius, R, and stagnation pressure, p, were run. They correspond to possible operating conditions of the present 2.0 cm I.D. (1 MW) arc heater and others of interest.

In order to run cases using the computer program, it is, of course, necessary to decide what values of the various plasma properites are to be used. This is no trivial matter with nitrogen because of large uncertainties which exist in the properties.

The plasma properties of particular interest are enthalpy, thermal conductivity, electrical conductivity, and specific radiated power as functions of the temperature and pressure. Other properties such as viscosity, etc., remained unchanged from the values already incorporated into the program as reported in Ref. 4.

In addition to examining the effects of parameters such as current and pressure, a major objective was to examine the results of using various groups of plasma properties chosen so as to reflect the present uncertainties in the properties, and to decide by comparison with experiment which of the theoretical property values were most nearly correct.

In order to accomplish this, three groups of properties were defined: "Yos-like", "Maecker-like", and "mixed". These classifications are discussed below.

B.1 Plasma Property Formulation

The work reported in Ref. 8 demonstrated that the pressure dependences of the properties can be closely approximated by powers of the pressure when the plasma properties are defined in a suitable manner. Since the computer program is set up so that all properties are evaluated at a given value of the enthalpy, h, and the pressure, p, while our plasma properties are given as functions of the thermal conductivity integral $\phi = \int_0^T K dT$ and p, the plasma properties are defined as follows.

First, a reference enthalpy at atmospheric pressure, h_a, is obtained from the given values of h and p by the following relationship:

$$h_a = h \left(\frac{p}{p_a} \right)^{x\{h\}} \tag{B.1}$$

where $x\{h\}$ is chosen in such a manner that the values of h at the various pressures corresponding to the same ϕ then have the same $h_a = h_a(\phi)$. The quantity h_a is directly associated with ϕ and thus when properties are evaluated at constant h_a, they are also being evaluated at constant ϕ.

The plasma properties are introduced in the following manner, beginning with the thermal conductivity integral ϕ, which is directly a function of h_a, as described above.*

$$\phi\{h,p\} = \phi\{h_a,p\} \tag{B.2}$$

The electrical conductivity is given by

$$\sigma\{h,p\} = \sigma_a\{h_a\} \left(\frac{p}{p_a} \right)^{s\{h_a\}} \tag{B.3}$$

*In all the equations in this section, functional relationship will be denoted by { }. For example, $\phi\{h_a\}$ means: ϕ is a function of h_a only.

Similarly, the specific radiated power is given by

$$u\{h,p\} = u_a\{h_a\} \left(\frac{p}{p_a} \right)^{t\{h_a\}} \qquad (B.4)$$

The various curves labeled "Yos-like" in Figs. B-1 and B-2 represent the properties of Ref. 1 fitted into the present formulation using powers of pressure.

Another grouping of nitrogen properties is based upon analytical inversions of measurements made on an arc device 0.5 cm in diameter at atmospheric pressure (Refs. 8 and 9). When these atmospheric pressure nitrogen properties are combined with the previously fitted powers of pressure from the "Yos-like" properties, the complete set of properties is called "Maecker-like". Calculations using these properties are illustrated in Figs. B-1 through B-5.

A third group of properties called "mixed" result when the high radiation values of the "Yos-like" properties are used with the "Maecker-like thermal and electric conductivity values.

B.2 Comparison of Cases

The various computer cases which were run are listed in Table B-1. The "skipped" numbers represent cases that were run with plasma properties read into the computer incorrectly. Several groups of related cases will now be discussed individually.

B.2.1 Calculations for a 0.5 cm Diameter Constrictor

For asymptotic arc columns in a 0.5-cm diameter (cascade) channel, the theoretical results agree with measurements (for nitrogen) when the "maecker-like" gas properties are used. The quantities which are measured in this experiment are electric field, total wall heat flux, and radiated power (through a quartz window). The agreement merely indicates consistency since the "Maecker-like" properties are based on the inversion of such measured data from a 0.5-cm cascade at one atmosphere.

Inlet region (or gas heater) calculations were made using the same gas properties for two typical operating conditions of the 0.5-cm research cascade (Ref. 3 and Appendix A). For the inlet region, some

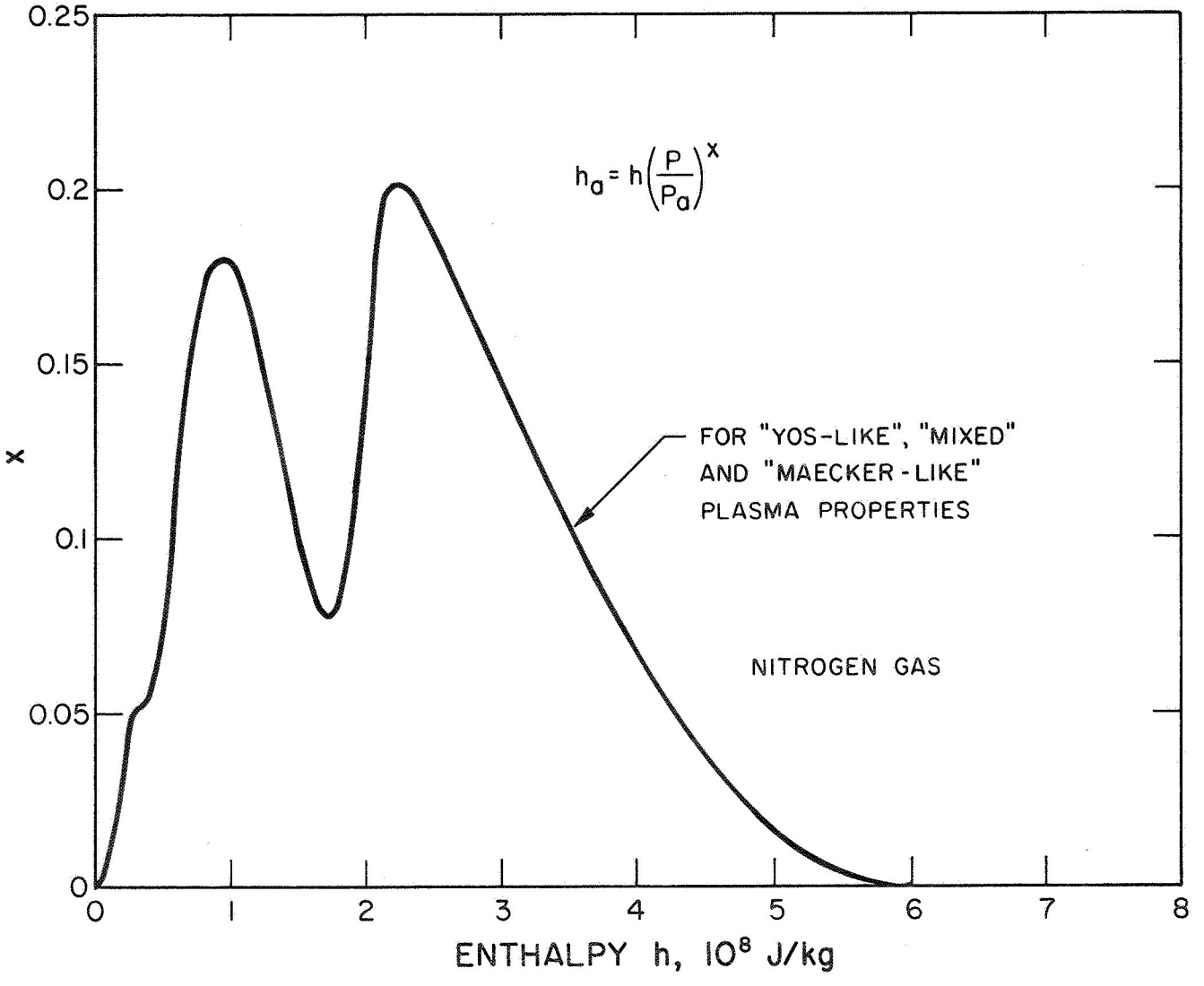

FIG. B-1 RELATIONSHIP BETWEEN ENTHALPY AND REFERENCE ENTHALPY

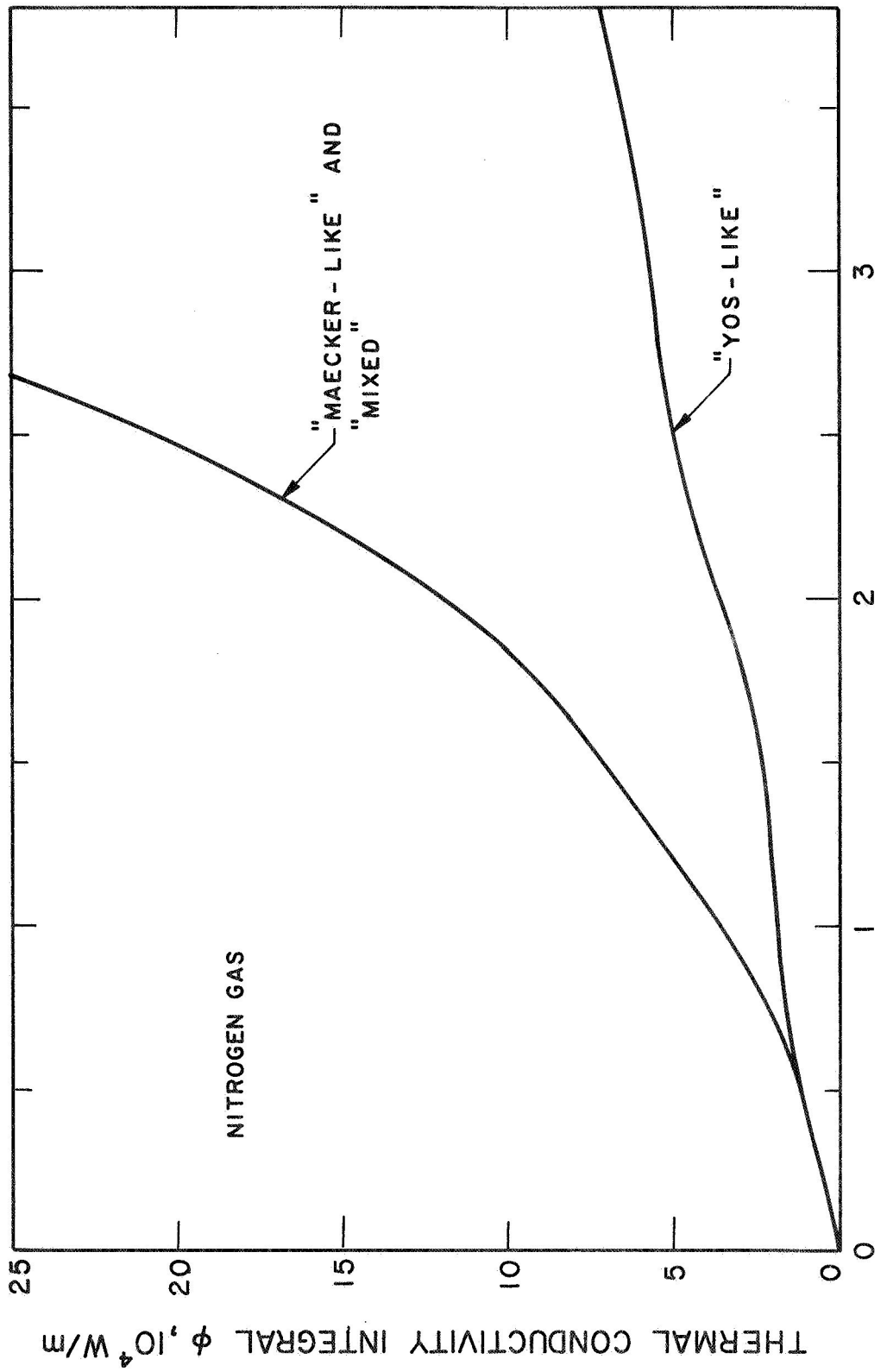

FIG. B-2 THERMAL CONDUCTIVITY INTEGRAL AS A FUNCTION OF REFERENCE ENTHALPY

73618264

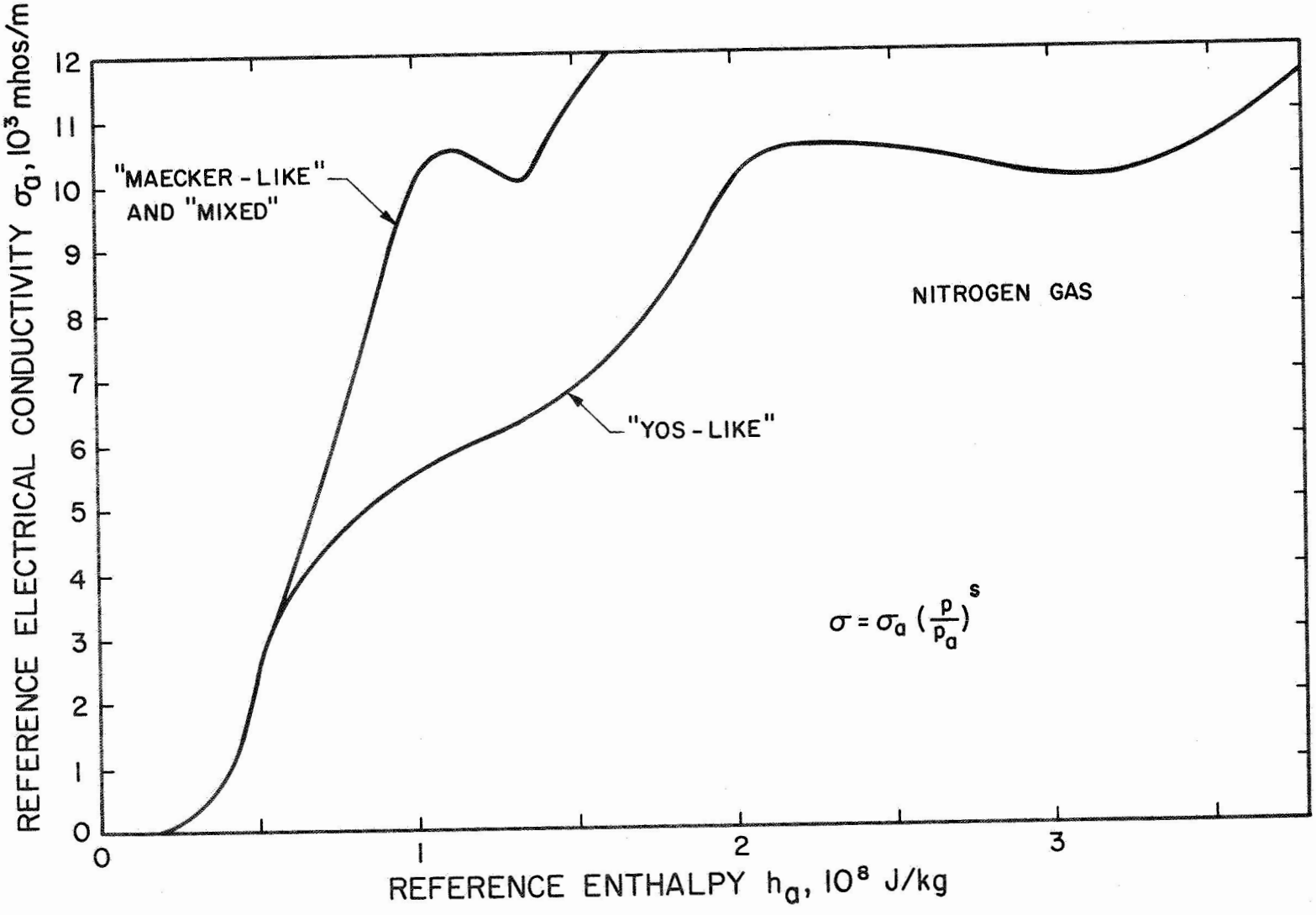

FIG. B-3 REFERENCE ELECTRICAL CONDUCTIVITY AS A FUNCTION OF REFERENCE ENTHALPY

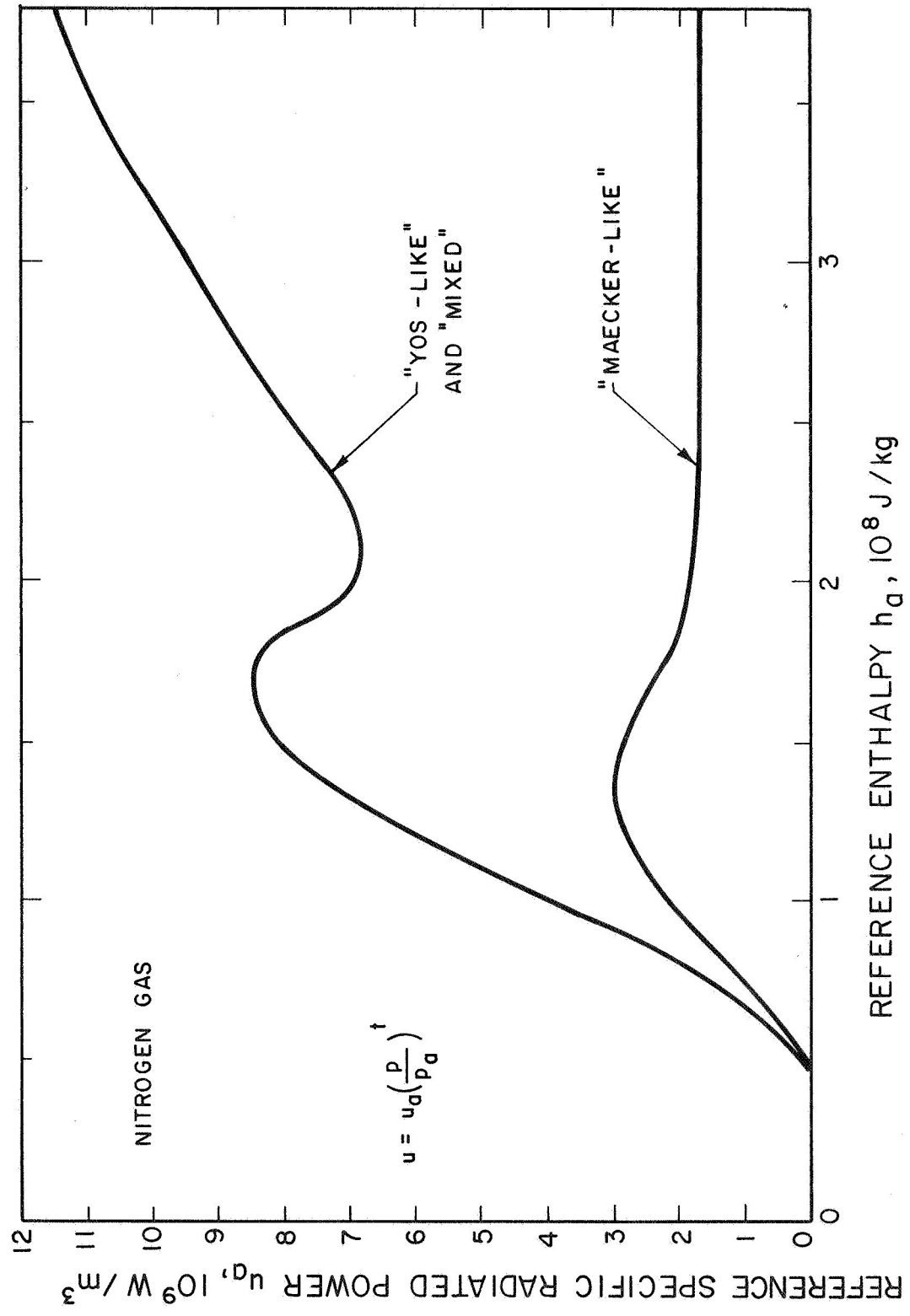

FIG. E-4 REFERENCE SPECIFIC RADIATED POWER AS A FUNCTION OF REFERENCE ENTHALPY

73618266

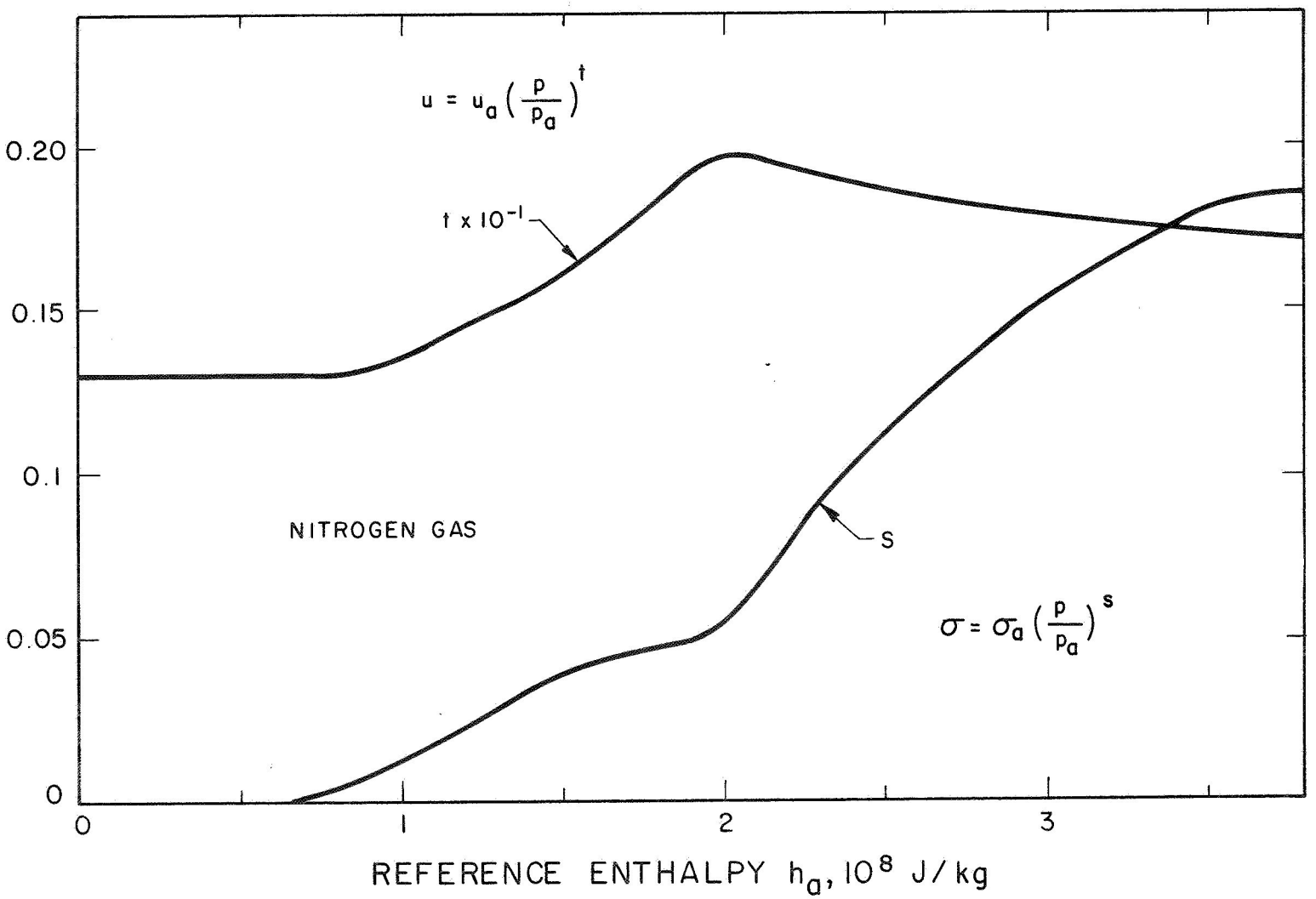

FIG. B-5 s AND t AS FUNCTIONS OF REFERENCE ENTHALPY

TABLE B-1

TABLE OF CASES

Case	Diameter (meters)	Current (Amps)	Pressure (Atm)	Flow Rate (kg/sec)	Plasma Properties
1	0.005	200	1.05	0.89×10^{-4}	Yos-like
4	0.02	1400	1.0	0.537×10^{-2}	Yos-like
12	0.005	200	1.02	0.89×10^{-4}	Maecker-like
13	0.005	100	1.02	0.89 xx 10^{-4}	Maecker-like
14	0.005	200	1.05	0.89×10^{-4}	Maecker-like
16	0.02	1400	1.0	0.537×10^{-2}	Maecker-like
17	0.02	1400	2.0	0.537×10^{-2}	Maecker-like
18	0.02	1400	4.0	0.537×10^{-2}	Maecker-like
19	0.02	1600	1.0	0.537×10^{-2}	Maecker-like
20	0.02	1900	1.0	0.537×10^{-2}	Maecker-like
21	0.02	2500	1.0	0.537×10^{-2}	Maecker-like
22	0.02	1500	1.0	0.537×10^{-2}	Mixed
23	0.07	17,000	1.0	0.07	Mixed

discrepancies between the experimental and the theoretical results appeared. These discrepancies are most pronounced in the mass flow averaged enthalpy which represents the difference between the power input ($I \int_o^L Edz$) and the integrated heat loss to the wall (Cf. Fig. 3-6). The mean enthalpy is neither measured nor calculated for the asymptotic case. Its calculation involves the radial distributions of enthalpy, density, and velocity, hence, also the viscosity.

When the "Yos-like" properties were used for the 200-ampere calculations, the following comparisons were indicated. While the axial dependence and the fully developed values of the mass-averaged enthalpy were almost identical to the "Maecker-like" calculation, the enthalpy profiles were considerably higher (on the order of 80 percent) and the mass flow considerably lower in the center of the discharge. Further, in the "Yos-like" case, the wall heat flux was lower (by 16 percent), radiation much higher (by 320 percent), and the electric field lower (by 16 percent). Hence, integrations using the "Yos-like" properties do not agree with the experiments.

B.2.2 Calculations for a 2.0 cm Diameter Constrictor, Comparing "Yos-like" and "Maecker-like" Properties

Cases 4 and 16 demonstrate the effects of using two different groups of plasma properties for a typical operating condition of a 2-cm heater.

The magnitudes and distributions of the various arc-gas flow quantities of interest are quite different for the two cases. Similar tendencies are present as with the smallest diameter calculations with respect to enthalpy, mass flux, and electric field. Now, however, radiation predominates in the wall heat flux and the greatly increased radiation of the "Yos-like" properties gives a "Yos-like" heat flux as much as 290 percent of the "Maecker-like" heat flux. In addition, the "Yos-like" case 4 took a length of almost 90 cm to choke, while the "Maecker-like" case 16 choked in 34 cm. A comparison will now be made dealing with the greatly different radiation values between the two groups of properties. In order to match a particular experimental operating point at 1500 amperes, a comparison was made between case 22, using the "mixed" properties (higher radiation), and the average of cases 16 and 19,

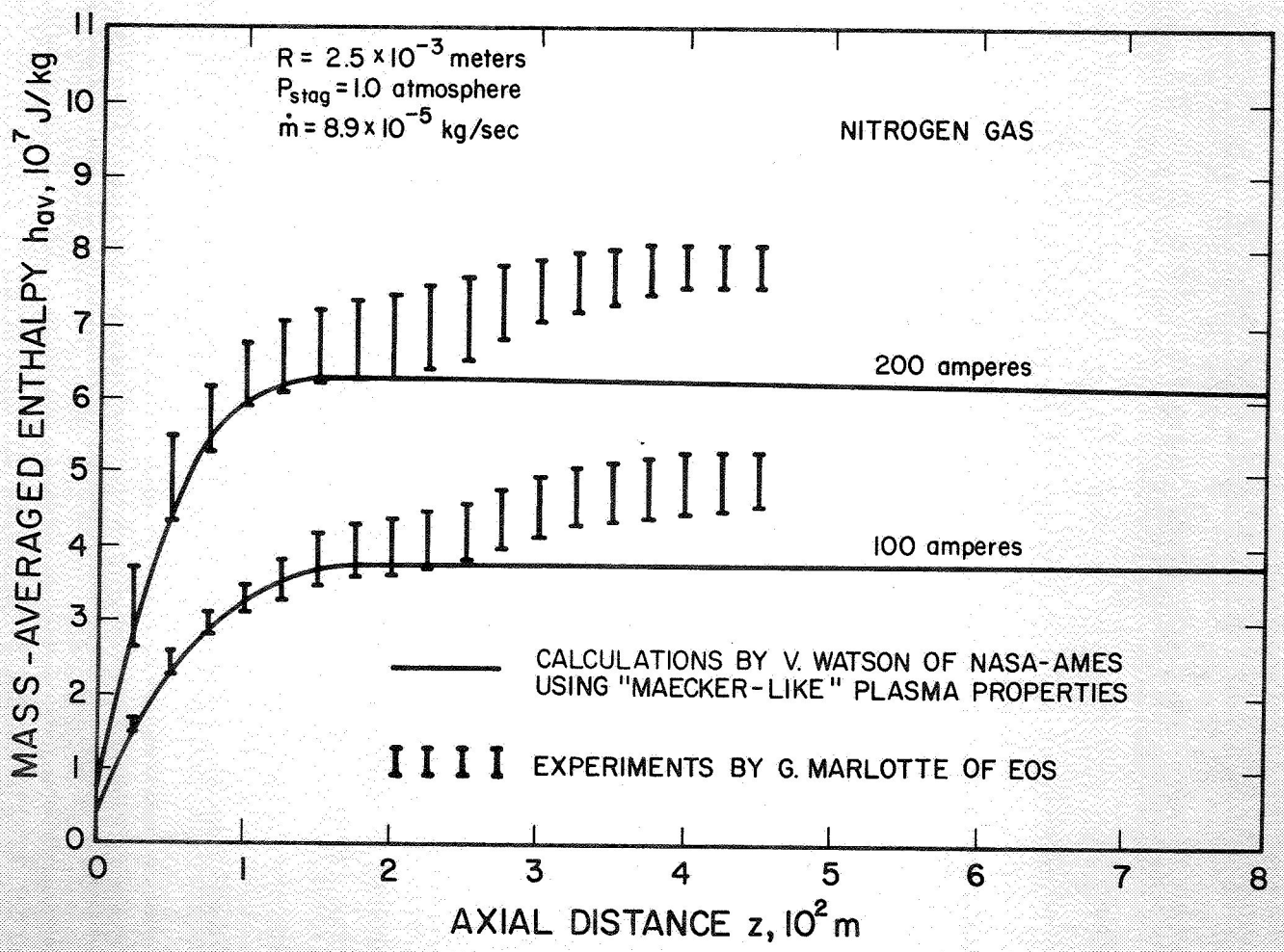

FIG. B-6 EXPERIMENTAL AND CALCULATED MASS-AVERAGED ENTHALPY AS A FUNCTION OF LENGTH FOR THE 0.5-cm-DIAMETER ARC DEVICE

using the "Maecker-like" properties (lower radiation). Figure B-7 shows the total heat fluxes together with the radiation components, while Fig. B-8 shows the electric field values. On Fig. B-7, experimental values of heat flux are plotted which tend to substantiate the higher "Yos-like" radiation values.

B.2.3 Calculations Showing Pressure Dependence for a 2.0 cm Diameter Constrictor

Cases 16, 17, and 18 in Table B-1 are similar except for a difference in inlet pressure. This particular sequence demonstrates one of the problems of drawing conclusions from the calculations; that is, which parameters should remain fixed to draw meaningful conclusions? Since the mass-flow remained the same in the three cases under discussion, while the inlet pressure was changed, the cases at the higher pressures did not choke in reasonable lengths.

Figure B-9 shows that values of mass-averaged enthalpy for the higher pressure calculations are reduced at a fixed axial coordinate. Figure B-10 demonstrates the large pressure dependence of radiation and the large role radiation can have. Of some interest is the fact that, in the region near the entrance to the heater, where the heat load is predominately radiation, the ratios of the magnitudes of the heat loads are given quite accurately by $(p/p_a)^t$, where $t \approx 1.3$ as may be obtained from Fig. B-5. Figure B-11 shows mainly the effect of increased radiation upon the electric field.

B.2.4 Calculations Showing Current Dependence for a 2.0 cm Constrictor

Cases 16, 19, 20, and 21 may be compared in order to examine current effects. The results are fairly self-explanatory and are given on Figs. B-12 through B-14. Some experimentally obtained electric fields at lower currents are also shown on Fig. B-14. Since the "Maecker-like" (low radiation) properties were used for this series of comparisons, the higher values for the experimental electric fields may be substantially due to higher radiation being present in the experiments.

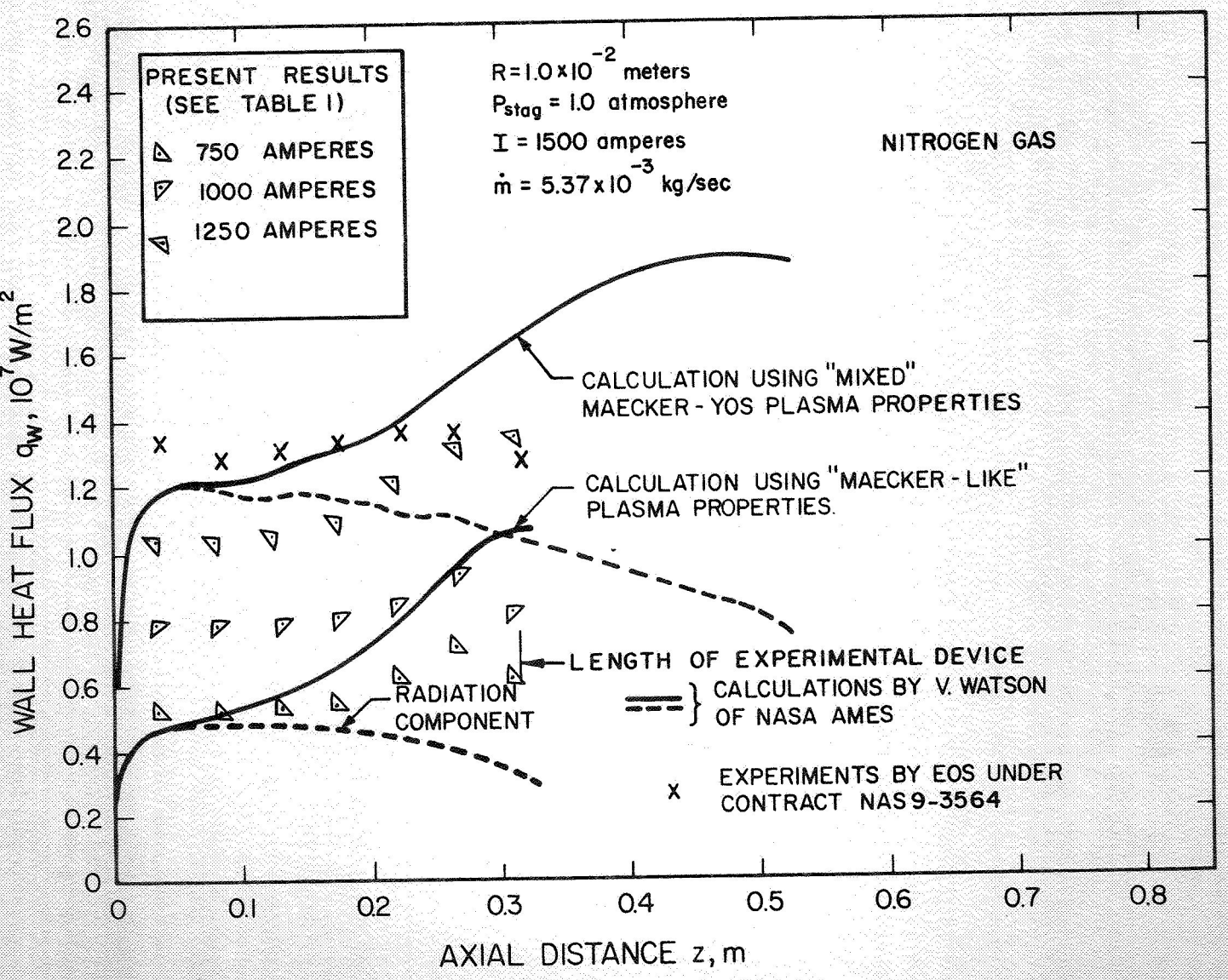

FIG. B-7 EXPERIMENTAL AND CALCULATED WALL HEAT FLUX AS A FUNCTION OF LENGTH FOR THE 2.0-cm-DIAMETER ARC DEVICE

73617978

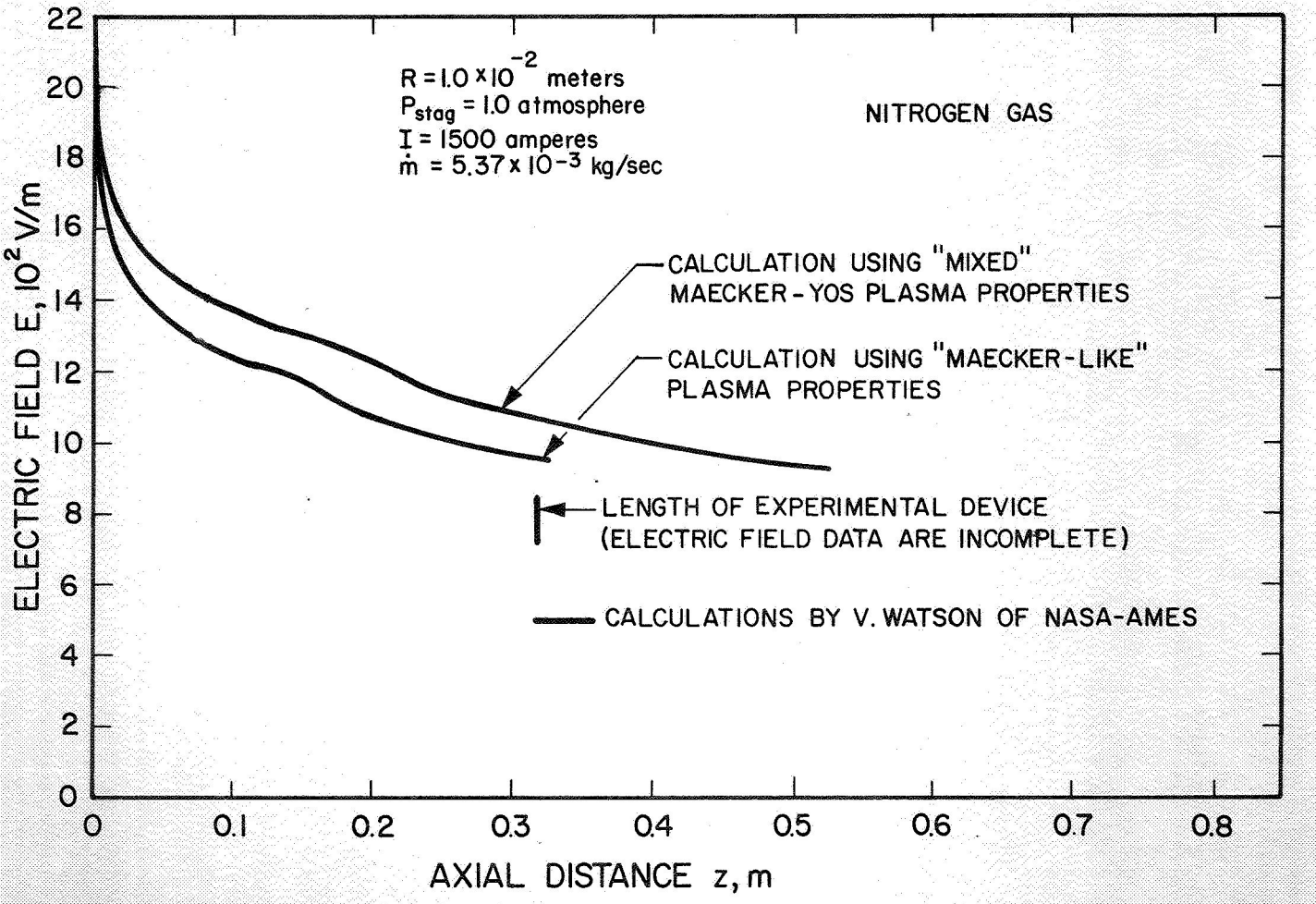

FIG. B-8 EXPERIMENTAL AND CALCULATED ELECTRIC FIELD AS A FUNCTION OF LENGTH FOR THE 2.0-cm-DIAMETER ARC DEVICE

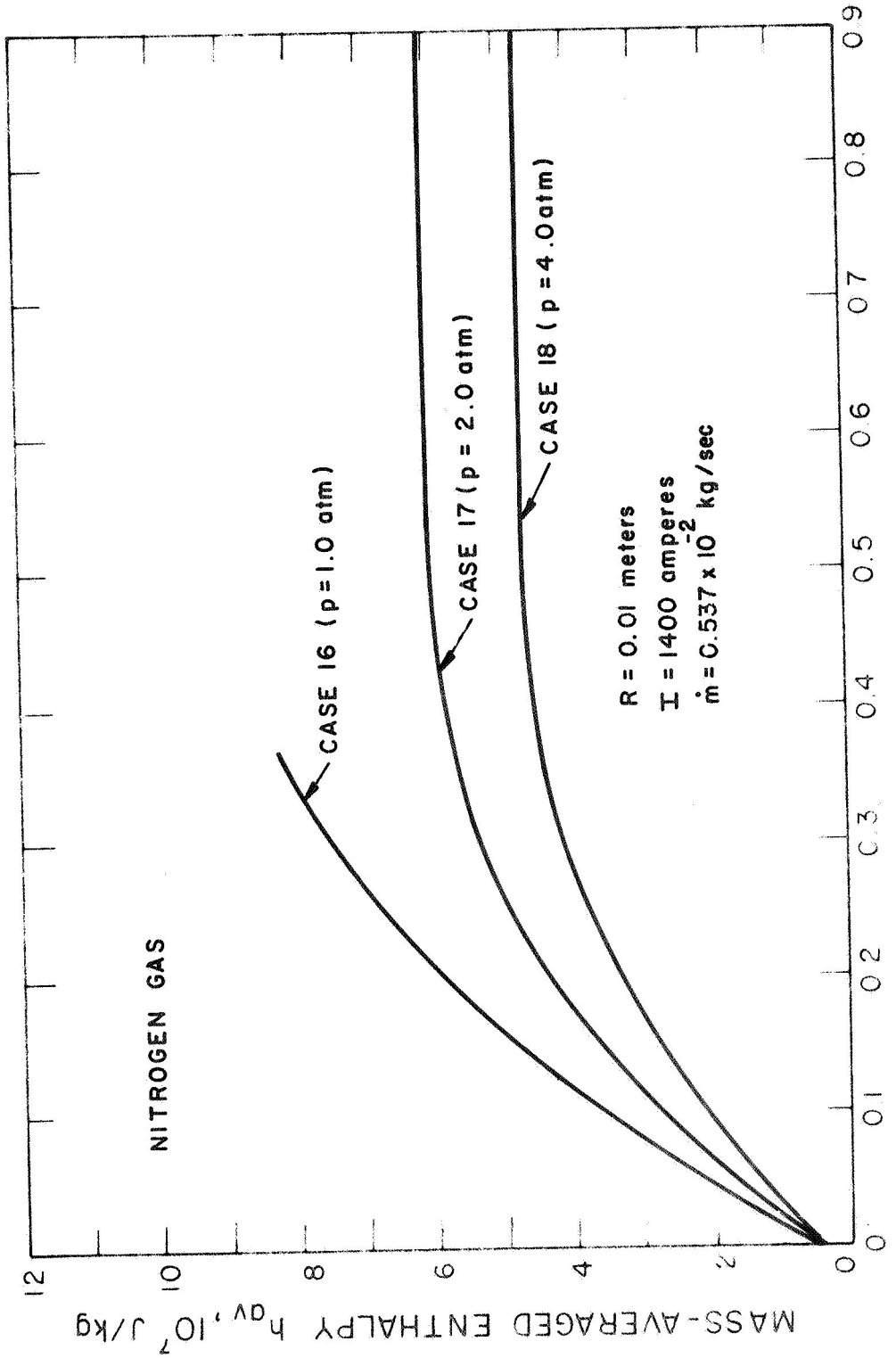

FIG. B-9 CALCULATIONS SHOWING PRESSURE DEPENDENCE OF MASS-AVERAGED ENTHALPY FOR A 2.0-cm-DIAMETER CONSTRICTOR

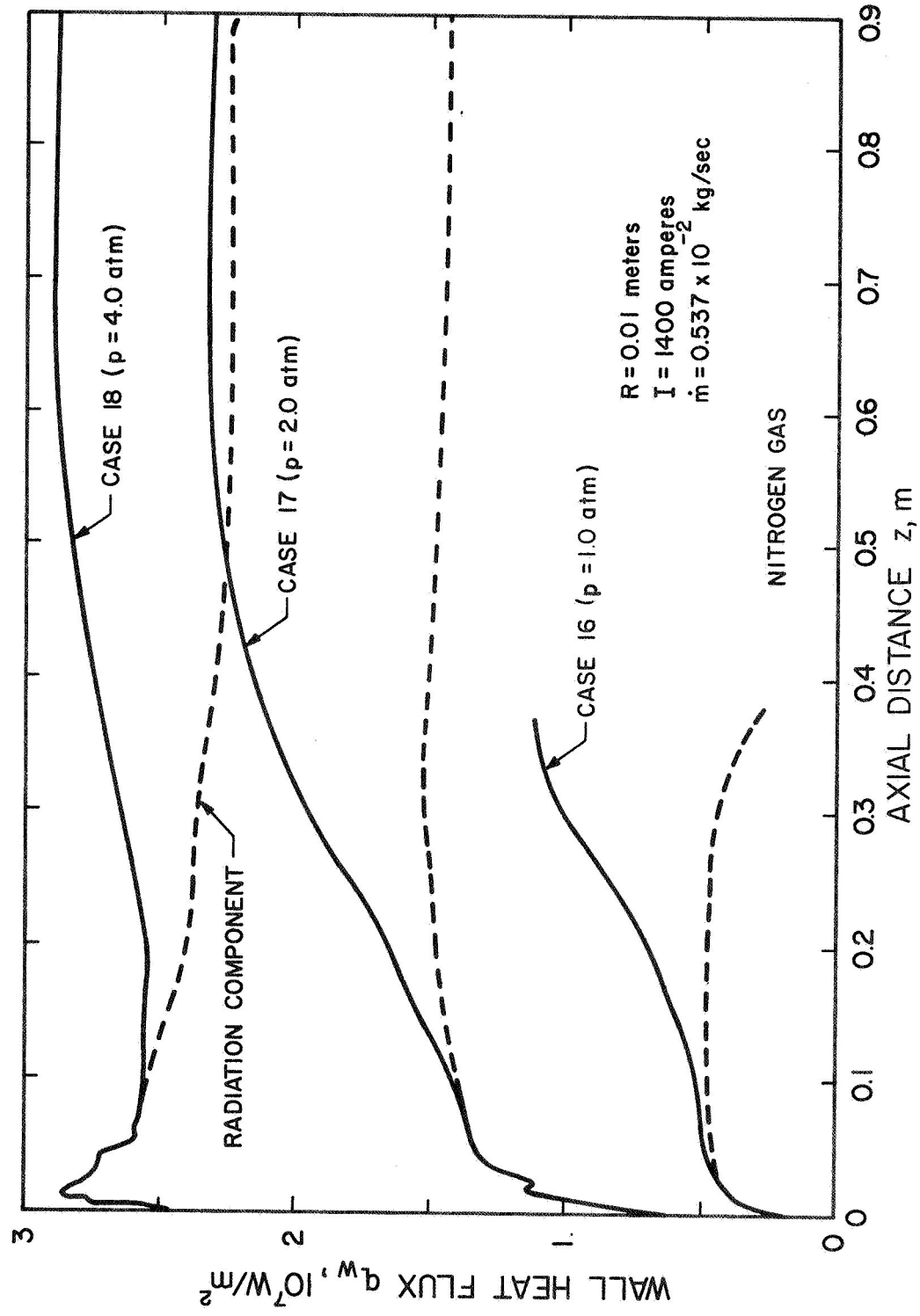

FIG. B-10 CALCULATIONS SHOWING PRESSURE DEPENDENCE OF WALL HEAT FLUX FOR A 2.0-cm-DIAMETER CONSTRICTOR

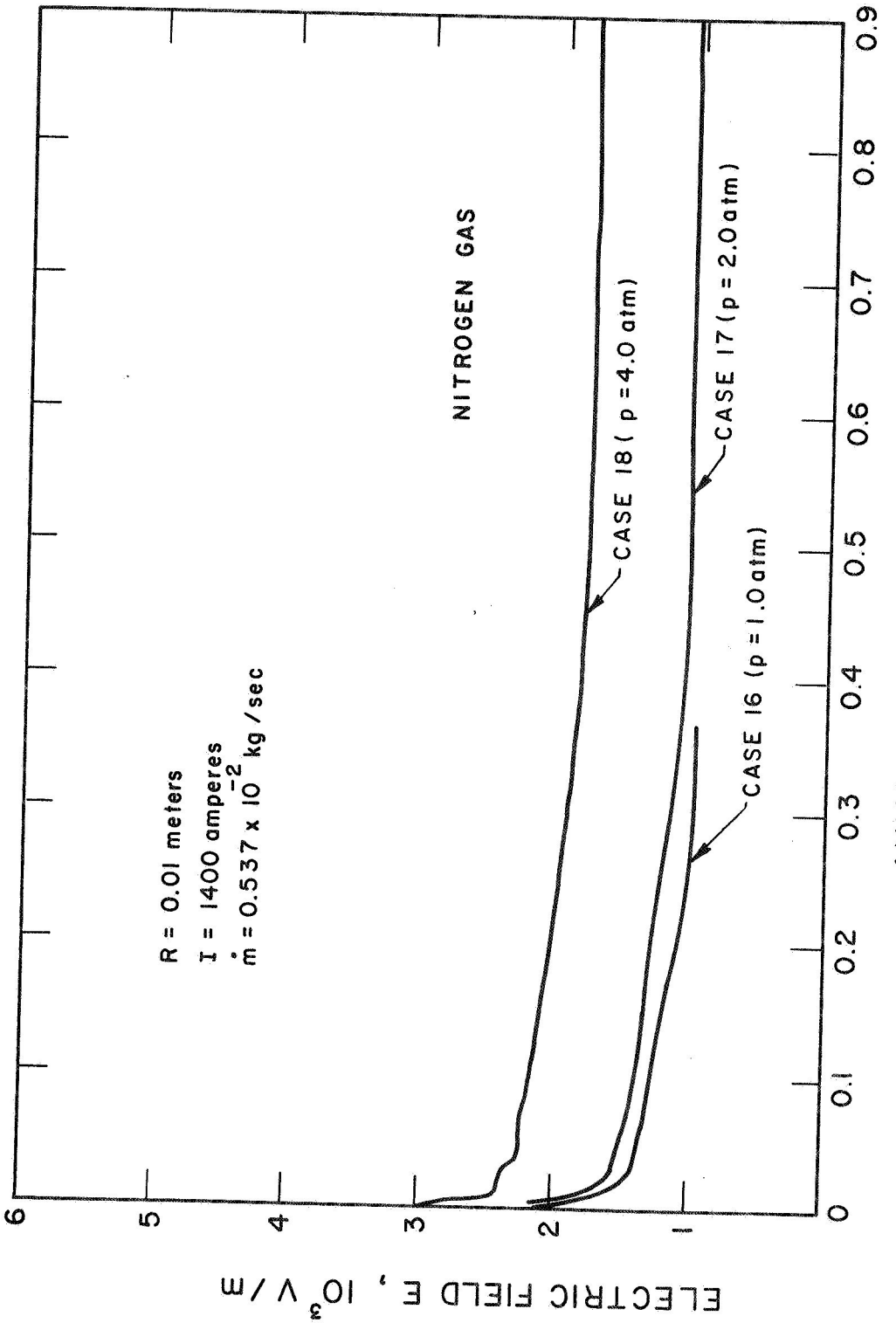

FIG. B-11 CALCULATIONS SHOWING PRESSURE DEPENDENCE OF ELECTRIC FIELD FOR A 2.0-cm-DIAMETER CONSTRICTOR

73618310

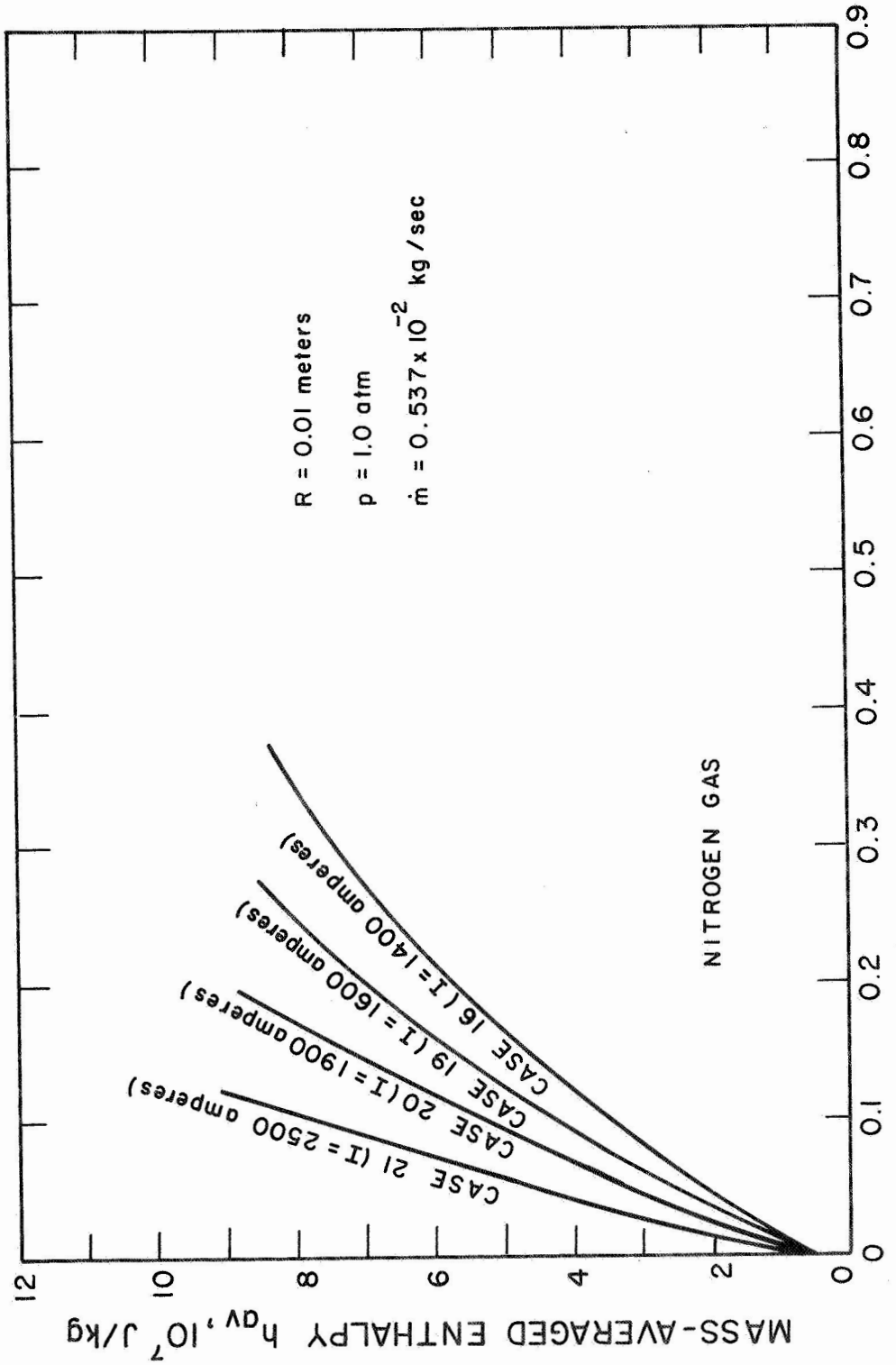

FIG. B-12 CALCULATIONS SHOWING CURRENT DEPENDENCE OF MASS-AVERAGED ENTHALPY FOR A 2.0-cm-DIAMETER CONSTRICTOR

3618312

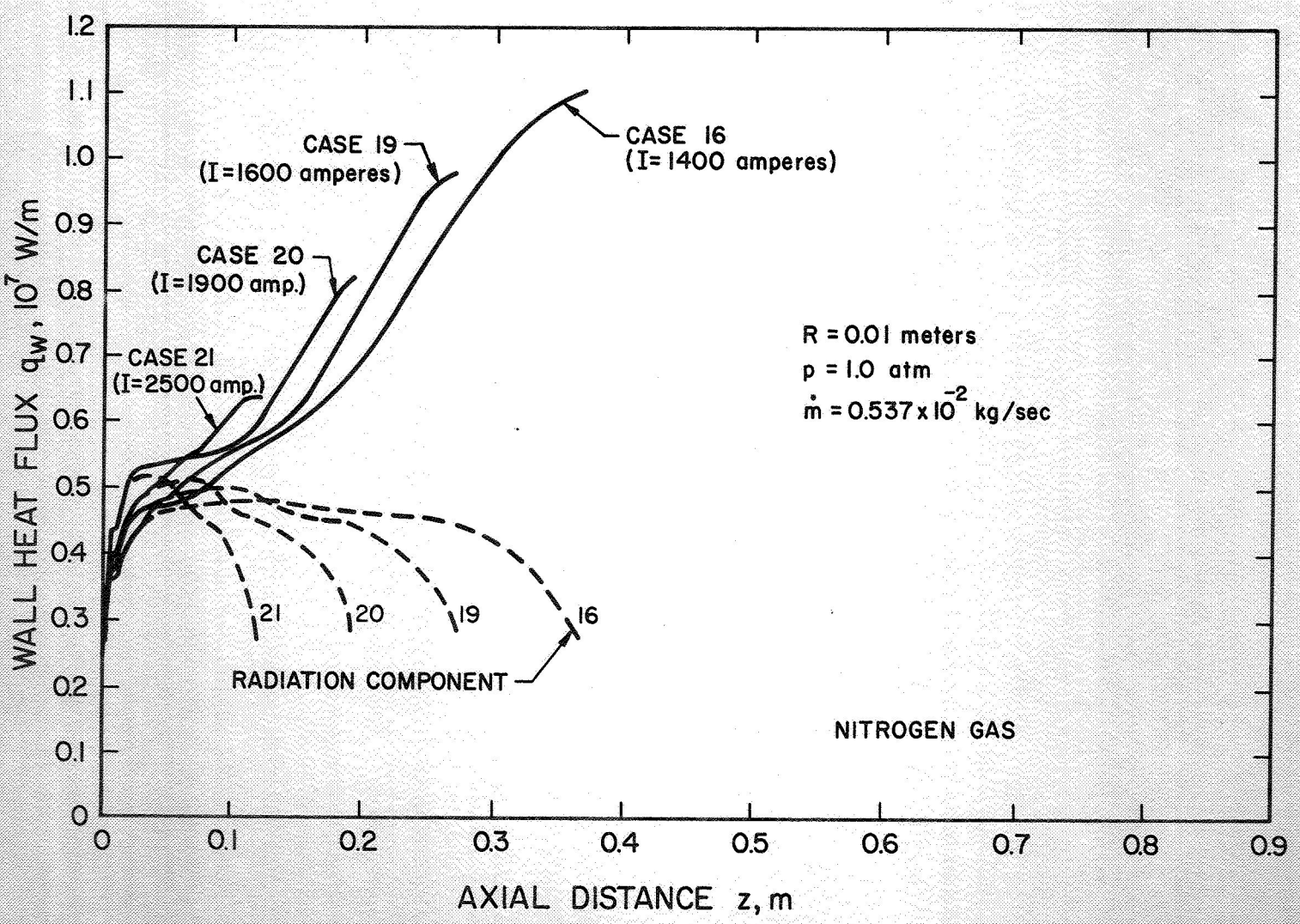

FIG. B-13 CALCULATIONS SHOWING CURRENT DEPENDENCE OF WALL HEAT FLUX FOR A 2.0-cm-DIAMETER CONSTRICTOR

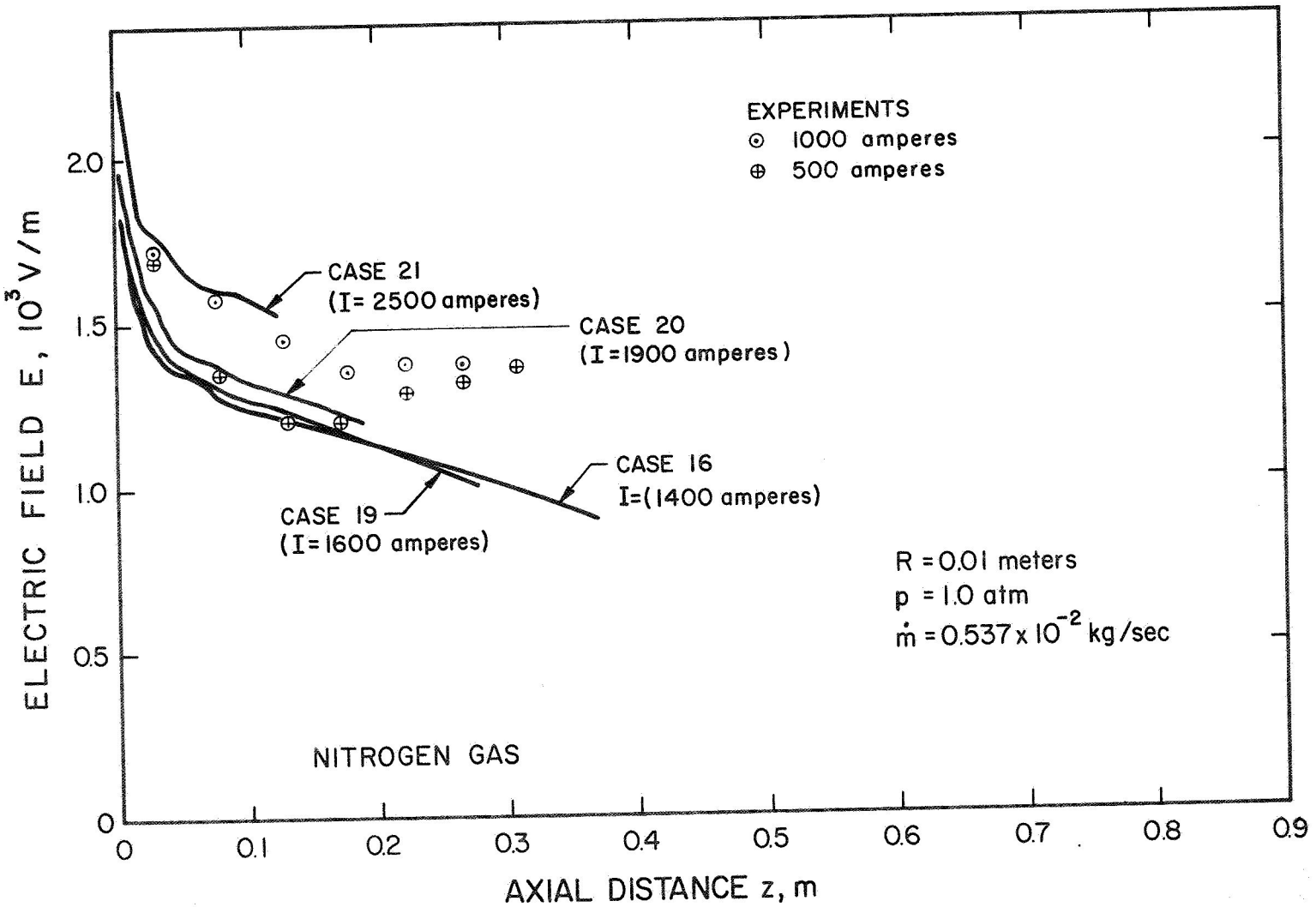

FIG. B-14 CALCULATIONS SHOWING CURRENT DEPENDENCE OF ELECTRIC FIELD FOR A 2.0-cm-DIAMETER CONSTRICTOR

Figure B-15 shows the calculated pressure drops for the four currents. The curves on Fig. B-15 indicate that, for the experimental currents of interest, a linear pressure drop is a good approximation.

B.3 Calculations for a Large High-Power Device

Case 23 (listed on Table B-1) is a trial calculation for an arc heater of much higher power with roughly the same mass-averaged enthalpy as the 2.0 cm heater developed in this program. When mass-averaged enthalpy is held constant in scaling, Ref. 3. Section 6 offers a convenient method of determining the various "scaled" parameters (radius, current, mass-flow, etc.). This method was used quite successfully; first, to determine the input and then to predict the results of the case 23 computer calculation.

Figure B-16 shows that the very high initial values of the radiation suppress the usual fast initial rise in mass-averaged enthalpy. Figure B-17 shows that conduction (the difference between the two curves) is an insignificant component of wall heat transfer in this device. Figure B-18 shows that the electric field is quite similar to the electric field in the smaller 2.0 cm device, as would be expected from simple theory and from experience.

The current (17,000A) for this 10 MW heater calculation was chosen on the basis of very simple scaling rules for radiation dominated arcs. These rules state that similar cases in this regime (i.e., same centerline temperatures, etc.) must have equal values of the current density, I/R^2. Now, for a given gas pressure and enthalpy

$$R^2 \propto \dot{M} \propto \dot{W}_G \text{ (power)}$$

Therefore the current I would scale up directly as the power.

The current chosen for this first try (17,000A) is clearly on the high side, and was chosen to insure that the desired enthalpy

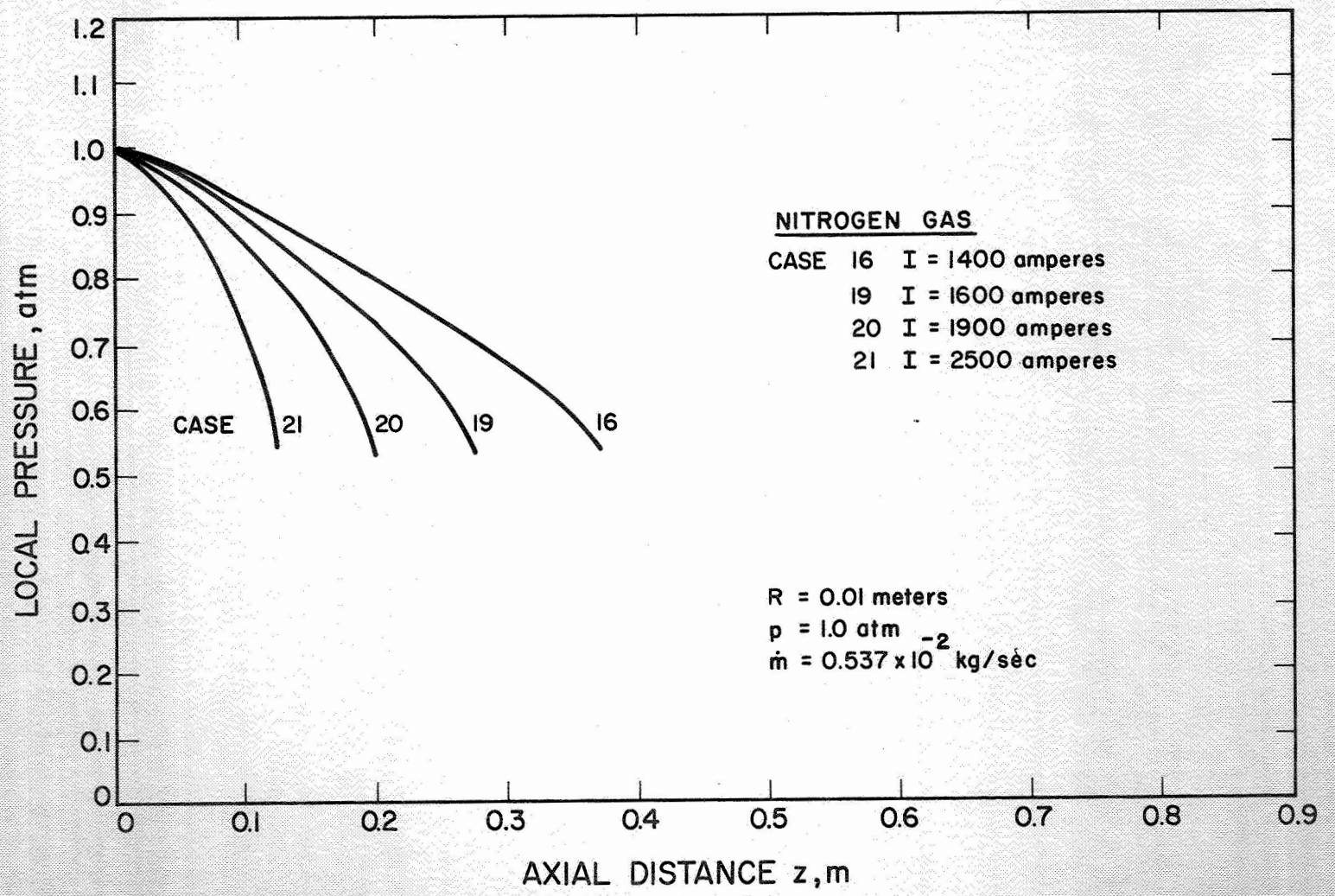

FIG. B-15 CALCULATIONS SHOWING CURRENT DEPENDENCE OF LOCAL PRESSURE FOR A 2.0-cm-DIAMETER CONSTRICTOR

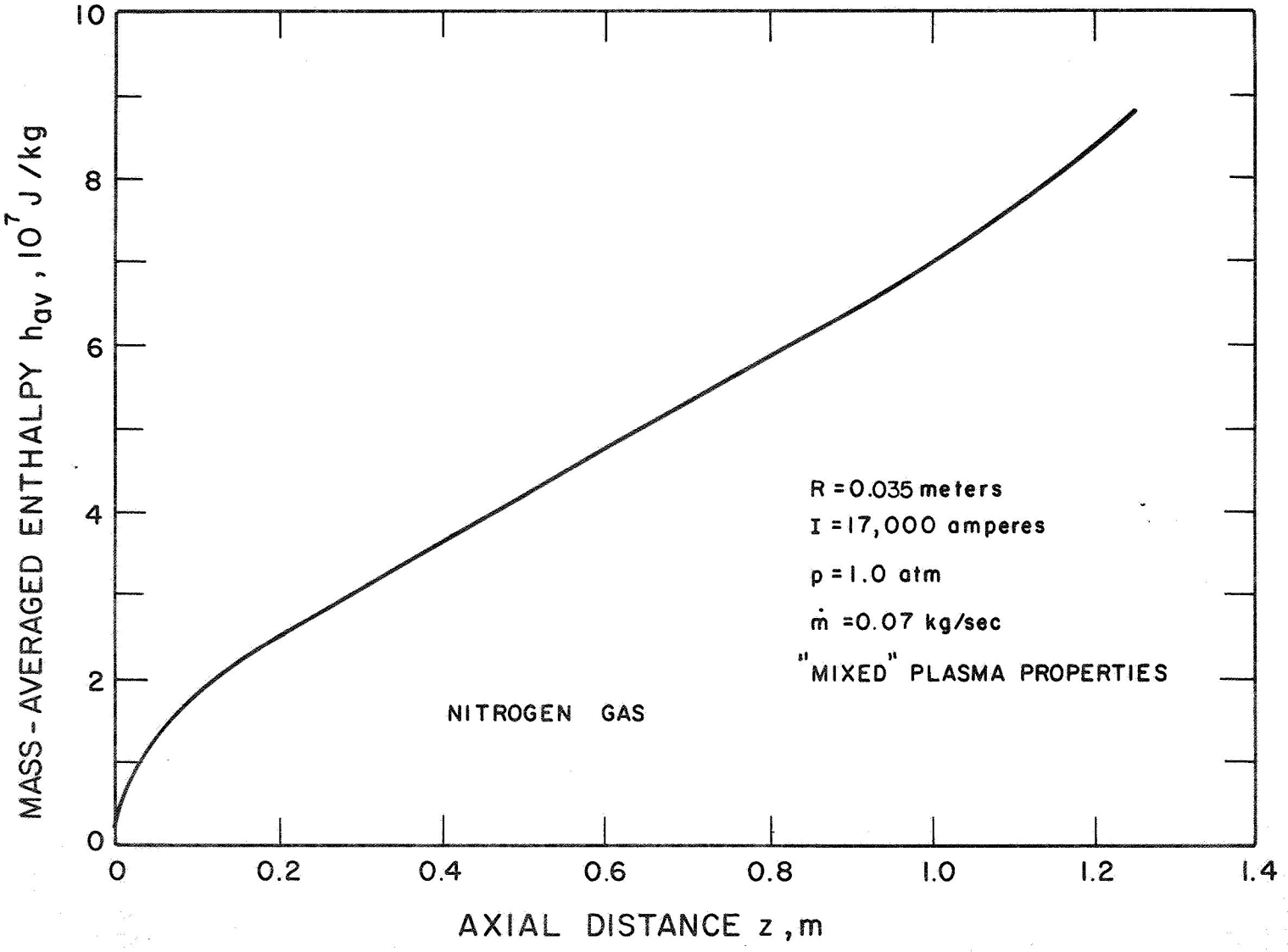

FIG. B-16 MASS-AVERAGED ENTHALPY CALCULATIONS FOR A LARGE HIGH-POWER DEVICE

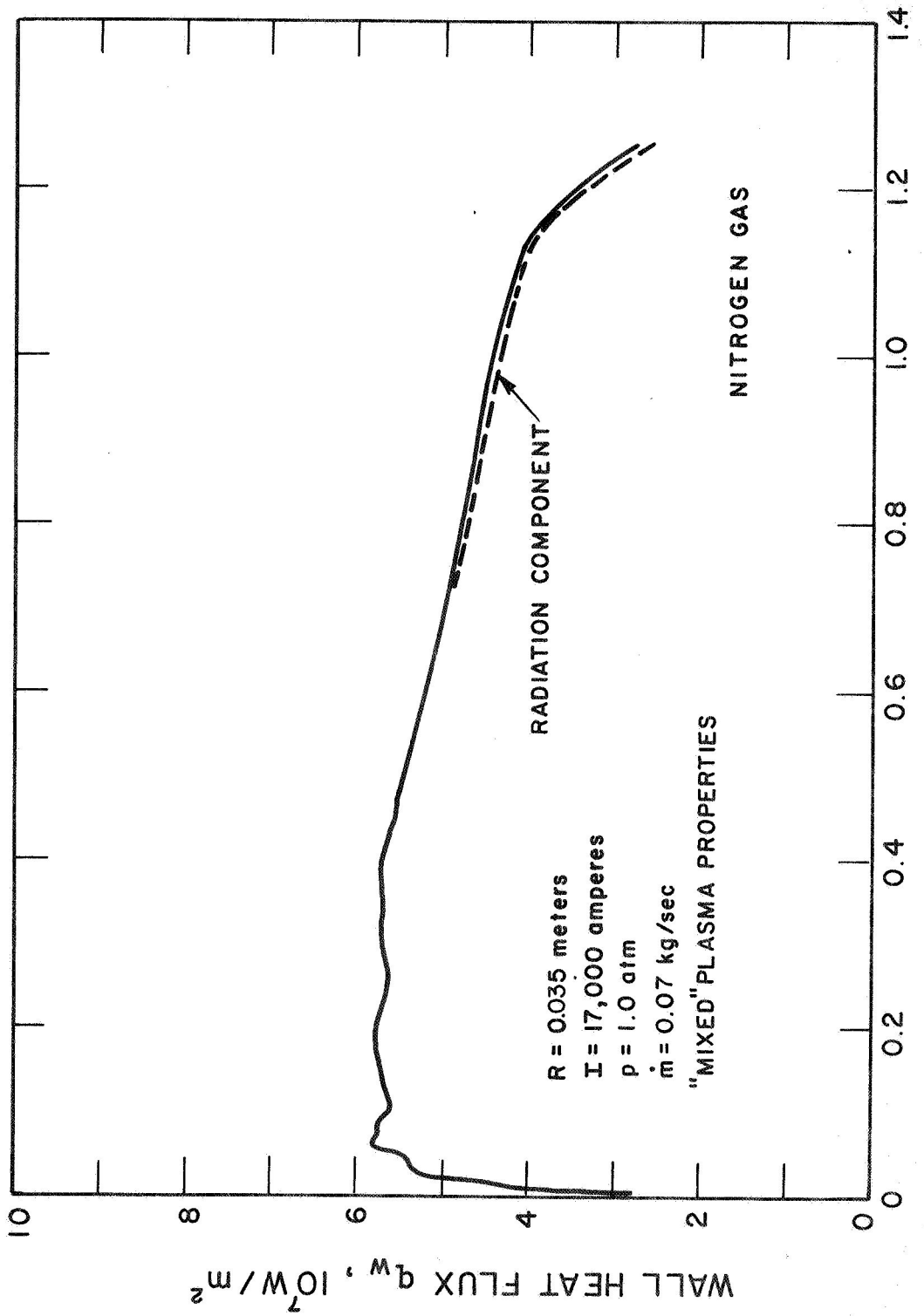

FIG. B-17 WALL HEAT FLUX CALCULATIONS FOR A LARGE HIGH-POWER DEVICE

73618315

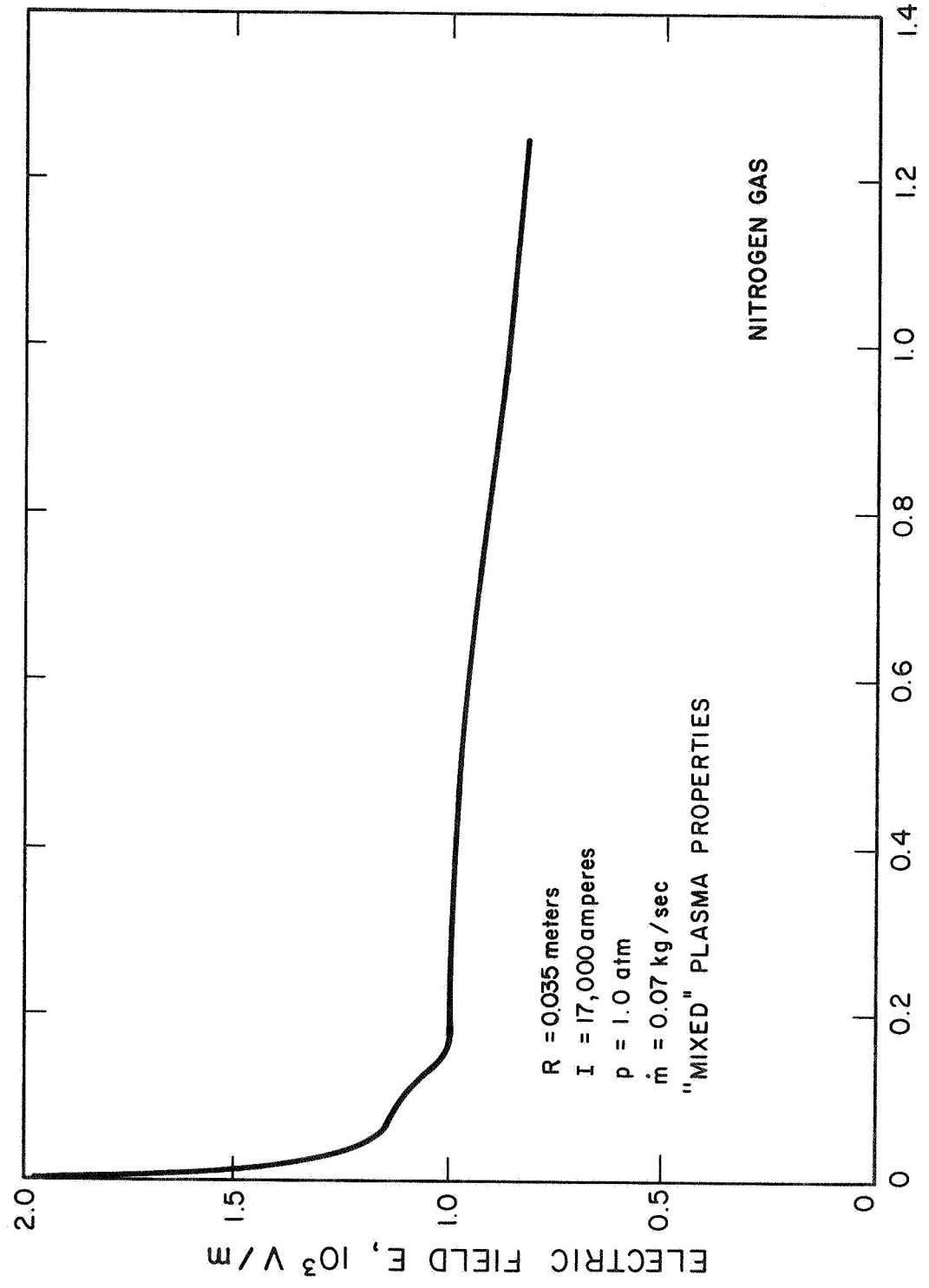

FIG. B-18 ELECTRIC FIELD CALCULATIONS FOR A LARGE HIGH-POWER DEVICE

would be reached in a heater of reasonable length. It is of interest to note that even with this large current the predicted constrictor wall heat loads are not yet completely out of reason, so they are rather high - $\sim$ 5-6 kW/cm^2 (see Fig. B-17).

Later when more information became available (see Section 6) it became clear that half of the above current, say 8000-9000A, would suffice for this heater, and would result in lower wall heat loads and better efficiency. The heat load for 8000A is now estimated at $\sim$ 2 kW/cm^2.

While this first computer case chosen for the 10 MW level is not yet close to an optimum design, it is interesting that the computer results for this case generally agree quite well with the semi-empirical design charts of Section 6. This is seen by substituting 17,000A into Fig. 6-4 and reading off the estimated heat load.

B.4 Conclusions

The numerical (computer) integration of the laminar flow-arc equations has already produced a great deal of valuable qualitative and quantitative insight, and it promises to become a most valuable aid for arc heater development in the future.

There are, however, several difficulties and uncertainties remaining which must be straightened out before the computer results will reach their full usefulness for engineering work.

The first is the basic difficulty of making meaningful full comparisons between numerical results and experimental data. This is particularly pronounced as long as only a few isolated points are available for both the theory and the experiments. When there is close agreement there is, of course, no problem. But when there is a known or suspected discrepancy in one quantity, say the electric field or conductivity, then it is difficult to judge whether other discrepancies are merely caused by this one or have different sources. It will require some ingenuity to find crossplotting, interpolating or other comparison schemes which will show clearly which trends

the theory predicts correctly and which it does not. Unfortunately, those integrated quantities which would be the easiest to compare, such as heater length or the pressure at a station, are also the least accurate results.

The second difficulty is in the well known uncertainties of the theoretical transport properties and of certain experimental measurements (e.g., total radiant power emitted). Only after the first difficulty has been resolved and many more well planned series of theoretical and experimental cases have been run can we hope to disentangle the transport property questions by careful comparisons.

The third major difficulty is the uncertainty regarding turbulence. Its presence would invalidate much of the present theoretical solution. Unfortunately the onset of turbulence must be expected in about the same regime in which radiation and self-absorption become important. Since both are highly uncertain and both will tend to produce somewhat similar results, namely a broadened temperature profile, it will be difficult to isolate these effects by mere comparisons between laminar theory and experiments with one gas. One must look for highly radiating low Reynolds number (laminar) cases and cases with high Reynolds number and low radiation fraction.

In summary there are still important unresolved discrepancies and uncertainties which at present limit the usefulness and reliability of the computer results for heater design. However, much progress has been made.

REFERENCES

1. AVCO, RAD Division, Theoretical and Experimental Investigation Arc Plasma Generation Technology, Part II, Vol. 2, ASD-TDR-62-729, Sept. 1963 (U)

2. G. L. Cann, R. D. Buhler, R. H. Harder, and R. A. Moore, "Basic Research on Gas Flows Through Electric Arcs Hot Gas Containment Limits," Aerospace Research Laboratories Report No. ARL 64-49, March 1964

3. G. L. Marlotte, et al, "Basic Research on Gas Flows Through Electric Arcs - Phase III: Studies of the Inlet Region," Electro-Optical Systems, March 1965, USAF Contract AF 33(657)-7940, Project 70192, to be issued as Aerospace Research Laboratories Report

4. H. A. Stine, V. R. Watson, and C. E. Shepard, "Effect of Axial Flow on the Behavior of the Wall Constricted Arc," (paper presented at the AGARD Specialists Meeting on Arc Heaters and MHD Accelerators for the Aerodynamic Purposes, Rhode-Saint-Genese, Belgium, 20-23 Sept. 1964)

5. K. S. Drellishak, D. P. Aeschlman, Ali Bulent Cambel, "Tables of Thermodynamic Properties of Argon, Nitrogen, and Oxygen Plasmas," AEDC-TDR-64-12, January 1964

6. J. Hilsenrath and M. Klein, "Tables of Thermodynamic Properties of Air from 90 to 15,000°K," AEDC-TDR-61-103, August 1961

7. H. E. Weber, "Growth of an Arc Column in Flow and Pressure Fields," AGARD Specialist Meeting on Arc Heaters and MHD Accelerators for Aerodynamic Purposes, Rhode-Saint-Genese, Belgium, Sept. 1964. Published as AGARDograph No. 84, pp. 845-881

8. Electro-Optical Systems, Inc., Basic Research on Gas Flows Through Electric Arcs - Measurement Techniques and Analytical Procedures, by G. L. Marlotte and M. L. Dalton, ARL 64-208, Contract AF 33(657)-7940, Pasadena, California, Nov. 1964

9. J. Uhlenbusch, "Berechnung der Materialfunktionen eines Stickstoff und Argonplasmas aus gemessenen Bogendaten," Z. Physik, Vol. 179, 1964, pp. 347-366

10. V. R. Watson, "Comparison of Detailed Numerical Solutions with Simplified Theories for the Characteristics of the Constricted Arc Plasma Generator," (paper presented at 1965 Heat Transfer and Fluid Mechanics Institute, University of California, Los Angeles, California, 21-23 June 1965